Posttranscriptional regulation of tapasin as an immune escape mechanism in melanoma and impact on immune microenvironment

Dissertation

to obtain the academic degree of
Doctor rerum medicarum (Dr. rer. medic.)
in the field of Medical Immunology

submitted to

the Faculty of Medicine of

Martin Luther University Halle-Wittenberg

by Yuan Wang

born on   in

Supervisor: Prof. Dr. Barbara Seliger

Prof. Dr. Claudia Wickenhauser

Reviewers: Prof. Dr. Manfred Kunz, Leipzig

PD Dr. Dagmar Riemann, Halle (Saale)

Date of the defense: 27.08.2024

Abstract

Deficient expression of the major components of the human leukocyte antigen class I (HLA-I) antigen processing and presentation machinery (APM) on tumor cells is one important immune escape strategy of tumors leading to an inhibition of CD8+ T cell recognition, which could be caused by a posttranscriptional regulation of APM molecules, including RNA binding proteins (RBPs) and microRNA (miRNAs). Furthermore, the suppressive tumor microenvironment (TME) also affects tumor progression. However, little information exists about the expression, function and clinical relevance of miRNAs and RBPs targeting tapasin (tpn) and affect the TME of melanoma. In this study, it was for the first time identified that miR-155-5p and hnRNP C can directly bind to tpn. MiR-155-5p bind to a repressive sequence in the tpn 3'untranslated region (3'UTR) thereby upregulating the HLA-I surface expression and increasing the recognition by CD8+ T cells, but a reduced NK cell cytotoxicity. The binding sequence was confirmed as a silencer by CRISPR/Cas9-mediated genomic deletion. Moreover, hnRNP C targets the tpn 3'UTR thereby inhibiting its expression leading to an reduced HLA-I surface expression on melanoma cells. TCGA SKCM and other *in silico* data demonstrated a link of miR-155-5p and hnRNP C with tpn in melanoma lesions and the patients' overall survival. Furthermore, hnRNP C and tumor-associated macrophages (TAMs) from TME can promote melanoma metastasis formation and could interact with each other via the CXCR3-hnRNP-MIF axis. Thus, these data identified miR-155-5p and hnRNP C can target tpn and their function on HLA-I pathway as well as their clinical relevance. In addition, new insights into unconventional functions of miR-155-5p and into the effect of hnRNP C on TAM and the metastatic phenotype of melanoma were demonstrated suggesting miR-155-5p and hnRNP C as a potential biomarker for tumor immunotherapy.

Referat

Eine defiziente Expression von wesentlichen Komponenten der Antigenprozessierungs- und -präsentationsmaschinerie (APM) der menschlichen Leukozyten-Antigenklasse I (HLA-I) auf Tumorzellen ist eine wichtige Strategie, der Erkennung durch CD8^{+} T-Zellen zu entkommen. Dies kann auf einer posttranskriptionellen Regulation von APM-Molekülen, einschließlich RNA-bindender Proteine (RBPs) und microRNA (miRNAs), beruhen. Gleichzeitig ist die suppressive Tumormikroumgebung (TME) mit der Tumorprogression assoziiert. Jedoch gibt es nur wenig Information über die Expression, Funktion und klinische Bedeutung von miRNAs und RBPs, die Tapasin (Tpn) als Zielstruktur haben und das TME von Melanomen beeinflussen. In der vorliegenden Arbeit wird zum ersten Mal gezeigt, dass sowohl miR-155-5p und als auch das RBP hnRNP C direkt Tpn binden: MiR-155-5p bindet an eine repressive Sequenz in der 3'untranslatierten Region (3'UTR) von Tpn und erhöht dadurch die HLA-I-Oberflächenexpression und die Erkennung durch T-Zellen, verringert aber die Zytotoxität von NK-Zellen. Diese Bindungssequenz wurde durch eine CRISPR/Cas9-vermittelte genomische Deletion als Silencer bestätigt. Darüber hinaus zielt hnRNP C auf die 3'UTR von Tpn ab und hemmt die Expression von Tpn, was zu einer verringerten HLA-I-Oberflächenexpression auf Melanomzellen führt. TCGA SKCM und andere *in-silico*-Daten zeigten eine Korrelation von miR-155-5p und hnRNP C mit der Tpn-Expression in Melanompatienten und ihrem Gesamtüberleben. Darüber hinaus zeigte sich, dass hnRNP C und tumorassoziierte Makrophagen (TAM) des TME die Metastasierung von Melanomen fördern, was über die Interaktion der CXCR3-hnRNP-MIF-Achse erfolgt. Zusammenfassend wurde in der vorliegenden Arbeit miR-155-5p und hnRNP C als Ziel von Tpn identifiziert und ihre Funktion auf den HLA-I-Signalweg sowie ihre klinische Relevanz charakterisiert, sowie neue Einblicke über unkonventionelle Funktionen von miR-155-5p und über Effekte von hnRNP C auf TAM sowie den metastasierenden Phänotyp, so dass miR-155-5p und hnRNP C als potenzielle Biomarker für Tumor-Immuntherapie postuliert werden.

Contents

Abbreviations

3'UTR	3'untranslated region
ab	Antibody
ALSA1	Delta-aminolevulinate synthase
APM	Antigen processing and presentation machinery
ARE	AU-rich element
CAF	Cancer-associated fibroblasts
CAR	Chimeric antigen receptor
CDS	Coding sequence
CRC	Colorectal cancer
CTL	Cytotoxic T lymphocytes
DCs	Dendritic cells
DHS	DNase I hypersensitive site
DHS	DNase hypersensitivity site
ECM	Extracellular matrix
ELISA	Enzyme-linked immunosorbent assay
EMT	Epithelial-mesenchymal transition
ENCODE	Encyclopedia of DNA Elements
ER	Endoplasmic reticulum
ERAP	Endoplasmic reticulum aminopeptidase
FCS	Foetal calf serum
FFL	Firefly luciferase
GAPDH	Glyceraldehyde-3-phosphate dehydrogenase
GSEA	Gene set enrichment analysis
HC	Heavy chain
HLA-I	Human leukocyte antigen class I
ICP	Immune checkpoint
ICPi	Immune checkpoint inhibitors

IGFBP2	Insulin growth factor-binding protein 2
MEM3	Muscle excess-3
MFI	Mean specific fluorescence intensity
MHC	Major histocompatibility complex
MIF	Migration inhibitory factor
miRNAs	microRNAs
miTRAP	MiRNA trapping by RNA *in vitro* affinity purification
NPC	Nasopharyngeal carcinoma
OS	Overall survival
PBMC	Peripheral blood mononuclear cells
PBS	Phosphate Buffered Saline
PCR	Polymerase chain reaction
PX458	pSpCas9 (BB)-2A-GFP plasmid
RBPs	RNA binding proteins
RL	Renilla luciferase
RLU	Relative light units
RT-qPCR	Reverse-transcription PCR
SD	Standard deviation
SDS	Sodium dodecyl sulfate
TAM	Tumor-associated macrophages
TAP	Transporter associated with antigen processing
TCGA-SKCM	TCGA Skin Cutaneous Melanoma
TME	Tumor microenvironment
tpn	Tapasin
VEGF	Vascular endothelial growth factor
β2-m	β2-microglobulin

1   Introduction

1.1 HLA class I antigen processing pathways and immune escape

Antigen presentation is a multi-step and complex process involving the human leukocyte antigen class I (HLA-I) antigen processing and presentation pathway. The classical HLA-I antigen processing pathway mainly presents intracellular proteins, since the proteasome can only degrade unfolded proteins, the intracellular proteins become linear proteins after ubiquitination and enter the proteasome where they are hydrolyzed into peptides[1]. These peptides cleave appropriate or truncated C- and N-terminus via endoplasmic reticulum aminopeptidase (ERAP) or cytosolic enzymes, are transported into the endoplasmic reticulum (ER) and bind to newly assembled HLA-I molecules. This size and sequence specific transport process is mainly mediated by the transporter associated with antigen processing (TAP) comprising of the TAP1 and TAP2 subunits. HLA-I molecules are composed of the heavy chain and the non-covalently bound β2-microglobulin (β2-m), HLA-I molecules are stabilized by calnexin and calreticulin, then the stable HLA-I molecules bind to TAP, ERp57, and tapasin (tpn) to form a peptide loading complex. ERp57 can balance the loading complex, and tpn promotes the stability of TAP and encourages peptides to bind to the loading complex[2]. The trimeric peptide-bound HLA-I complex is stably folded and transported via the trans-Golgi to the cell surface and there presented to CD8+ T cells[3]. CD8 as a coreceptor can bind to the α3 domain of HLA class I molecules independently thereby enhancing T-cell receptor binding to presented antigens and activating downstream signaling[4] (Figure 1).
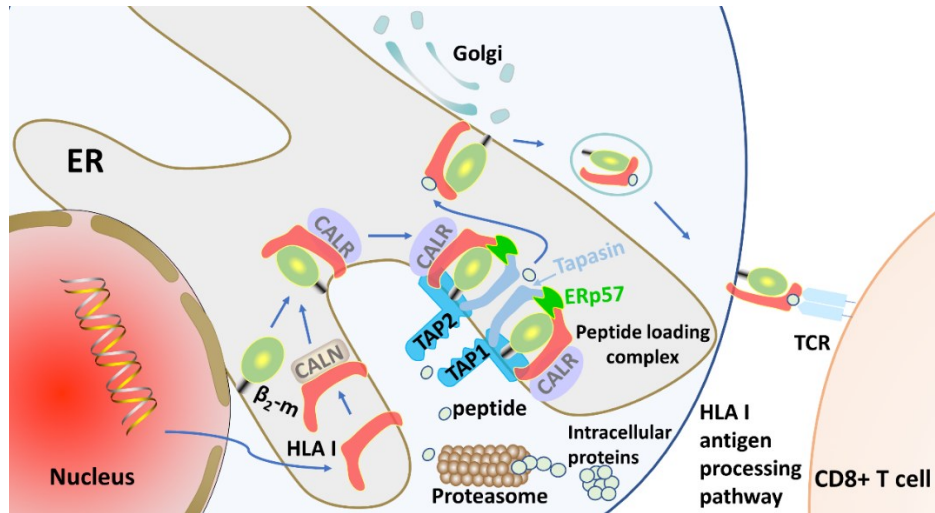
Figure 1 Schematic diagram of HLA-I antigen processing and presentation pathway.
Intracellular proteins are hydrolyzed to oligopeptides via the proteasome pathway, which are subsequently delivered to the ER by the TAP transporter complex, which forms the peptide loading complex with tpn and HLA-I dimer. After loading the peptide, the complex dissociates and the peptide/ HLA-I complex is transported to the cell surface via Golgi. Figure created independently with PowerPoint.

Major breakthroughs have been achieved with the ongoing development of tumor-related immunotherapies with the introduction of immune checkpoint inhibitors (ICPi), chimeric antigen receptor (CAR)-based T and natural killer (NK) cell therapies as well as cancer vaccines[5-8]. The core mechanism of immunotherapies so far driven by T cell recognition of tumor antigens presented by HLA[9], including HLA-I presented peptides to CD8+ T cells. However, only a few numbers of patients achieve durable responses to these treatments[10-12] suggesting that more diverse tumor-associated immunotherapies are urgently needed. In addition to the expression of inhibitory immune checkpoint (ICP) molecules, the loss of components of the HLA-I antigen processing machinery (APM) is characteristic mechanism of tumor immune evasion. By comparing nonmalignant corresponding tissues, neoplastic malignant counterparts, and metastases, the loss of HLA-I is progressive[13-15]. Histological and experimental evidence [15]demonstrated a high frequency of defects in the expression of APM components in many tumor types of distinct origin (Table 1). The loss of APM could occur at any step of antigen processing thereby affecting HLA-I cell surface expression and immune cell recognition. Several studies have shown dysregulated expression of components of APM in several types of tumors in different stages of malignancy has

2

link with patients' overall survival, HLA-I cell surface expression and effector immune cells responses[4][13][16-19]. HLA-I consists of a heavy chain encoded by HLA-A, B, C genes, and a light chain named β2-microglobulin. There are numerous reports on the loss of HLA-A, B, C, and β2-m from 7% to 89% in different types of cancer: bladder cancer[14], breast cancer[20], lung cancer[21], melanoma[22], and so on. In addition to this, the loss of the key transport associated proteins, including LMP2, LMP7, TAP1, TAP2, and the chaperone tpn also can lead to impaired HLA class I antigen processing in many solid and hematopoietic malignancies: liver cancer[23], pancreatic cancer[24], oral tongue cancer[25], acute myeloid leukemia[26], and so on. Though the description of the defects of HLA-I molecules has increased during the past decade, the mechanism is still quite unclear. Several studies have revealed that the loss of HLA-I molecules is one strategies of tumor immune evasion[4][13][18][19], and the heart of immune escape is the inability of tumor cells to be recognized and killed by T cells. When T cells are abundant in tumor microenvironment (TME), immune checkpoint inhibitors[27] can activate CD8+ cytotoxic T lymphocyte (CTL) and HLA-I on the surface of tumor cells could be recognized by T cells. The understanding of this tumor immune escape strategy will improve T cell recognition of tumor cells and guide immunotherapies[16].

Table 1 The Defects of HLA-I APM Components in Cancers[4][28-30]

Components	Cancer Types	Frequency of Defects in %
HLA-I	Melanoma	15.3 - 37
	Lung Cancer	20 - 80
	Breast Cancer	18.1 - 86
	Colorectal Cancer	12.3 - 80
	Head and Neck Cancer	15 - 50
	Esophageal Cancer	46.9 - 89
$β_2$-m	Lung Cancer	75
	Head and Neck Cancer	20 - 49
	Bladder Carcinoma	40 - 44
	Laryngeal Carcinoma	41
	Colorectal Carcinoma	11 - 46.9
	Breast Cancer	29 - 79
	Melanoma	8 - 37.5
	Renal Cell Carcinoma	7
TAP1	Lung Cancer	38
	Head and Neck Cancer	5 - 28
	Breast Cancer	8 - 20

	Colorectal Carcinoma	14 - 81.5	
	Esophageal Cancer	29.8 - 44	
	Melanoma	33 - 38	
TAP2	Head and Neck Cancer	0 - 40	
	Breast Cancer	8	
	Colorectal Carcinoma	15 - 58.6	
	Esophageal Cancer	35	
	Melanoma	24	
tpn	Colorectal Carcinoma	28.9 - 80	
	Esophageal Cancer	32	
	Melanoma	33	
LMP2	Colorectal Carcinoma	0 - 67	
	Esophageal Cancer	45 - 47	
	Melanoma	31	
LMP7	Colorectal Carcinoma	20 - 90	
	Esophageal Cancer	40 - 48	
	Melanoma	38	
LMP10	gastric cancers	20 - 40	
	breast carcinoma	47.5	
ERAP	cervical carcinoma	9 - 15	

1.2 Posttranscriptional modifications of HLA-I antigen processing pathways

As already described above, dysregulation or loss of HLA-I components can impair the function or expression of the APM components, including HLA-I, LMP2, LMP7, TAP1, TAP2 and tpn, which can be due to many reasons, including genetic alterations, epigenetic regulation, transcriptional and even post-transcriptional regulation via the expression of immunoregulatory RBPs and immunomodulatory microRNAs (miRNAs)[31-36]. Recently, immune-related post-transcriptional control has gradually been recognized and numerous APM components have been identified in multiple tumors.

Over the past decade, microRNAs, as small RNAs of about 20 bp in length, have been shown to play an important role as post-transcriptional regulators of gene expression due to their classically resulting in a down-regulation in cancer and other diseases suggesting their potential therapeutic targets[37-41]. MiR-148a is associated with HLA-A, -B, -C in esophageal cancer and affects outcome[35]. In nasopharyngeal carcinoma (NPC), miR-9, which is associated with cell proliferation, epithelial-mesenchymal transition (EMT), invasion and

metastasis, was also found to up- or down-regulate the expression of HLA-B, -C[42]. In lung cancer, miR-19 overexpression was implicated in regulating the expression of immune and inflammatory response genes in cancer cells, including HLA-B, -E, -G, suggesting a novel role of miR-19 in linking inflammation and cancer[43]. Interestingly, O'Guigin and coauthor showed that the common ancestor of all extant HLA-C alleles was suppressed by miR-148a, which directly affects the expression of HLA-C in cell surface[44]. In addition, in comparison to HLA A, -B, -C, many miRNAs have been demonstrated to target and bind he 3' UTR of HLA-G, such as miR-148a and miR-152[45] and miR-365[46]. Our previous study showed that downregulate the expression of HLA-G and enhance NK cell-mediated cytotoxicity via in vitro CD107a activation assays[47]. We also demonstrated that miR-200a-5p, miR-26b-5p and miR-21-3p, which target TAP1, affect melanoma patients' outcome by improving the expression of HLA-I molecules suggesting them as biomarkers or therapeutic targets for HLA-I^{low} melanoma cells[48][49]. At the same time, in esophageal adenocarcinoma, increased levels of miR-125a have been found to reduce the level of TAP2 protein, which is accompanied by a poor outcome for patients[35].

In addition, a few unconventional positive regulatory roles for miRNAs have been described, where miRNAs can regulate both protein production and mRNA stability. [50-52]. For example, Eiring and co-authors reported that the negative regulation of CEBPA mRNA by hnRNP E2 was attenuated by miR-328 competing with CEBPA mRNA for binding to hnRNP E2[53]. Subsequently, miR-709 can control the biogenesis of other miRNAs, such as miR-15a and miR-16-1, by directly interacting with their nuclear primary transcripts, thereby regulating apoptosis through the miR-16/Bcl-2 pathway[54]. Furthermore, Vasudevan and coauthors showed that miRNAs bind to AU-rich elements (ARE), which promote a translational activation signal, thereby inducing upregulation of target mRNAs[55]. We have recently shown that the binding of miR-16 to the coding sequence (CDS) of classical and non-classical HLA molecules induces their up-regulation[56]. This unconventional upregulation of target genes is known as miRNA-mediated RNA or protein activation, an emerging field of miRNA biology[57]. However,

5

the mechanisms of miRNA-mediated activation are not uniform and their diversity, as well as how they affect tumor progression, remains to be fully elucidated.

RBPs are proteins binding to the RNA sequences thereby participating in the formation of ribonucleoprotein (RNP) complexes and regulating mRNA processes[58].[59-61]. Based on their deregulation in various tumor samples compared to normal tissues, there is evidence that RBPs also have a critical function in tumors[62]. Friedrich et al.[63] have summarized the members of muscle excess-3 (MEX3) and heterogeneous nuclear ribonucleoprotein R (HNRNPR) as target components of APM. They bind to the 3'UTR of HLA-A and HLA-G, respectively, and cause the target proteins to degrade. MEX3B and Syncrip have been identified to target HLA-A[36][64], while a possible RBP gene is in HLA-DR[65]. Furthermore, RBPs have been shown to modulate EMT progression and tumor metastasis. For example, PCBP1 regulate breast cancer invasiveness[66], hnRNP A1 affect hepatocellular carcinoma migration[67] and MEX3A promotes angiogenesis in colorectal cancer[68]. In addition, the heterogeneous nuclear ribonucleoprotein C1/C2 (hnRNP C) associated with pre-mRNAs in the nucleus and known to influence pre-mRNA processing, is an RNA-binding protein (RBP) with heterogeneous nuclear RNA (hnRNA)[69]. Recent studies have explored that hnRNP C is closely linked to the development of many tumors [70][71] and associated with tumor metastasis in different cancers[72][73] including melanoma[74][75].

1.3 Characteristics of silencer

Our knowledge of silencers is still limited[76][77], despite the fact that Brand and colleagues identified sequence-specific silencer functions that repress gene expression 30 years ago[78]. Silencers have come back into the spotlight with the rapid iteration of sequencing technologies in recent years[79-82]. Huang and co-authors directly used the H3K27me3-DNase I hypersensitive site (DHS) peak for the identification of silencers in the genome[83], demonstrating an overlap of these silencer regions with the H3K27me3 marker and chromatin

accessibility as detected by DHS sequencing. Different heterochromatin histone marks, such as H3K27me3 and H3K9me3 associated with inactivation of genes, were found to overlap with silencers, which was confirmed by Cai and co-authors suggesting a silencer function for the H3K27me3 regions[84]. Furthermore, Pang and Snyder systematically identified silencers using ReSE screens in cells, which showed that GC-rich areas are present in most silencing regions[85]. In addition to these features, silencers can occur throughout the genome[86] including the 3'untranslated region (3'UTR)[87]. Although some silencers have been identified, little remains known about how they interact with other molecules[88]. Until now, how silencers in the 3'UTR interact with other molecules, such as non-coding RNAs, has not been well studied.

1.4 Tumor microenvironment and tumor-associated macrophages

Besides tumor cells, the TME consists of immune, endothelial, and stromal cells, including their produced and released molecules. These non-cancerous cells gradually modulate the environment surrounding the tumor into an immunosuppressive microenvironment, making it difficult to treat tumors[89]. The function of non-tumor cells in the TME is currently being explored in this context. These include dendritic cells (DCs), which influence the tumor immune modulation and tolerance[90]; T cells, the tumor is "hot" when cytotoxic T lymphocyte are rich in TME, and can be activated to kill tumor cells, when the tumor is "cold" with less cytotoxic T cells, more T_{regs} and other suppressor cells, the immune suppressive microenvironment could be formed and the patients' prognosis is not better[91]; cancer-associated fibroblasts (CAF) 's that may secrete growth factors, extracellular matrix (ECM) proteins, and inflammatory ligands to affect cancer cell proliferation, migration, and immune evasion[92][93], and NK cells, which are often dysfunctional in the fight against cancer[94]. Tumor associated macrophages (TAM) is one of the most abundant immune cell types in the TME, a plastic and heterogeneous cell population that feeds and metabolizes tumor cells[95]. In addition, TAM can promote tumor growth, angiogenesis, migration, invasion, and metastasis in many types of solid tumors. They can also activate immune suppression and increase the resistance of cancer cells to

chemotherapy and radiotherapy[96]. But the exact way in which TAM affect all these different aspects of cancer and their regulation is still unclear.

TAM "crosstalk" with tumor cells, influencing their tumorigenicity. Small extracellular vesicles may upregulate PD-L1 in TAM to induce immune evasion in colorectal cancer (CRC)[97]. In addition, Tumor-derived UBR5 promotes the recruitment of TAM and their activation via cytokines to induce the metastasis of ovarian cancer[98]. Furthermore, CPEB3 is involved in cross-talk between CRC cells and TAM via the cytokine IL6/STAT3 axis to inhibit EMT[99]. Most of these cross-talks are mediated by cytokines, which are not only macrophage-derived but also tumor-derived. By altering macrophage phenotypes, these cytokines further promote tumor progression and immune evasion, such as the migration inhibitory factor (MIF)[100], the vascular endothelial growth factor (VEGF)[101], and the insulin growth factor-binding protein 2 (IGFBP2)[102]. However, due to the diversity and complexity of cytokines, their role in the tumor cell-macrophage crosstalk, especially with RBPs like hnRNP C, is not well understood.

2 Aim

Immunotherapy has recently revolutionized the treatment of tumor patients[103]. However, only a limited number of patients do respond to this therapy, which might be related to the diversity of immune escape mechanisms[10]. Loss of HLA-I APM is one of the strategies for tumor immune escape and post-transcriptional regulation on immune-related molecules has been gradually investigated[15]. However, the link of tpn, a key protein of the HLA-I APM, and post-transcriptional regulation has not yet been investigated. Therefore, the aim of this thesis was to investigate the role of the post-transcriptional regulation of tpn and its effect on HLA-I expression and the immune microenvironment in melanoma with the following questions:

1. Which molecules target and bind to tpn 3'UTR including miRNAs and RBPs?
2. Has the correlation between these molecules and tpn in melanoma cell lines and the clinical relevance?
3. How do these molecules regulate tpn and the HLA-I pathway components?
4. Do these molecules effect the phenotype of melanoma, like migration of melanoma and how?
5. Do these molecules also regulate immune microenvironment in melanoma?

3 Materials and Methods

3.1 Materials

3.1.1 Chemicals and plastic ware

A. Chemicals

Materials	Distributor
0.5% Trypsin-EDTA (10x)	Gibco® Invitrogen, Carlsbad, USA
100 bp DNA Ladder	Thermo Fisher Scientific, Waltham, USA
1 x plus Amplification Diluent	PerkinElmer, Waltham, USA
1k bp DNA Ladder	Thermo Fisher Scientific, Waltham, USA
2 x SYBR qPCR Master Mix	Nanjing Vazyme Biotech, Nanjing, China
2 x RNA Loading Dye	Thermo Fisher Scientific, Waltham, USA
4-20% gradient SDS-PAGE gels	SERVA, Heidelberg, Germany
Ampuwa® water	Fresenius Kabi GmbH, Bad Homburg, Germany
Actinomycin D	Merck, Darmstadt, Germany
Ampicillin	CARL ROTH GmbH & Co. KG, Karlsruhe, Germany
Acrylamide	Sigma-Aldrich Chemie GmbH, Taufkirchen bei Munchen, Germany
Antigen Retrieval Reagent, pH6（10x）	AKOYA Biosciences, Marlborough, USA
Agarose	BioLine GmbH, Luckenwalde, Germany
Antigen Retrieval Reagent, pH9（10x）	AKOYA Biosciences, Marlborough, USA
Amylose resin beads	New England Biolabs, MA, USA
Ammonium persulfate (APS)	AppliChem GmbH, Darmstadt, Germany
Bolt™ 4-12% Bis-Tris Plus Gel	Thermo Fisher Scientific, Waltham, USA
β-mercaptoethanol (C2H6OS)	AppliChem GmbH, Darmstadt, Germany
Benzonase	Novagen, San Diego, CA, USA
BamHI	New England Biolabs, MA, USA
BCA Protein Assay Reagent	Thermo Fisher Scientific, Waltham, USA
Bovine Serum Albumin (BSA)	Sigma-Aldrich Chemie GmbH, Taufkirchen bei Munchen, Germany
CCL2 Elisa Kit	Biolegend, San Diego, USA
CD14 microbeads	Miltenyi, Bergisch Gladbach, Germany
Chloroform (CHCl3)	Sigma-Aldrich Chemie GmbH, Taufkirchen bei Munchen, Germany
CellTiter-Glo® 2.0 Reagent	Promega, Madison, WI, USA
CXCL10 (IP10) Elisa Kit	Biolegend, San Diego, USA
CXCL8Elisa Kit	Biolegend, San Diego, USA
DNase I	Promega, Madison, WI, USA
DpnI	New England Biolabs, MA, USA
Dual-Luciferase® Reporter Assay System	Promega, Madison, WI, USA
Dimethyl sulfoxide (DMSO)	CARL ROTH GmbH & Co. KG, Karlsruhe, Germany

Dulbecco's Modified Eagle Medium (DMEM)	Gibco® Invitrogen, Carlsbad, USA
Dulbecco's Phosphate Buffered Saline (PBS)	Sigma-Aldrich Chemie GmbH, Taufkirchen bei Munchen, Germany
EHUEGFP	Sigma-Aldrich Chemie GmbH, Taufkirchen bei Munchen, Germany
Ethanol absolute for analysis	Sigma-Aldrich Chemie GmbH, Taufkirchen bei Munchen, Germany
Ethidium bromide (C21H20BrN3)	AppliChem GmbH, Darmstadt, Germany
Ethylene diamine tetra-acetic acid (EDTA)	Sigma-Aldrich Chemie GmbH, Taufkirchen bei Munchen, Germany
Fetal Calf Serum (FCS)	Anprotec, Bruckberg, Germany
GeneRuler DNA Ladder	Thermo Fisher Scientific, Waltham, USA
Glycogen	Thermo Fisher Scientific, Waltham, USA
HEPES	Gibco® Invitrogen, Carlsbad, USA
HindIII	Thermo Fisher Scientific, Waltham, USA
Hydrochloric acid (HCl)	CARL ROTH GmbH & Co. KG, Karlsruhe, Germany
Human xl cytokine array kit	R&D Systems, Inc., Minneapolis, MN, USA
Horse serum	CC pro, Oberdorla, Germany
HaltTM Protease & Phosphatase inhibitor Cocktail (100x)	Thermo Fisher Scientific, Waltham, USA
iBlotTM 2 NC Regular Stacks	Thermo Fisher Scientific, Waltham, USA
iBlot 2 Dry Blotting System	Thermo Fisher Scientific, Waltham, USA
Isopropanol (C3H8O)	Sigma-Aldrich Chemie GmbH, Taufkirchen bei Munchen, Germany
KpnI	Thermo Fisher Scientific, Waltham, USA
LB-agar	CARL ROTH GmbH & Co. KG, Karlsruhe, Germany
L-glutamine	Lonza, Basel, Switzerland
Lipofectamine RNAiMAX	Thermo Fisher Scientific, Waltham, USA
Lipofectamine 2000	Thermo Fisher Scientific, Waltham, USA
LB-medium	CARL ROTH GmbH & Co. KG, Karlsruhe, Germany
Methanol	CARL ROTH GmbH & Co. KG, Karlsruhe, Germany
Geltrex™ LDEV-free basement membrane matrix	Thermo Fisher Scientific, Waltham, USA
MES SDS Running Buffer (20x)	Thermo Fisher Scientific, Waltham, USA
M-CSF	Biolegend, San Diego, USA
miR-155-5p mimics	Sigma-Aldrich Chemie GmbH, Taufkirchen bei Munchen, Germany
Minimum Essential Medium Non-Essential Amino Acids (MEM NEAA,100x)	Gibco® Invitrogen, Carlsbad, USA
Magnesium chloride (MgCl2)	CARL ROTH GmbH & Co. KG, Karlsruhe, Germany
MIF Elisa Kit	Biolegend, San Diego, USA
MEGAclear™ transcript purification kit	Thermo Fisher Scientific, Waltham, USA
Minimum Essential Medium (MEM)	Gibco® Invitrogen, Carlsbad, USA

Natriumchlorid (NaCl) sodium chloride	CARL ROTH GmbH & Co. KG, Karlsruhe, Germany
negative control mimics (NC)	Sigma-Aldrich Chemie GmbH, Taufkirchen bei Munchen, Germany
NheI	Thermo Fisher Scientific, Waltham, USA
Optimem	Gibco® Invitrogen, Carlsbad, USA
Opal Fluorophore Reagent Packs	AKOYA Biosciences, Marlborough, USA
Opal Antibody Diluent/Block	AKOYA Biosciences, Marlborough, USA
Thermo Fisher Scientific, Waltham, USA	Thermo Fisher Scientific, Waltham, USA
T7 RiboMAX™ kit	Promega, Madison, WI, USA
Penicillin-Streptomycin Mix	Sigma-Aldrich Chemie GmbH, Taufkirchen bei Munchen, Germany
Pierce Classic Magnetic IP/Co-IP kit	Thermo Fisher Scientific, Waltham, USA
Phosphatase inhibitor cocktail	Sigma-Aldrich Chemie GmbH, Taufkirchen bei Munchen, Germany
Polysorbate 20 (Tween 20)	AppliChem GmbH, Darmstadt, Germany
Parafilm	IDL GmbH & Co. KG, Nidderau, Germany
Pierce protease inhibitor	Thermo Fisher Scientific, Waltham, USA
Phusion® High-Fidelity DNA-Polymerase	New England Biolabs, MA, USA
PspOMI	New England Biolabs, MA, USA
Puromycin	Sigma-Aldrich Chemie GmbH, Taufkirchen bei Munchen, Germany
Q5® High-Fidelity DNA-Polymerase	New England Biolabs, MA, USA
Q5® site-directed mutagenesis kit	New England Biolabs, MA, USA
RevertAid First Strand cDNA synthesis kit	Thermo Fisher Scientific, Waltham, USA
RNase A	MACHEREY-NAGEL GmbH & Co. KG, Düren, Germany
RPMI 1640 media	Gibco® Invitrogen, Carlsbad, USA
SignalFire ECL Reagent	Cell Signaling, Danvers, USA
siHNRNPC	Sigma-Aldrich Chemie GmbH, Taufkirchen bei Munchen, Germany
Skim milk powder	BD Biosciences, Heidelberg, Germany
Sodium dodecyl sulfate (SDS)	AppliChem GmbH, Darmstadt, Germany
Sodium phosphate dibasic dihydrate (Na2HPO4 * 2H2O)	CARL ROTH GmbH & Co. KG, Karlsruhe, Germany
Spectral DAPI	AKOYA Biosciences, Marlborough, USA
Trizol	Thermo Fisher Scientific, Waltham, USA
T4 DNA-Ligase	Promega, Madison, WI, USA
Tris(hydroxymethyl)aminomethane (TRIS, C4H11NO3)	AppliChem GmbH, Darmstadt, Germany
Trypan bleu (C34H28N6Na4O14S4)	Gibco® Invitrogen, Carlsbad, USA
Tween® 20	AppliChem GmbH, Darmstadt, Germany
Trypsin/EDTA (10x)	Gibco® Invitrogen, Carlsbad, USA
VEGF Mini TMB ELISA	PeproTech Germany, Hamburg, Germany
VECTASHIELD® HardSet™ Antifade Mounting Medium for fluorescence	VECTOR Laboratories, Newark, USA
Xylol /ROTICLEAR	CARL ROTH GmbH & Co. KG, Karlsruhe, Germany
yeast tRNA	Thermo Fisher Scientific, Waltham, USA

B. Consumables and plastic ware

Name	Company
0.2 mL Thin Wall PCR Tubes	Greiner Bio-One GmbH, Frickenhausen, Germany
1.5 mL tubes	Greiner Bio-One GmbH, Frickenhausen, Germany
12 well plate (flat bottom)	SARSTEDT AG & Co. KG, Nümbrecht, Germany
15 mL tubes	SARSTEDT AG & Co. KG, Nümbrecht, Germany
24 well plate (flat bottom)	SARSTEDT AG & Co. KG, Nümbrecht, Germany
24-well transwell plate	Corning, USA
25 mL serological pipettes	SARSTEDT AG & Co. KG, Nümbrecht, Germany
25, 75 and 175 cm2 cell culture flasks	SARSTEDT AG & Co. KG, Nümbrecht, Germany
5 mL serological pipettes	SARSTEDT AG & Co. KG, Nümbrecht, Germany
50 mL tubes	SARSTEDT AG & Co. KG, Nümbrecht, Germany
6 well plate (flat bottom)	SARSTEDT AG & Co. KG, Nümbrecht, Germany
70 µm pre-separation filters	Miltenyi, Bergisch Gladbach, Germany
96 well plate (flat bottom)	SARSTEDT AG & Co. KG, Nümbrecht, Germany
Coverslips (24 x 32 mm)	CARL ROTH GmbH & Co. KG, Karlsruhe, Germany
Counting chambers	Paul Marienfeld GmbH & Co. KG, Marienfeld, Germany
FACS tubes	SARSTEDT AG & Co. KG, Nümbrecht, Germany
LS columns	Miltenyi, Bergisch Gladbach, Germany
Multiplate PCR Plates,96-well	Bio-Rad, Hercules, USA
NucleoSpin RNA isolation kit	Machery-Nagel, Düren, Germany
Pipette tips (0-10 µL, 10-100 µL, 20-200 µL, 100-1000 µL)	SARSTEDT AG & Co. KG, Nümbrecht, Germany
Safe seal micro tube 1.5 mL, PP	SARSTEDT AG & Co. KG, Nümbrecht, Germany
Pipettes	Eppendorf AG, Hamburg, Germany
Safe seal micro tube 2.0 mL, PP	SARSTEDT AG & Co. KG, Nümbrecht, Germany
5 mL, 10 mL, 25 mL, 50 mL sterile pipets	Greiner Bio-One GmbH, Kremsmünster, Austria

C. Antibodies used for immunocellochemistry

Name	Dilution	Company
Primary antibodies		
Anti-TPN	1:500	Abcam, Cambridge, UK
Anti-H3K27me3	1:500	Diagenode, Seraing, Belgium
Secondary antibody		
Opal Polymer HRP mouse + rabbit, AKOYA, Biosciences, Marlborough, USA		
Fluorochrome		
Opal 520 Reagent and Opal 570 Reagent, AKOYA, Biosciences, Marlborough, USA		

D. Antibodies used for Western Blot analysis

Antibody	Dilution	Source	Company

Primary antibodies			
Anti-GAPDH	1:2500	Rabbit	Cell Signaling, Danvers, Massachusetts, USA
Anti-TPN	1:1000	Rabbit	Abcam, Cambridge, UK
Anti-HNRNPC	1:1000	Rabbit	Thermo Fisher Scientific, Waltham, USA
Anti-β-actin	1:1000	mouse	Abcam, Cambridge, UK
Anti-vimentin	1:1000	Rabbit	Abcam, Cambridge, UK
Secondary antibodies			
Anti-mouse IgG, HRP-linked antibody	1:1000	Horse	Cell Signaling, Danvers, USA
Anti-rabbit IgG, HRP-linked antibody	1:1000	Goat	Cell Signaling, Danvers, USA

E. Antibodies used for flow cytometry

Name	Fluorophore	Company
Anti-CD86	BV605	BD Biosciences, Heidelberg, Germany
Anti-CD68	PE-Cy™7	BD Biosciences, Heidelberg, Germany
Anti-CD163	PE	BD Biosciences, Heidelberg, Germany
Anti-CD206	BV421	BD Biosciences, Heidelberg, Germany
Anti-HLA-DR	APC	Miltenyi, Bergisch Gladbach, Germany
Anti- HLA-ABC	FITC	Beckman, Brea, California, USA
Anti- HLA-BC	APC	Thermo Fisher Scientific, Waltham, USA
Anti-CD107a	APC	Biolegend, San Diego, USA
Anti-CD3	PE-Cy™7	Miltenyi, Bergisch Gladbach, Germany
Anti-CD16	Vioblue	Miltenyi, Bergisch Gladbach, Germany
Anti-CD56	PE	Miltenyi, Bergisch Gladbach, Germany

F. Antibodies used for neutralization assay

Name	Company
anti-CXCL10	R&D Systems, Inc., Minneapolis, MN, USA
anti-IL8	R&D Systems, Inc., Minneapolis, MN, USA
anti-CXCR1	R&D Systems, Inc., Minneapolis, MN, USA
anti-CXCR2	R&D Systems, Inc., Minneapolis, MN, USA
anti-CXCR3	R&D Systems, Inc., Minneapolis, MN, USA

3.1.2 Equipment and Software

A. Equipment

Name	Company
96-well labcycler gradient	SensoQuest GmbH, Göttingen, Germany
Allegra X-15R Centrafuge	Beckman Coulter, Krefeld, USA
BD LSRFortessa™	BD Biosciences, Heidelberg, Germany
Biometra® Power Pack P25 T	Biometra GmbH, Göttingen, Germany
BD FACSCanto™	BD Biosciences, Heidelberg, Germany
Centrifuge 5414C	Eppendorf AG, Hamburg, Germany
CFX Connect™ Real-time system	Bio-Rad, Hercules, USA
Cold centrifuge 5425R	Eppendorf AG, Hamburg, Germany
CO2 Incubator	BINDER GmbH, Tuttlingen, Germany
Heraeus Incubator	Heraeus Company, Bitterfeld-Wolfen, Germany
Evos FLoid™ Imaging System	Thermo Fisher Scientific, Waltham, USA
Hoefer EPS 2A200 Electrophoresis Power Supply	Marshall Scientific, Hampton, NH, USA
iBlot™ 2 Gel Transfer Device	Thermo Fisher Scientific, Waltham, USA
iBright750 imaging system	Thermo Fisher Scientific, Waltham, USA
Infinite® 200Pro microplate reader	Tecan Group Ltd., Mannedorf, Switzerland
LAS 3000 CCD camera system	FujiFilm, Tokyo, Japan
MMM Medcenter™ Venticell™ Drying Ovens	MMM Medcenter Company, Planegg, Germany
Microcentrifuge Z233 MK-2	Hermle Labortechnik GmbH, Wehingen, Germany
Mini Gel Tank	Thermo Fisher Scientific, Waltham, USA
Manitowoc ice maker	Manitowoc Company, Manitowoc, USA
PowerPac™ Basic Power Supply	Bio-Rad, Hercules, USA
Rotor-Gene	Qiagen, Venlo, Netherlands
Navios flow cytometer	Beckman Coulter, Krefeld, Germany
Thermomixer F1.5	Eppendorf AG, Hamburg, Germany
Trans-Blot® Tank	BIO-RAD Laboratories, Inc., California, USA
SimpliAmp™ Thermal Cycler	Thermo Fisher Scientific, Waltham, USA
Vectra Polaris Automated Quantitative Pathology Imaging System	PerkinElmer, Waltham, USA
VILBER Gel Documentation system	VILBER Company, Eberhardzell, Germany
Vectra Polaris	PerkinElmer, Waltham, USA
ZipTips®	Sigma-Aldrich Chemie GmbH, Taufkirchen bei Munchen, Germany

B. Software

Software	Company
Adobe Photoshop CC 2015.5	Adobe, San Jose, USA
Acrobat Reader DC	Adobe, San Jose, USA
BD CellQuest Pro Software	BD Biosciences, Heidelberg, Germany
Bio-Rad CFX	Bio-Rad, Hercules, USA
Endnote 9	Thomson Reuters, Canada
ENCORI	http://starbase.sysu.edu.cn/rbpClipRNA.php
GraphPad Prism 8.0.0	GraphPad Software, San Diego, USA
Image Reader LAS3000 software	Fuji GmbH, Düsseldorf, Germany
FlowJo_V10.8.1	DONGLE
FACSDiva software package	BD Biosciences, Heidelberg, Germany
GSEA software	Broad Institute, SanDigo, USA
ImageJ 1.53k	National Institute of Health, Bethesda, USA
inForm Tissue Finder	AKOYA Biosciences, Marlborough, USA
Kaluza® Flow Analysis Software	BECKMAN, Brea, California, USA
miRDB	http://www.mirdb.org/
Microsoft Excel 2010	Microsoft, Washington, USA
Microsoft Word 2010	Microsoft, Washington, USA
Microsoft PowerPoint 2010	Microsoft, Washington, USA
miRBase	http://mirbase.org/
NEBaseChanger software	New England Biolabs, MA, USA
Rstudio Desktop	Rstudio company, Boston, USA
R2 Genomics Analysis and Visualization Platform	https://hgserver1.amc.nl/cgi-bin/r2/main.cgi?open_page=login
RNA hybrid	BiBiServ
Xenabrowser	UCSC Xena (xenabrowser.net)

C. Oligonucleotides

Name	Applikation	Sequence
tpn 3'UTR-1 fw	cloning	AAAGGATCCCCACCTGCAAGGATTCAAAG
tpn 3'UTR-1 rev	cloning	AAACTCGAGCGGATCACCAGGTTAGGAGA
tpin 3'UTR-2 fw	cloning	AAAGAATTCCTCGGACTACAGGCGTCCTC
tpn 3'UTR-2 rev	cloning	AAAGGATCCTCTGGCCGACCGTCCTGACT
T7 tpn 3'UTR-1 fw	PCR	GCGGAGATCTAATACGACTCACTATAGGCCACCTGCAAGGATTC
T7 tpn 3'UTR-2 fw	PCR	GCGGAGATCTAATACGACTCACTATAGGCCACCTGCAAGGATTCAAAG
tpn fw	qPCR	TGGGTAAGGGACATCTGCTC
tpn rev	qPCR	ACCTGTCCTTGCAGGTATGG

ALAS1 fw	qPCR	TGAGACAGATGCTAATGGATGC
ALAS1 rev	qPCR	CACCGTAGGGTAATTGATTGCT
ACTB fw	qPCR	TCCTGTGGCATCCACGAAACT
ACTB rev	qPCR	GAAGCATTTGCGGTGGACGAT
GAPDH fw	qPCR	GAGAAGGCTGGGGCTCATTTG
GAPDH rev	qPCR	GGACTGTGGTCATGAGTCCTTC
general reverse miR-primer	qPCR	GTGCAGGGTCCGAGGT
miR-155-5p fw	qPCR	CACGCATTAATGCTAATCGTGAT
miR-155-5p SLRT	qPCR	TCGTATCCAGTGCAGGGTCCGAGGTATTCGCACTGGATACGACACCCCT
U6 snRNA fw	qPCR	CGGCAGCACATATACTAAAATTGGA
U6 snRNA rev	qPCR	AATATGGAACGCTTCACGAATTTGC
sil 1 del fw	cloning	AGAGACGGGGTTTCACCG
sil 1 del rev	cloning	CAACAGAGCGAGACTCTGTC
sil 4 del fw	cloning	GAACCCGTACTCTAGGGC
sil 4 del rev	cloning	CTCACGCCTGTAATCCCA
del fw	cloning	GGGACCTAAGGCCCACTG
del rev	cloning	GACAGGCATTTAACGACGAC
ARE del fw	cloning	GTGATCGTGTGAGTCGTC
ARE del rev	cloning	CAACTGTGGTGAACCGCA
AU del fw	cloning	GGGCTCCTCGAGGACAGG
AU del rev	cloning	CCGCGGGGAGACAGGCAT
GC del fw	cloning	ATCATGGGCTCCTCGAGG
GC del rev	cloning	AGACAGGCATTTAACGACG
GA del fw	cloning	CTGGCCTGTCTGTCCACTG
GA del rev	cloning	GAGGAGCCCATGATCCGC
Sg R3 fw	cloning	CACCGCGCCGCGCGTCCCTCTTGTG
Sg R3 rev	cloning	AAACCACAAGAGGGACGCGCGGCGC
Sg R9 fw	cloning	CACCGCTGTAACCCCGCGCCGGCAT
Sg R9 rev	cloning	AAACATGCCGGCGCGGGGTTACAGC
tapasin KO fw	PCR	TTTGTGTTTTTAGTAGAGACGGGG
tapasin KO rev	PCR	TTTGGAAGCACTGGAATACAGCTT

sil 3 del fw	cloning	ACCACAGTTGTATTTAAGTGATCGTG
sil 3 del rev	cloning	GGACTGGGACCTGGAGGT
TAP1 fw	PCR	GGAATCTCTGGCAAAGTCCA
TAP1 rev	PCR	TGGGTGAACTGCATCTGGTA
TAP2 fw	PCR	CCAAGACGTCTCCTTTGCAT
TAP2 rev	PCR	TTCATCCAGCAGCACCTGTC
HLA-ABC fw	PCR	GCCTACCACGGCAAGGATTAC
HLA-ABC rev	PCR	GGTGGCCTCATGGTCAGAGA
HLA-B fw	PCR	CTACCCTGCGGAGATCA
HLA-B rev	PCR	ACAGCCAGGCCAGCAACA
HLA-C fw	PCR	TGGTGGTGCCTTCTGGACAA
HLA-C rev	PCR	CCAAGGACAGCTAGGACAACC
HNRNPC fw	PCR	TCGAAACGTCAGCGTGTATC
HNRNPC rev	PCR	TCCAGGTTTTCCAGGAGAGA
Vimentin fw	PCR	GAGTCCACTGAGTACCGGAG
Vimentin rev	PCR	ACGAGCCATTTCCTCCTTCA
NF-kB fw	PCR	ACCTCGACGCATTGCTGTG
NF-kB rev	PCR	CTGGCTGATCTGCCCAGAAG
MMP2 fw	PCR	ATGGCTACCGCTGGTGCGG
MMP2 rev	PCR	GGTGCAGCTCTCATATTTGTTGCG
SNAIL2 fw	PCR	GACCCTGGTTGGTTGCTTCAAGGA
SNAIL2 rev	PCR	TGTTGCAGTGAGGGCAAGAA

3.2 Methods

3.2.1   Cell lines and cell culture

The human metastatic melanoma cell lines Buf1402 and Buf1379 kindly provided by Soldano

Ferrone (Department of Surgery, Massachusetts General Hospital, Harvard Medical Scholl,

Boston, MA, USA). The human metastatic melanoma cell lines FM81 (ECACC 13012428),

FM3 (ECACC 13012407), and MZ-Mel2 (CVCL-1435) were acquired from the European Searchable Tumor Cell Line and Data Bank (ESTDAB project; https://www.ebi.ac.uk/ipd/estdab/). The human embryonic kidney cell line HEK293T and the NK cell-sensitive erythroleukemic cell line K-562 (ATCC®CCL-243™) were obtained from the American Tissue Culture Collection (ATCC, Manassas, USA). Melanoma cell lines were grown in Roswell Park Memorial Institute 1640 medium (RPMI1640, Invitrogen, Carlsbad, CA, USA) according to the guidelines. HEK293T and K-562 cells were grown in Dulbecco's modified Eagles medium (DMEM, Invitrogen) and all cell lines were tested for mycoplasma contamination. Cell culture was performed at 37°C in 5%CO2 humidified air in a medium supplemented with 10% foetal calf serum (FCS) (PAN, Aidenbach, Germany), 1% L-glutamine (Lonza, Basel, Switzerland) and 1% pen/strep (Sigma-Aldrich, Missouri, USA).

3.2.2 MiRNA enrichment analysis

MiRNA trapping by RNA *in vitro* affinity purification (miTRAP) was used to identify specific miRNAs that target the 3'UTR of tpn, as described previously[104]. Briefly, the 3'UTR of tpn (accession number: NM_001410875.1) was cloned upstream of two MS2 "stem-loop" structures in recombinant plasmid pcDNA™ 3.1(+) (Invitrogen). The fusion protein was then in vitro transcribed (IVT) overnight using the T7 RiboMAX™ kit (Promega, Madison, Washington, USA) and purified using the MEGAclear™ transcript purification kit (Invitrogen). Amylose resin beads (NEB, Ipswich, MA, USA) were incubated with the fusion protein, including the MBP domains and the MS2 loop, to which the IVT RNAs had been immobilized. To allow specific binding of miRNAs to the 3'UTR of tpn, bait RNAs and cell lysate were added after blocking with yeast tRNA (Invitrogen). The eluted miRNA was purified by chloroform-RNA isolation and sent to Novogene (Hong Kong, China) for small RNA sequencing.

3.2.3 Identification of RNA-binding proteins via RNA affinity purification and mass spectrometry

The RNA affinity purification method for the enrichment of RBPs was performed as previously

described[105] to study the RBPs that target the 3'UTRs of tpn, using the same plasmid as for miTRAP. MZ-Mel2 cell pellets with a packed cell volume (pcv) of at least 700 µL were used to prepare cytoplasmic extracts, which were then incubated with the IVT 3'UTR of tpn. The co-purified proteins were separated on 4-20% gradient SDS-PAGE gels (4-20% mini-PROTEAN® TGX™ pre-cast protein gel, SERVA, Heidelberg, Germany) and analyzed by mass spectrometry.

3.2.4 Transfection of microRNA and siRNA

To investigate the effect of miR-155-5p on tpn expression, 2.2×10^5 melanoma cells/well were seeded into 6-well plates including FM81, MZ-Mel2, FM3. After 16 hours, cells were transfected with a final 30 nM miR-155-5p mimics (UUAAUGCUAAUCGUGAUAGGGGU, Sigma-Aldrich, St. Louis, MO, USA) or negative control (NC) 1 (GGUUCGUACGUACACUGUUCA, HMC0002, Sigma-Aldrich) using 9µl Lipofectamine RNAiMAX (Invitrogen). Cells were harvested after 48 hours for further analysis. In addition, Melanoma cells including Buf1379 and Buf1402 were seeded at 2.4×105 cells/well in 6-well plates, 1×105 cells/well in 24-well plates or 1.8×105 cells/well in 12-well plates to study the function of hnRNP C. After 16-20 hours, melanoma cells were transfected with siRNA (siHNRNPC, 2ng/ml, EHU133931, Sigma-Aldrich, St. Louis, MO, USA) or negative control (NC, 2ng/ml, EHUEGFP, Sigma-Aldrich) using 9 µl Lipofectamine RNAiMAX (Invitrogen) according to the manufacturer's instructions. For subsequent RNA and protein analyses, cells were harvested after 48 hrs.

3.2.5 Isolation of macrophages and co-culture with melanoma cells

Macrophages were isolated and differentiated from peripheral blood mononuclear cells (PBMC). Briefly, cells were isolated directly from PBMC according to the manufacturer's instructions using CD14 microbeads (Miltenyi Biotec, Bergisch Gladbach, Germany). M-CSF (100ng/ml, 574806, BioLegend, San Diego, California, USA) was added every 2 days to differentiate mononuclear cells

into macrophages (M0) for further study after 6 days. TAM was differentiated after 48 hrs by co-culturing with parental melanoma cells in conditioned medium. Additionally, melanoma cells were co-cultured with TAM and M0 for 24 hrs using 12-well trans-well systems (0.4 µm pore size; Corning, USA). RNA and protein were then isolated from melanoma cells for q-PCR, Western blot, while M0 macrophages and TAM were collected for flow cytometry after incubation with siHNRNPC, siNC and parental cell conditioned medium supernatants.

For the antibody (ab) neutralization assay, monoclonal antibody (mAb) anti-CXCL10 (MAB266), anti-IL8 (MAB208), anti-CXCR1 (MAB330), anti-CXCR2 (MAB331) and anti-CXCR3 (MAB160) (2 µg/mL, R&D Systems, Inc., Minneapolis, MN, USA) were added to TAM and M0, respectively, and proteins were analyzed by Western blot as described below.

3.2.6 RNA preparation and real-time quantitative reverse-transcription PCR (RT-qPCR)

Total RNA was isolated using TRIzol reagent (Invitrogen) to determine the effect of miR-155-5p and hnRNP C and co-culture with TAM on mRNA levels, according to the manufacturer's instructions. Total RNA was used for cDNA synthesis (Thermo Scientific, Rockford, IL, USA) with the specific stem-loop primers and general primers as described in Chen et al.[106]. RT-qPCR was performed using SYBR qPCR Master Mix (Vazyme, Nanjing, PRC), and data were normalized to housekeeping genes including glyceraldehyde-3-phosphate dehydrogenase (GAPDH), delta-aminolevulinate synthase (ALSA1) and β-actin for mRNA levels, while RNU6A was used as a control for miRNA data.

3.2.7 Protein extraction and Western blot analysis

Total protein was isolated from transfected cell pellets. Using protease inhibitor/phosphatase inhibitor lysis buffer (Thermo Scientific), followed by quantification using Pierce BCA protein assay kit (Thermo Scientific). 25µg protein per sample was separated on Bolt™ 4-12% mini protein gels (Invitrogen) and transferred to Blot 2 transfer stacks (Invitrogen). These were incubated overnight at 4°C with primary abs: anti-TPN (1:1000, ab13518, Abcam, Cambridge,

UK), anti-GAPDH (1:2000, 14C10, CST, Danvers, Massachusetts, USA), anti-β-actin (1:2500, ab6276, Abcam, Cambridge, UK), anti-HNRNPC (1:1000, PA5-24221 Thermo Scientific) and anti-vimentin (1:1000, ab92547, Abcam) and anti-HLA-I HC (1:750; HC-10), courtesy of Professor Soldano Ferrone (Harvard University, Boston, USA). Horseradish peroxidase-conjugated goat anti-mouse/rabbit Ab (CST) was used as secondary antibody. A LAS-3000 imaging system (Fujifilm, Tokyo, Japan) was used to image the chemiluminescent blots. Densitometric analysis of signal intensity was performed with ImageJ[107].

3.2.8 Wound healing assay and transwell assay for migration and invasion

To analyses the migration of melanoma cells after transfection with siHNRNPC or co-culture with TAM and M0, a wound healing assay was used. Briefly, cell monolayers grown at around 90% confluence were scratched with a plastic pipette tip and images were taken immediately after scratching and after incubation at 37°C, 2 hours, 4 hrs, 24 hrs, or 48 hrs. For invasion, 5 × 10^4 cells/well were seeded after transfection or co-culture in 100 μL culture medium with 1% FBS into the upper chamber of a 24-well transwell plate (8 μm pore size; Corning, USA) and Matrigel (Geltrex™ LDEV-free basement membrane matrix, A1413201, Thermo Fisher Scientific Inc., USA). 500 μL culture medium with 10% FCS was added to the lower chamber. After 24 hrs incubation, 110 μl of CellTiter-Glo® 2.0 Reagent (G924A, Promega, Madison, USA) was added to the bottom of the upper chamber for 10 min, followed by detection of cells using a spectrophotometer (TECAN, Männedorf, Switzerland). The transwell migration assay was performed in the same way as the invasion assay but without Matrigel.

3.2.9 Flow cytometry

To investigate the HLA-I surface expression of melanoma cells and macrophage markers for TAM and M0, flow cytometric analyses were performed. Briefly, $2x10^5$ transfected melanoma cells and TAM were washed twice with phosphate buffered saline (PBS), incubated with Ab against HLA-ABC (Beckman, Brea, California, USA) or HLA-BC (Invitrogen) for melanoma

cells or Abs against CD86 (562999, BD Biosciences, Heidelberg, Germany), CD68 (565595, BD Biosciences), CD163 (556018, BD Biosciences), CD206 (564062, BD Biosciences), HLA-DR (130-123-843, Miltenyi Biotec) for macrophages and TAM, followed by incubation for 30 min at 4°C, washing and measurement on an LSR-Fortessa (BD Biosciences, Heidelberg, Germany) or a Navios 3L10C (Beckman Coulter GmbH, Krefeld, Germany) flow cytometer. Data were analyzed and reported as mean specific fluorescence intensity (MFI) using FACS Diva (BD Biosciences) and Kaluza (Beckmann) analysis software.

3.2.10 Luciferase reporter assay

To verify the direct interaction between miR-155-5p and the 3'UTR of tpn, the dual luciferase reporter assay was performed. Briefly, the wide type (wt) tpn3'UTR was cloned into the pmiR-Glo dual luciferase miRNA target expression vector (vector) (Promega). Using the Q5® site-directed mutagenesis kit (NEB) and primers designed with the NEBaseChanger software (https://nebasechanger.neb.com/, NEB), the predicted miR-155-5p (del) binding site and other elements (AREdel, AUdel, GCdel, GAdel, sil1del, sil3del, sil4del) were deleted in the luciferase reporter gene construct. Lipofectamine 2000 (Invitrogen) was used to transfect HEK293T cells with 5 ng of the different pmiR-Glo vectors and (i) 30 nM miR-155-5p mimic, (ii) a negative control or (iii) different concentrations of siRNA specific for different RBP. After 48 hours, cells were lysed in lysis buffer (Promega). Luciferase activity was assessed using the Dual-Luciferase® Reporter Assay System (Promega) according to the manufacturer's instructions. Relative light units (RLU) were determined by normalizing firefly luciferase (FFL) activity to Renilla luciferase (RL) activity expressed in the pmiR-Glo vector as an internal control.

3.2.11 CRISPR/Cas9-guided silencer knock-out and cell sorting

CRISPR/Cas9 experiments were performed to verify the function of the miR-155-5p binding site in the melanoma cell lines. Guide RNAs targeting the miR-155-5p binding site in the 3'UTR of tpn were designed using the web tool (https://chopchop.cbu.uib.no/). The guide RNAs were

separately cloned into the pSpCas9 (BB)-2A-GFP (PX458) plasmid (Addgene, Watertown, USA). The cloned plasmids were co-transfected into melanoma cells. Successful GFP+ cells were selected by cell sorting (BD FACSAriaTM Fusion, Heidelberg, Germany). Individual clones were amplified. Correct recombination was verified by Sanger sequencing (Microsynth Seqlab GmbH, Göttingen, Germany) and agarose gel electrophoresis. TPN expression was assessed by RT-qPCR after normalization with housekeeping genes such as GAPDH, ALAS1 and β-actin.

3.2.12 Actinomycin D assay

To determine mRNA decay after transfection with miR-155-5p mimics, the actinomycin D assay was used. FM81 cells were transfected with miR-155-5p mimics or NC mimics control as described and immediately treated with actinomycin D (10 µg/mL, Merck, Darmstadt, Germany). The RNA was isolated at different time points and the levels of tpn mRNA were determined by qRT-PCR as described in the previous section.

3.2.13 CD107a degranulation assay

The susceptibility of tumor cells to NK cells was investigated using the CD107a degranulation assay. Briefly, healthy donor PBMC were obtained from the Martin Luther University blood bank and used as effector cells. MZ-Mel2 cells transfected with miR-155-5p or negative control were co-incubated with the effector cells in a 1:1 ratio at 37°C. After 1hour, anti-CD107a Ab (Biolegend, San Diego, California, USA) was added, and after a total of 4 hours, the culture was stained with anti-CD3, anti-CD16 (both from Biolegend) and anti-CD56 Ab (Thermo Scientific) to detect NK cells within the PBMCs. To assess the functionality of the different PBMC preparations, K562 cells were used as a positive control.

3.2.14 Immune cytofluorescence

To investigate the correlation between tpn and H3K27me3 expression,

immunocytofluorescence was performed. Briefly, cells were seeded on chamber slides (Lab-Tek, Thermo Scientific) 48 hours after transfection with miR-155-5p and negative control mimic, fixed with paraformaldehyde, and stained with anti-TPN ab (1:500 dilution, Abcam) and anti-H3K27me3 Ab (1:500 dilution, Abcam): 500 dilution, Diagenode, Seraing, Belgium) for 30 min at room temperature followed by secondary Ab (Opal anti-Ms+Rb HRP, AKOYA, Mariborough, MA, USA) and fluorochrome (Opal 520 Reagent and Opal 570 Reagent, AKOYA) staining before fluorescence microscopy (EVOS FLoid Bildgebungssystem, Invitrogen). PowerPoint was used for image processing after data acquisition.

3.2.15 Immunoprecipitation

Immunoprecipitation was used to investigate correlation between TPNs and H3K27me3 markers. Briefly, after transfection with miR-155-5p mimics and negative controls for 48 hrs, 2 µg of H3K27me3 ab (Diagenode, Seraing, Belgium) was added to the FM81 melanoma cell lysis and incubated overnight at 4°C, followed by incubation with Protein A/G magnetic beads (Pierce Classic Magnetic IP/Co-IP kit, Thermo Fisher Scientific Inc, MA, USA) for 1 hrs. After elution, the sample/ab mixture was subjected to immunoprecipitation. After elution, the antigen sample/ab mixture was subjected to Western blot analysis as described above.

3.2.16 Determination of cytokines

The proteome profiler human xl cytokine array kit (ARY022B, R&D Systems) was used to examine secreted cytokines in the cell supernatants of tumor cells after co-culture, using 200 µl of supernatant per sample according to the manufacturer's instructions. Chemiluminescent blots were imaged using an iBright750 imaging system (Invitrogen) and signal intensity for densitometric analysis was determined using ImageJ. Enzyme-linked immunosorbent assay (ELISA) was performed to determine supernatant concentrations of selected cytokines. The ELISA MAXTM Deluxe Set Kits (Biolegend) were used for the analysis of CCL2 (438804), CXCL10 (439904) and IL8 (431504), the ELISA LEGEND MAXTM Kit (Biolegend) for the

analysis of MIF (438407) as well as the human VEGF Mini TMB ELISA Development Kit (900-TM10, PeproTech Germany, Hamburg, Germany) for VEGF concentration according to the manufacturer's instructions.

3.2.17 Gene set enrichment analysis (GSEA)

In order to investigate the association between hnRNP C and the protein complex of the major histocompatibility complex (MHC), a GSEA was carried out. [108]. Briefly, we used GSEA software (UC SanDigo, Broad Institute) to analyze the RNA-seq data of 67 metastatic melanoma cases from the TCGA-SKCM data set, and the molecular signature data bank (MSigDB) to determine which genes are correlated with hnRNP C.

3.2.18 Bioinformatics and statistical analysis

The correlation of miR-155 and tpn expression with overall survival (OS) of melanoma patients was investigated in different public datasets (GSE65904, TCGA-SKCM). The probability of OS of melanoma patients was determined by Kaplan-Meier estimation according to hnRNP C expression using 459 cases from "SKCM Cancer" and "Bhardwaj" and 44 cases of metastatic melanoma patients from R2 database (https://hgserver1.amc.nl/cgi-bin/r2/main.cgi). Within the TCGA Skin Cutaneous Melanoma (TCGA-SKCM) dataset, the relationship between tpn and miR-155 as well as their immune infiltration was evaluated in depth using the CIBERSORT website for 63 distant metastatic melanoma samples with available miRNA seq data. The correlation between CD8+ T cells and miR-155 was verified using the infiltration ratio data from CIBERSORT, which also using for determine the link of M1 macrophages and cytokines through the TCGA-SKCM dataset. Furthermore, 67 distant metastatic melanoma samples from the TCGA-SKCM dataset were used to determine the association between hnRNP-C expression and immune infiltration. GAPIA, ENCORI and GSEA webtools were used to correlate pan-cancer hnRNP C expression with TPN and MHC I expression. Possible miRNAs that also bind to the same sequence of the tpn 3'UTR as miR-155-5p were identified using the

26

R language. The dataset "R2: Hynes - 83 - MAS5.0 - u133a" from the R2 Genomics Analysis Web Tool (https://hgserver1.amc.nl/cgi-bin/r2/main.cgi) was used for the analysis of hnRNP C expression and immune cell infiltration in primary and metastatic melanoma lesions. The results of the graphical data were presented as mean ± standard deviation (SD) of at least three experiments. Analysis was performed using Microsoft Office (Microsoft Corporation, Redmond, WA, USA), ImageJ (NIH, Bethesda, Maryland, USA) and GraphPad Prism (GraphPad Software, LLC, San Diego, USA). Unless otherwise stated, statistical significance was determined using paired or unpaired t-tests, assuming P values of $P<0.05$ (*), $P<0.01$ (**), $P<0.001$ (***) or $P<0.0001$ (****).

4 RESULTS

4.1 Unconventional role of microRNA by enhancing the HLA class I antigen processing pathway due to the interaction with a silencer

4.1.1 MiR-155-5p bind to 3'UTR of tpn

miTRAP followed by small RNA sequencing and *in silico* analysis were performed to gain insights into the miRNA-mediated regulation of tpn using the human melanoma cell line MZ-Mel2 as a model thereby identifying miRNAs binding to the tpn 3'UTR[109]. First, RNAhybrid (https://bibiserv.cebitec.uni-bielefeld.de/rnahybrid/) was used to predict the binding site of the miR-155-5p in the tpn 3'UTR (Figure 2 A). Next, luciferase reporter assays in the HEK293T cells indicated a higher RLU value of wt 3'UTR when compared to the del 3'UTR (Figure 2 B), which is the opposite of the conventional transcriptional downregulation induced by miRNAs.
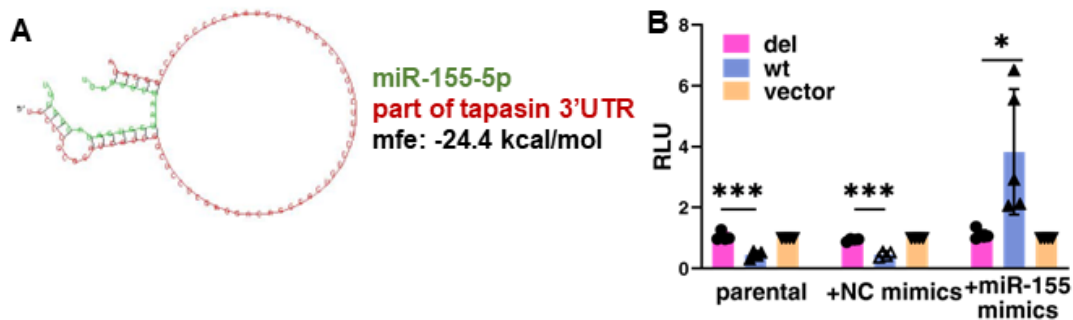
Figure 2 Identification of miR-155-5p targeting tpn
(A) The binding site predicted tpn 3'UTR (red) and miR-155-5p (green) interactions, including sequence alignment, secondary structure and free energy (mfe = -24.4 kcal/mol) were obtained using the RNAhybrid online database. (B) Direct miR-155-5p and tpn interaction identified by dual luciferase reporter assay using HEK293T cells and pmiR-GLO plasmid. The Firefly luciferase (FFL) activities were normalized to Renilla luciferase activities to give the relative light units (RLU) as described in Materials and Methods. The data represent the mean ± SD of three biological replicates upon their normalization to parental cells.

4.1.2 MiR-155-5p upregulates tapasin mRNA and protein level

To analyze function of the miR-155-5p binding in more detail, three human tpn expressing melanoma cell lines (FM81, MZ-Mel2, FM3) were transfected with miR-155-5p mimics and investigated for their expression of tpn. In all three melanoma cell lines, overexpression of miR-155-5p (Figure 3 A) increased tpn mRNA (Figure 3 B) and protein levels (Figure 3 C and D). Since the mRNA of programmed death ligand 1 (PD-L1), another target of miR-155-5p[110], was downregulated in the miR-155-5p-transfected MZ-Mel2 cell line (Figure 3 E) suggesting this upregulation was specific for tpn. Thus, miR-155-5p displayed the opposite behavior with respect to the other miRs during data validation.
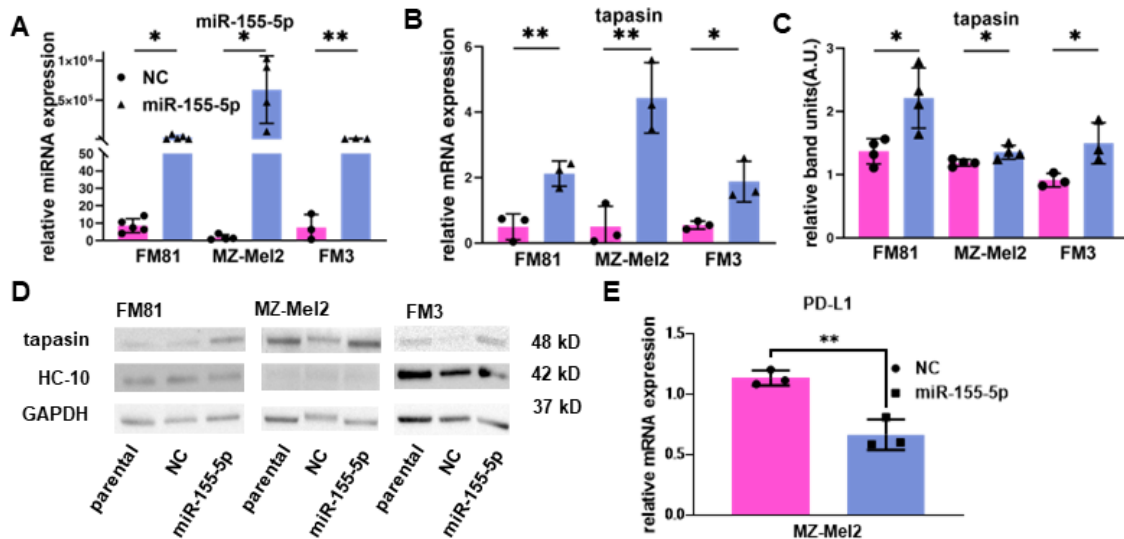
Figure 3 miR-155-5p upregulates tpn at the mRNA and protein level
(A, B) RT-qPCR was performed to determine the mRNA expression of miR-155-5p and in three metastatic melanoma cell lines after transfection of miR-155-5p mimic or miR mimic NC for 48 hrs. The data represent the mean ± SD upon their normalization to parental cells. (C, D) The Western blot analyses were performed as described in Materials and Methods to determine the expression of the tpn protein after transfection with miR-155-5p or NC. In each group, the relative band intensities (A.U., arbitrary units) were compared to that of the corresponding parental melanoma cells and normalized to the corresponding GAPDH signals (mean ± SD, n = 3 biological replicates). (E) To determine PD-L1 mRNA expression via RT-qPCR after transfection of the metastatic melanoma cell line MZ-Mel2 with miR-155-5p mimic or NC mimic for 48 hrs. Data were presented as A – C.

4.1.3 MiR-155-5p activates the HLA-I pathway

After overexpression of miR-155-5p, the expression of HLA-I at the protein level and at the cell surface has also to be checked. While the overall protein levels of HLA-I heavy chain (HC) were not altered in the miR-155-5p transfectants (Figure 3 D and Figure 4 A), HLA-ABC and HLA-BC cell surface antigens were upregulated on FM81 and MZ-Mel2 cells (Figure 4 B and C), not on FM3 cells. The latter might probably be due to their high constitutive levels of HLA-I HC when compared to FM81 and MZ-Mel2 cells (Figure 3 D).

To get further insights into the role of miR-155-5p in the transcription process, miR-155-5p transfectants, the negative control (NC), and parental human FM81 cells were treated with actinomycin D (act D) immediately after transfection. As shown in Figure 4 D, the mRNA half-life of tpn increased significantly over time in the miR-155-5p transfectants when compared to the NC and parental FM81 cells. In addition, the effect of miR-155-5p on the susceptibility of melanoma cell lines to NK cells was analyzed using a CD107a degranulation assay to evaluate the functional consequences of this increased HLA-I surface expression[111]. In comparison to the negative control group, MZ-Mel2 transfected with miR-155-5p induced lower numbers of CD107a-positive NK cells (Figure 4 E).
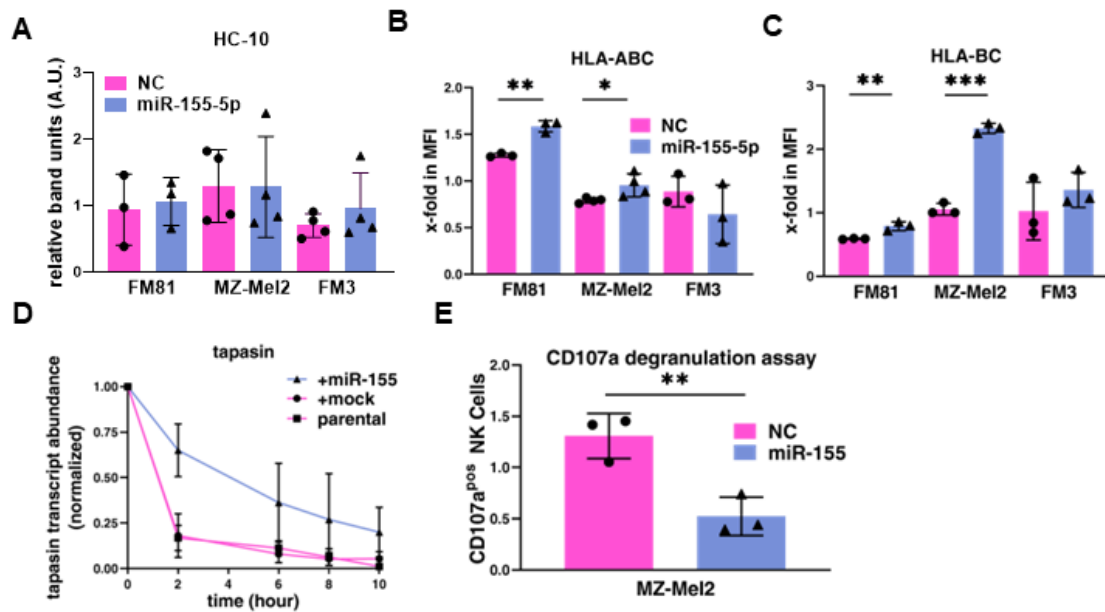
Figure 4 miR-155-5p activates the HLA-I pathway via tpn upregulation

(A) Western blot analyses were performed to explore the expression of HLA-I HC after transfection with miR-155-5p or NC as described in Materials and Methods. The relative band intensities (A.U., arbitrary units) of each group were compared with the corresponding parental melanoma cells and normalized to the corresponding GAPDH signals (mean ± SD, n = 4 biological replicates). (B, C) To determine the HLA-I surface expression via flow cytometry. For staining of melanoma cells, Abs directed against HLA-ABC and HLA-BC were employed. The data were presented as mean fluorescence intensities (MFI) to parental cells (mean ± SD, n = 3 biological replicates). (D) The half-life of the tpn mRNA was determined via act D mRNA stability assay upon determination of the tpn mRNA expression during different treatment time points after transfection as previously described using RT-qPCR normalized to the mRNA expression of ALAS1 (mean ± SD, n = 3 biological replicates). (E) Using CD107a degranulation assay to determine the miR-155-5p-mediated effect on HLA-I cell surface expression in association to NK cell cytotoxicity (mean ± SD, n = 3 biological replicates). *p < 0.05, **p<0.01 and ***P < 0.001.

4.1.4 Clinical relevance of miR-155-5p and APM

In light of the positive effect of miR-155-5p on tpn, the "R2: Genomics Analysis and Visualization Platform (http://r2.amc.nl)" web tool and several public available datasets were explored regarding the clinical relevance of miR-155 in melanoma. A positive correlation of the expression of the miR-155 host gene (miR-155HG) with the OS time of patients[112] (Figure 5 A) as well as with tpn (Figure 5 B) and HLA-A (Figure 5 C) expression levels was demonstrated after analyzing the Jönsson dataset comprising 214 metastatic melanoma cases with patients' outcomes thereby confirming our *in vitro* experiments. Subsequently, the analysis of an independent TCGA-SKCM dataset or of 63 cases of distant metastatic melanoma with available miRNA sequencing (seq) results within the SKCM dataset confirmed the positive correlation of miR-155 expression with patients' OS (Figure 5 D) and between tpn and miR-155 (Figure 5 E).
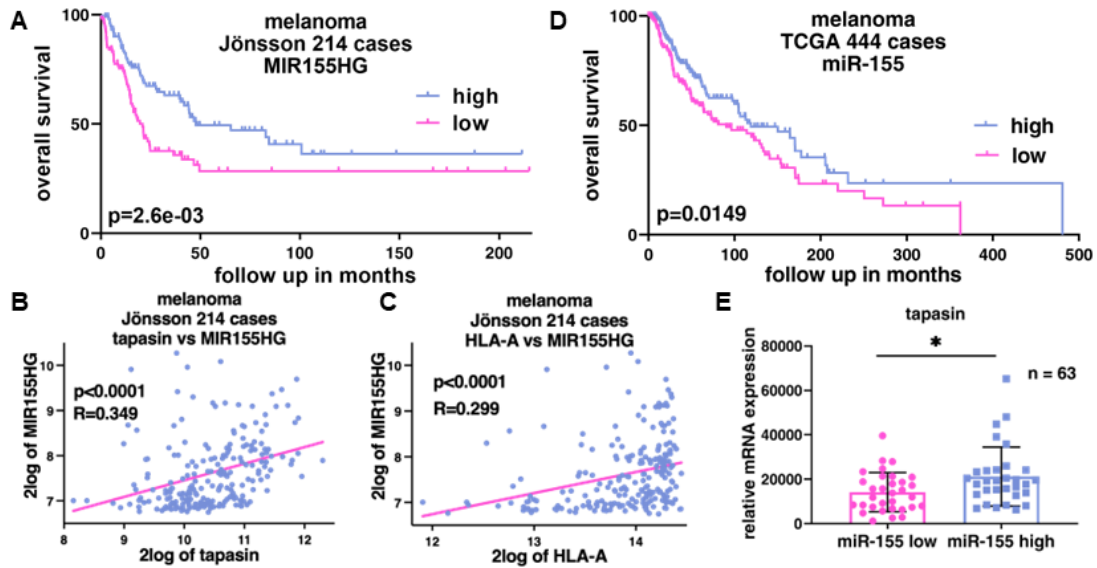
Figure 5 Clinical significance of miR-155-5p
(A to C) To evaluate the patient's OS determined by the Kaplan Meier estimation curve and correlations of MIR155HG expression with tpn or HLA-A via the datasets (GSE65904). (D) Using the TCGA-SKCM dataset to investigate the patients' OS upon miR-155 expression. (E) To verify the association between tpn and miR-155, 63 metastatic melanoma cases with available RNA and miRNA seq data in the TCGA-SKCM dataset was determined. *p < 0.05.

4.1.5 Relevance of miR-155-5p and immune cells

The immune infiltrate of the 63 cases of the "SKCM" dataset was correlated to the expression of miRNAs discovered by miTRAP and RNA seq via using the CIBERSORT web tool demonstrating a very strong positive correlation between miR-155 and CD8⁺ T cells (Figure 6 A and B). Thus, miR-155-5p has not only a significant impact on the OS rate of melanoma patients, but also influences the TME, tumor immunogenicity and immune cell recognition.
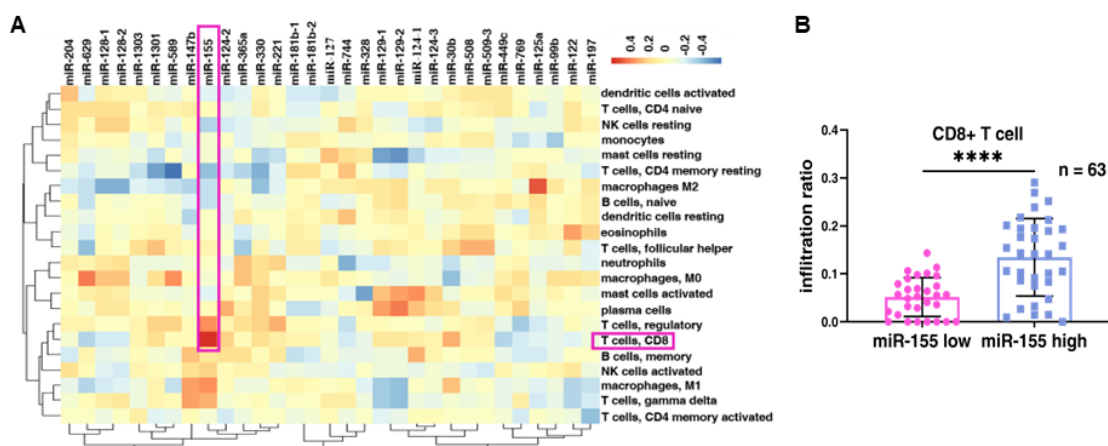
Figure 6 Relationship of miR-155-5p and immune cell infiltration
(A, B) Using 63 cases of distant metastatic melanoma with available miRNA sequencing (seq) results within the SKCM dataset, the effect of miRNAs on immune cells expressing and the relationship between CD8⁺ T cell infiltration as well as the expression of miR-155 was analyzed by the generation of a heat map. (mean ± SD, n = 3 biological replicates), ****P < 0.0001.

Table 2 Characteristics of the silencer sequence including the miR-155-5p binding site in three different cell lines of distinct tissue origin

chrom osome	start	end	cell line	tissue	organ	species	method	nearest gene	regulatory gene
chr6	3326 5041	3326 8136	fetal intestine small	small intestin e	intestin e	home sapiens	SVM	PFDN6	TAPBP
chr6	3326 5041	3326 8136	h1 derived neuronal progenitor cultured cells	brain	brain	home sapiens	SVM	PFDN6	TAPBP
chr6	3326 5041	3326 8136	gastric	stoma ch	stoma ch	home sapiens	SVM	PFDN6	TAPBP

4.1.6 Silencer characteristics of miR-155-5p binds sequence

Subsequently, the underlying mechanism(s) of the unexpected miR-155-5p-mediated upregulation of tpn were explored in detail. Based on the luciferase assays, an intrinsic direct or indirect inhibitor effect on the transcription process was analyzed via miR-155-5p binding sequence using the Encyclopedia of DNA Elements (ENCODE) [113] to characterize this binding site sequence in depth. As shown in Figure 7 A, this sequence contains a high GC content and a DNase hypersensitivity site (DHS). Interestingly, GC-rich sequences have a direct association with the mRNA decay from several reports[114 115], which is also further supported by the silencer database silencerDB web tools [80] suggesting that this sequence is a part of a silencer with direct inhibitory effects (Table 2, Figure 7 B).

Figure 7 Characteristics of miR-155-5p binding site sequence
Using the Homo sapiens suprapubic skin tissue dataset in ENCODE to examine the sequence of the tpn 3'UTR. The binding site area of miR-155-5p is a high GC content region and has DNase hypersensitivity sites as well as peaks of H3K27me3. (B) 3095 bp silencer sequence was identified by using the silencer database SilencerDB. In addition, a part of this silencer is the miR-155-5p binding site located in the 3'UTR of tpn (ENST00000434618.2).
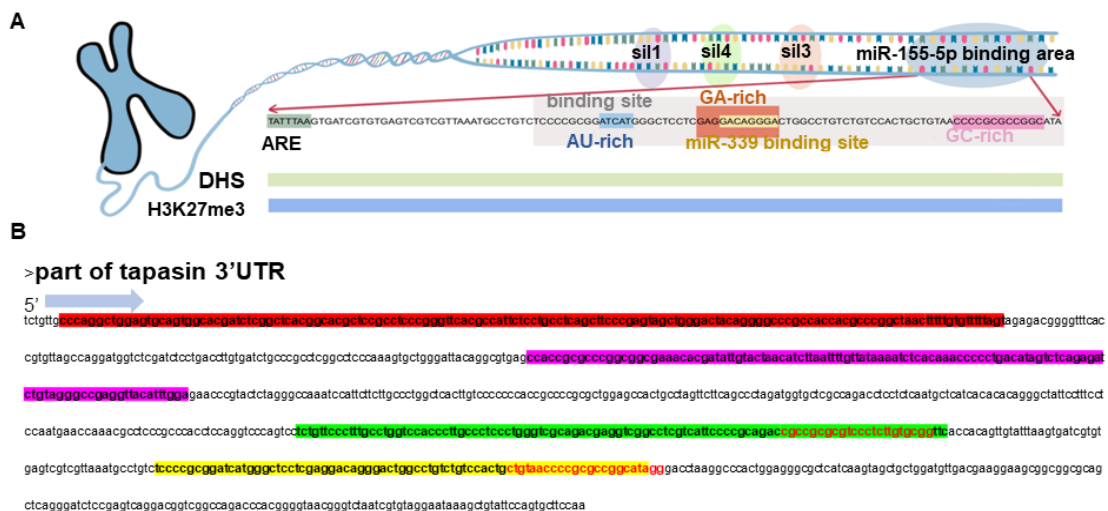

Figure 8 Diagram representing the sequence deletion in the tapasin 3'UTR
(A) Simulation diagram for the sequence of the binding site, elements around this binding site and characteristics of this sequence. (B) The deleted regions of sil1, sil3 and sil4 are marked by red, green and pink boxes, respectively. The yellow box highlights the miR-155-5p binding site on the 3'UTR. The two sequences in red are the target sequences for the clipping sites of CRISPR/Cas9, respectively.

33

Three sequences (sil1, sil3, sil4) deleted upstream of the binding site, an AU-rich element predicted via the ARE site web tool[116] and the potential GA-, AU- and GC-rich areas within the miR-155-5p binding site from the tpn 3'UTR (Figure 8 A and B) were cloned into the miR-GLO vector to determine the length of the silencer around the miR-155-5p binding site and to exclude other possible functional elements, which overlap with the binding site.

Using transfected HEK 293T with ARE, AU, GC or GA sequence knockout, respectively, highlighted the disappearance of the suppressive effects in negative control (NC) transfectants and parental cells as well as of the positive effect in miR-155-5p transfectants via luciferase assays in comparison to the wt 3'UTR. Deletion of these elements, which belong to the binding site of miR-155-5p, have disrupted the binding site leading to the loss of the positive function after transfection confirming that these sequences are a part of the miR-155-5p binding site. These sequences represent a core part of a silencer, since there is also a loss of the intrinsic suppressive effect. Whereas the positive effect of all three sil constructs was much lower than in wt group, the repressive effect in the deletion of sil1, sil3 or sil4 groups found in both NC and parental cells was similar to the wt 3´UTR upon miR-155-5p mimic transfection (Figure 9 A). Thus, the secondary mRNA structures, which were disrupted by those partial sequence deletion might explain that the upregulation induced by miR-155-5p binding to the tpn 3'UTR is more effective in wt sequences than upon deletion of sil1, sil3 and sil4 sequences (Figure 9 B-K). In contrast, these sil sequences did at least not individually display intrinsic silencing activity.
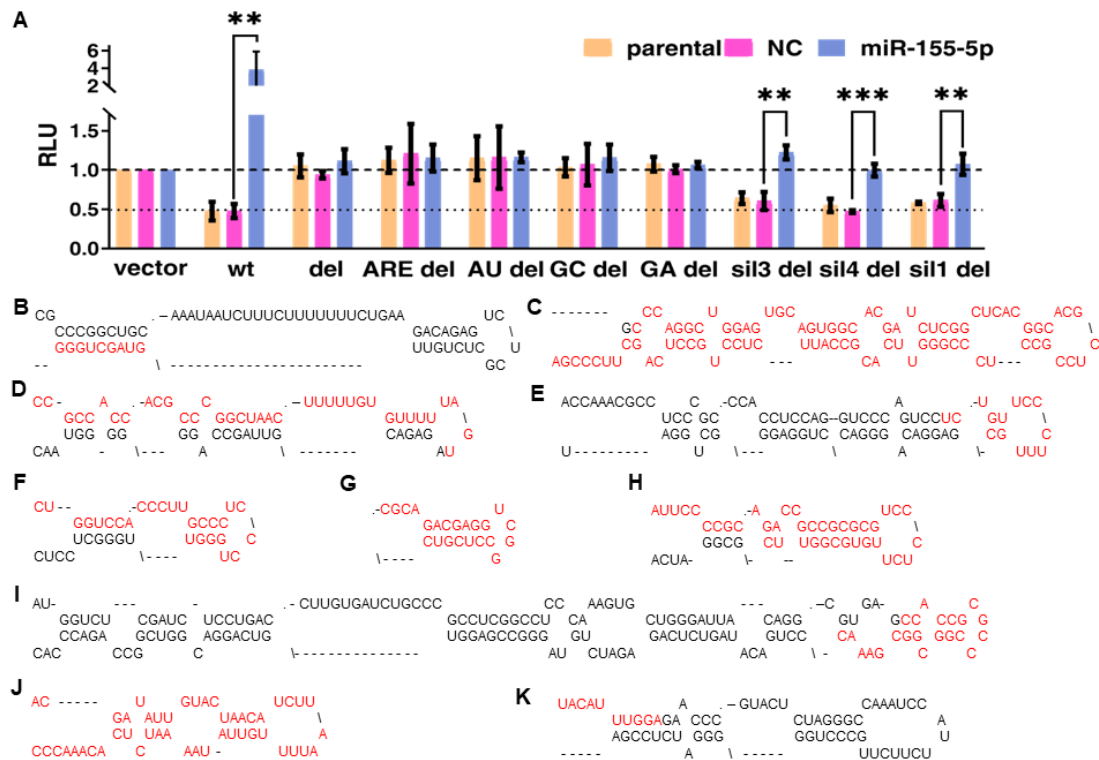
Figure 9 Luciferase assays and prediction of several secondary structures
(A) Luciferase assays were used to investigate the activity of this area upon deletion of the binding sites and some possible functional elements cloned into pmiR-GLO vector after transfection with miR-155-5p mimics or negative control mimics (mean ± SD, n = 3 biological replicates). (B-K) Using the UNAFold Web server (http://www.unafold.org/) to predict the secondary structure of tpn 3'UTR. RNA folding results show structure 1 folding bases 1 to 2065 of NM_001410875 1 Homo sapiens TAP binding protein [T Initial ΔG = -697.50]. (B to C) Sil1 deletion area overlap with the secondary structures (red). (D to G) Sil3 deletion area overlap with the secondary structures (red). (H to J) Sil4 deletion area overlap with the secondary structures (red).

To further confirm the silencer function, a CRISPR/Cas9-mediated deletion[117] of the miR-155-5p binding site sequence in the tpn 3'UTR was generated in the FM3 melanoma cell line upon transfection of the pSpCas9 (BB)-2A-GFP plasmid (PX458) with two guide RNAs (Figure 10 A and Figure 8 A). Sanger sequencing (data not shown) and PCR amplification (Figure 10 B) demonstrated the successful deletion of the miR-155-5p binding site (R3R9), which resulted in tpn mRNA and protein levels when compared to the mock vector (PX458) (Figure 10 C-E).
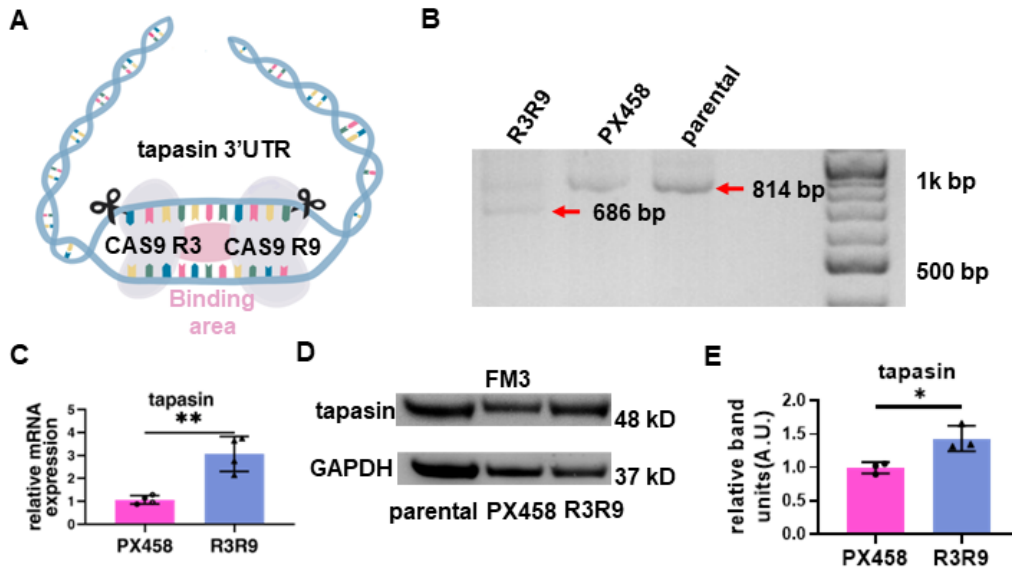
Figure 10 CRISPR/Cas9-mediated knock out of the miR-155-5p binding site sequence
(A) Simulation diagram that using CRISPR/Cas9 system to knock out sequence of the binding site area. (B) Approximately 128 bp sequences were knocked out in the R3R9 group via CRISPR/Cas9 compared to PX458 and parental groups (814 bp). (C) To investigate the tpn mRNA expression through RT-PCR after knocking out the binding site via vector R3 and R9 (R3R9) as well as negative control PX458 empty vector (PX458) (mean ± SD, n = 3 biological replicates), respectively. (D, E) To determine the expression of the tpn protein through Western blot analyses after knocking out the binding site via CRISPR/Cas9. The relative band intensities (A.U., arbitrary units) of each group were compared to that of the corresponding parental FM3 melanoma cells and normalized to the corresponding GAPDH signals (mean ± SD, n = 3 biological replicates).

Using fluorescence immunocytochemical staining of the three melanoma cell lines transfected with miR-155-5p and NC mimics to determine whether the identified silencer interacts with H3K27me3. As shown in Figure 11 A, tpn has a higher expression (green fluorescence) in the miR-155 group than in the other two groups, while the expression of H3K27me3 (red fluorescence) was inversely correlated. Subsequently, immunoprecipitation was performed after transfection of the FM81 melanoma cell line with miR-155-5p and NC mimics. Tpn was found to directly or indirectly bind to the histone mark H3K27me3 (Figure 11 B) via using Western blot analysis. These data are consistent with previous reports demonstrating a suppressor function of silencers overlapping with H3K27me3[83-85]. In conclusion, the deletion of the miR-155-5p binding site as well as its "occupation" upon miR-155-5p overexpression confirm its role as a silencer.
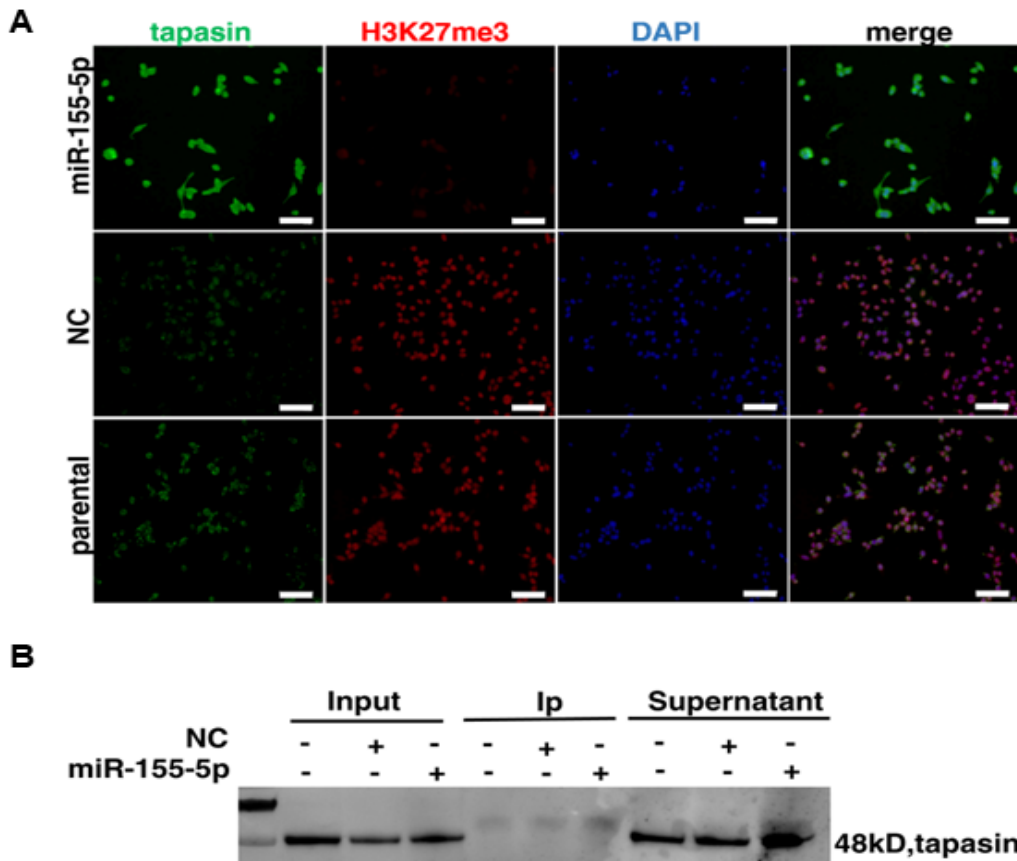
Figure 11 Link of tpn and H3K27me3 in melanoma cell lines
To investigate the correlation between tpn (green) and H3K27me3 (red) after transfection with miR-155-5p mimics and NC mimics via immune cytofluorescence. (B) To determine the expression of the tpn protein after immunoprecipitation and transfection with miR-155-5p or NC in FM81 melanoma cell line through the Immunoprecipitation and Western blot analyses as described in Materials and Methods. Ip represented the immunoprecipitation group and the supernatant was the residual liquid after separation and precipitation, the Input group was used as a control, which was not subjected to immunoprecipitation.

To determine whether the inhibitory effect of this sequence is caused by the binding with other molecules or due to intrinsic effects, mass spectrometry after sodium dodecyl sulfate (SDS) gel separation was used to identify RBPs interacting with the tpn 3'UTR. Then, four proteins (HNRNPL, HNRNPC, IGF2BP1, IGF2BP3) were identified, which bind to the tpn 3'UTR, by using the RBP suite web tool (http://www.csbio.sjtu.edu.cn/bioinf/RBPsuite/) to predict the precise binding site. While the HNRNPC and HNRNPL predicted binding sites in the tpn 3'UTR were distant from the miR-155 binding site (Figure 12 A and B), the IGF2BP1 and IGF2BP3 predicted binding sites overlap with that of miR-155 (Figure 12 C and D). The miR-155-5p binding site is a part of the IGF2BP1 and IGF2BP3 potential binding site and include a GC- as well as an AU-rich element as determined by after the analysis of the overlap between the binding site sequences of IGF2BP1 and miR-155-5p on the tpn 3'UTR (Figure 12 E). Using concentration gradient silencing assays for IGF2BP1 and IGF2BP3, the possible role for both RBPs were determined in the silencer function of the sequence, which resulted in the lack of

rebound effects of the inhibitor upon protein downregulation (Figure 12 F-H) thereby excluding the interaction between miR-155-5p and RBPs that upregulate tpn expression.
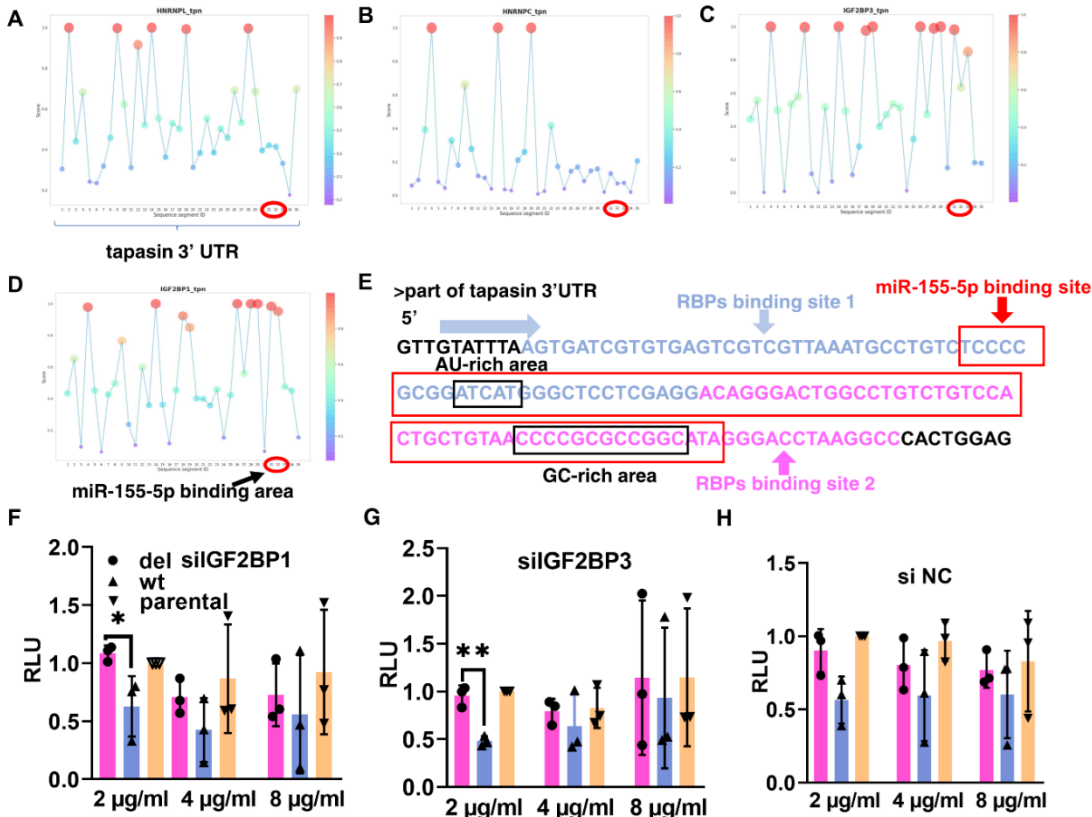

Figure 12 Simulation diagram of the overlap of the binding sites and the concentration gradient silencing assays

(A-D) Using RBPsuite to predict the binding sites of the four proteins on tpn 3'UTR. The position circled in red is the binding site for miR-155-5p. The red dots represent the binding sites with higher probability. (A and B) HNRNPC and HNRNPL predicted results. (C and D) IGF2BP1 and IGF2BP3 predicted results, the miR-155-5p binding site overlap with some of their binding sites. (E) The miR-155-5p binding site (red box) overlap with the predicted binding site 1 (blue) and site 2 (pink) of IGF2BP1 and IGF2BP3 on the tpn 3'UTR. GC- and AU-rich areas are the black boxes. (F-H) Using luciferase assays to investigate the effects of concentration gradient silencing IGF2BP1 and IGF2BP3 on the binding site sequence after transfection of siRNAs (IGF2BP1, IGF2BP3, negative control) and cloned miR-GLO vector into HEK 293T cell lines (mean ± SD, n = 3 biological replicates). $*p < 0.05$ and $**p<0.01$.

Not only RBPs, but also other miRNAs might bind to the tpn 3'UTR thereby competing with miR-155-5p. Using R language to calculate and predict miRNAs that overlap with miR-155-5p binding site, a few miRNAs were identified (Table 3). MiR-339-5p is a candidate miRNA with a binding site overlapping with miR-155-5p as demonstrated by *in silico* analysis (Figure 8 A). However, a similar loss of the intrinsic suppressive activity was found in the parental and NC transfectants in luciferase experiments upon depletion of the GA-, AU- and GC-rich elements (Figure 9 A). Thus, miR-339-5p is not involved in this process. Therefore, a competition with miR-339-5p for the tpn 3'UTR do not enhance activity of miR-155-5p. In addition, and the miR-

155-5p binding site in the tpn 3'UTR is a significant part of the silencer and miR-155-5p acts directly on it.

Table 3 MiRNAs identified to bind within the tapasin 3'UTR (miR-155-5p region)

miRNA	type	miRNA	type	miRNA	type	miRNA	type	miRNA	type
hsa-miR-151a-5p	8-mer	hsa-miR-15a-3p	6-mer	hsa-miR-744-5p	6-mer	hsa-miR-4421	6-mer	hsa-miR-6849-5p	6-mer
hsa-miR-339-5p		hsa-miR-28-5p		hsa-miR-922		hsa-miR-4438		hsa-miR-6852-3p	
hsa-miR-151b		hsa-miR-214-3p		hsa-miR-937-3p		hsa-miR-4454		hsa-miR-6889-5p	
hsa-miR-1972		hsa-miR-194-3p		hsa-miR-1225-3p		hsa-miR-4479		hsa-miR-10396a-5p	
hsa-miR-3138		hsa-miR-409-5p		hsa-miR-1233-3p		hsa-miR-4633-5p		hsa-miR-12115	
hsa-miR-4520-3p		hsa-miR-146b-3p		hsa-miR-1910-5p		hsa-miR-4634			
hsa-miR-1324	7-mer	hsa-miR-193b-5p		hsa-miR-3120-3p		hsa-miR-4650-5p			
hsa-miR-2114-5p		hsa-miR-505-5p		hsa-miR-3131		hsa-miR-4717-5p			
hsa-miR-2277-5p		hsa-miR-455-3p		hsa-miR-3139		hsa-miR-4784			
hsa-miR-4519		hsa-miR-611		hsa-miR-4274		hsa-miR-4800-5p			
hsa-miR-4641		hsa-miR-640		hsa-miR-3619-5p		hsa-miR-5588-3p			
hsa-miR-4706		hsa-miR-542-5p		hsa-miR-3681-5p		hsa-miR-5693			
hsa-miR-4749-5p		hsa-miR-670-5p		hsa-miR-3909		hsa-miR-5699-3p			
hsa-miR-4524b-3p		hsa-miR-761		hsa-miR-3150b-3p		hsa-miR-6499-3p			
hsa-miR-6748-3p		hsa-miR-708-5p		hsa-miR-676-3p		hsa-miR-6777-5p			

4.2 Identification of RNA-binding protein hnRNP C targeting TAP-associated glycoprotein tapasin in melanoma

4.2.1 Clinical relevance of hnRNP C expression regarding the survival of pan-cancer patients

Mass spectrometry results suggested that hnRNP C bind to the tpn 3'UTR. Therefore, hnRNP C was intensively studied demonstrating that has been associated with a few cancer types. Using the R2 genomic analysis web tool the prognostic relevance of hnRNP C expression was investigated in melanoma patients using the datasets "R2: Tumor Melanoma – Bhardwaj – 44 – MAS5.0 – u133p2" and "R2: Tumor Melanoma – TCGA – 470– rsem - tcgars". In both datasets, the OS probability was linked to lower hnRNP C mRNA transcript levels (Figure 13 A and B) suggesting an association of a better OS of melanoma patients with lower hnNRP C expression. For other cancer types, comparable results were obtained (Figure 13 C).
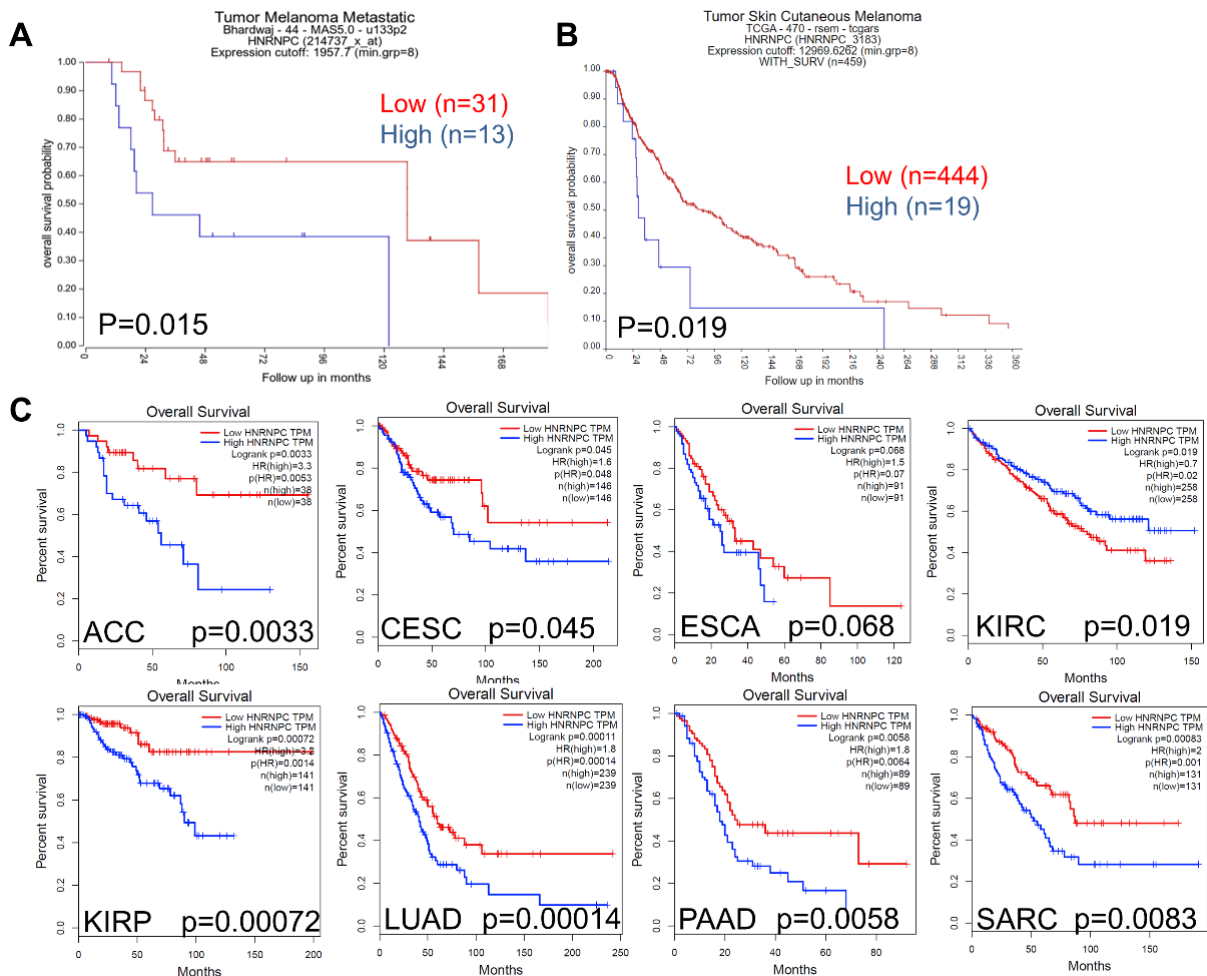
Figure 13 Correlation of the hnRNP C expression with the overall survival of melanoma and pan-cancer patients
The OS probability of melanoma patients with Kaplan-Meier estimation depending on hnRNP C expression including (A) 44 cases metastasis melanoma patients and (B) 459 cases from

the "SKCM Cancer" dataset, both analyzed from web database (https://hgserver1.amc.nl/cgi-bin/r2/main.cgi). (C) Correlation of the expression of hnRNP C with the OS in pan-cancer via TCGA dataset using GAPIA web tool (ACC: adrenocortical carcinoma, CESC: cervical squamous cell carcinoma and endocervical adenocarcinoma, ESCA: esophageal carcinoma, KIRC: kidney renal clear cell carcinoma, KIRP: kidney renal papillary cell carcinoma, LUAD: lung adenocarcinoma, PAAD: pancreatic adenocarcinoma, SARC: sarcoma).

Using the TCGA-SKCM dataset with the GAPIA web tool, the expression of hnRNP C in different tumor types and corresponding normal tissues was analyzed and results were shown in Figure 14. In most cancer types, the tumor tissues expressed higher hnRNP C transcript levels than the non-neoplastic tissues suggesting a possible tumor-promoting effect from hnRNP C.
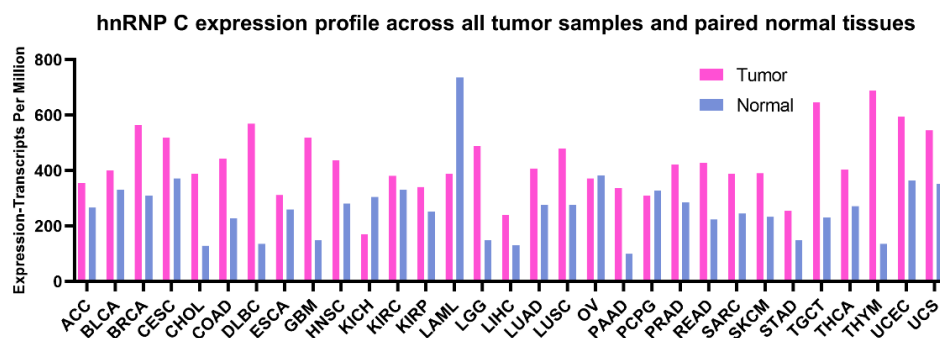
Figure 14 Higher hnRNP C expression levels in tumor samples compared to paired tumor-adjacent samples in pan-cancer
The expression of hnRNP C mRNA levels was compared in tumor tissues and paired normal tissues in 31 TCGA cancer datasets including melanoma via the GAPIA web tool. (BLCA: bladder urothelial carcinoma, BRCA: breast invasive carcinoma, CHOL: cholangiocarcinoma, COAD: colon adenocarcinoma, DLBC: lymphoid neoplasm diffuse large B cell lymphoma, GBM: glioblastoma multiforme, HNSC: head and neck squamous cell carcinoma, KICH: kidney chromophobe, LAML: acute myeloid leukemia, LGG: brain lower grade glioma, LIHC: liver hepatocellular carcinoma, LUSC: lung squamous cell carcinoma, OV: ovarian serous cystadenocarcinoma, PCPG: pheochromocytoma and paraganglioma, PRAD: prostate adenocarcinoma, READ: rectum adenocarcinoma, SKCM: skin cutaneous melanoma, STAD: stomach adenocarcinoma, TGCT: testicular germ cell tumors, THCA: thyroid carcinoma, THYM: thymoma, UCEC: uterine corpus endometrial carcinoma, UCS: uterine carcinosarcoma).

4.2.2   Link between hnRNP C, tpn and HLA-I in pan-cancer

Using the ENCORI web tool the link of hnRNP C mRNA levels and tpn expression of the TCGA datasets was analyzed, since hnRNP C has been shown to bind to the 3'UTR of tpn. In 13 different cancer types, a negative correlation of tpn and hnRNP C was found including melanoma with a high correlation coefficient (R value) (Figure 15) suggesting that hnRNP C inhibit tpn expression via binding to the tpn 3'UTR.
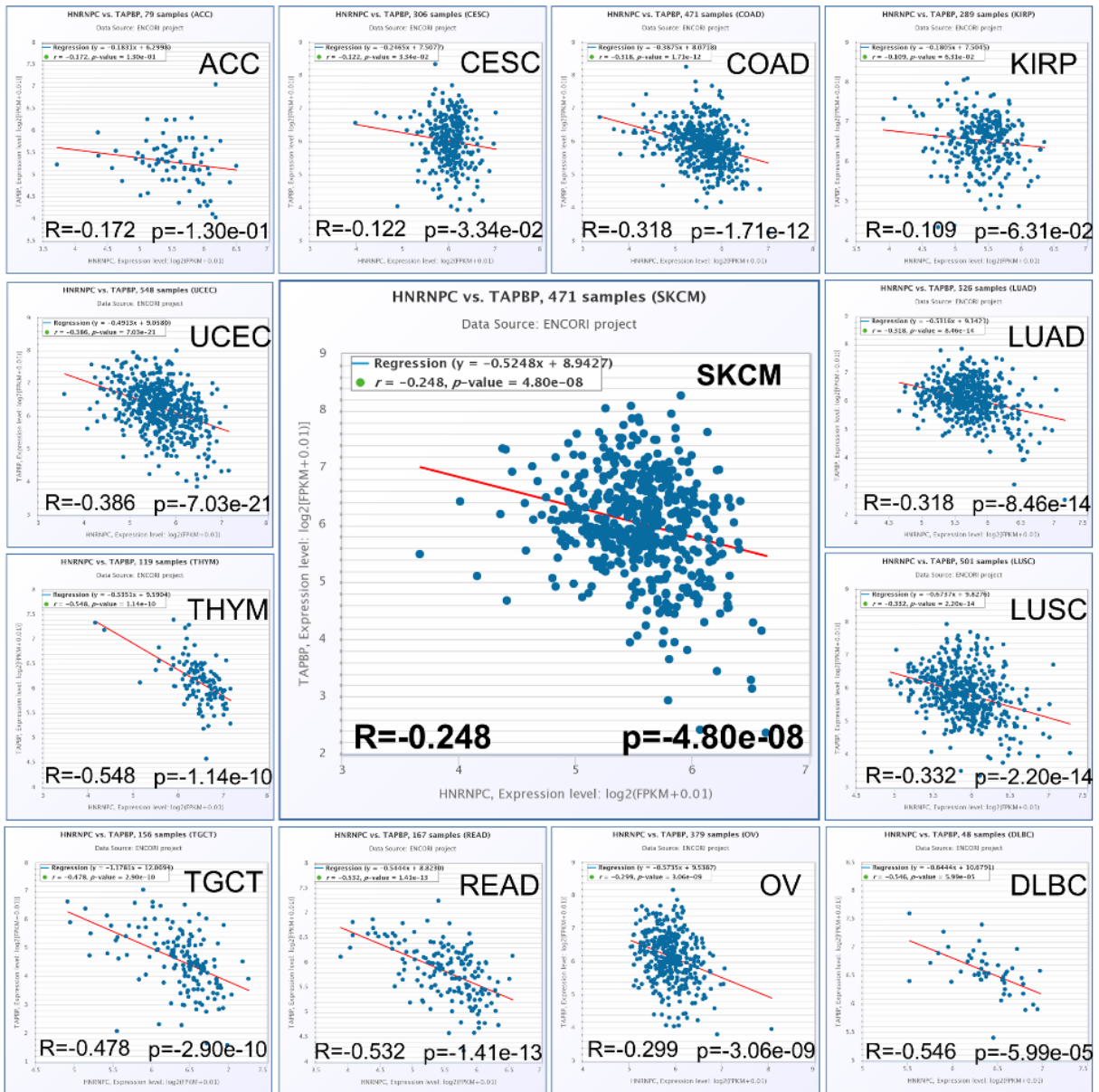
Figure 15 Co-expression analysis of hnRNP C and tpn in pan-cancer
The association of the mRNA expression levels between tpn and hnRNP C was determined in different cancer types through the TCGA data set via ENCORI web tool (https://rnasysu.com/encori/index.php). Each dot represents mRNA expression levels of a tumor sample. The expression values from RNA-seq data were scaled with log2 (FPKM + 0.01). (ACC: Adrenocortical carcinoma, CESC: Cervical squamous cell carcinoma and endocervical adenocarcinoma, COAD: colon adenocarcinoma, KIRP: Kidney renal papillary cell carcinoma, LUAD: Lung adenocarcinoma, LUCS: Lung squamous cell carcinoma, DLBC: lymphoid neoplasm diffuses large B cell lymphoma, OV: ovarian serous cystadenocarcinoma, READ: rectum adenocarcinoma, TGCT: Testicular Germ Cell Tumors, THYM: thymoma, UCEC: uterine corpus endometrial carcinoma, SKCM: skin cutaneous melanoma).

GSEA was used to further verify the relationship between hnRNP C and MHC class I APM components in 67 metastatic melanoma cases from the TCGA-SKCM dataset. A negative correlation of hnRNP C mRNA levels and the MHC class I complex "GOBP-PEPTIDE-

42

ANTIGEN-ASSEMBLY-WITH-MHC-PROTEIN-COMPLEX" (Figure 16, Table 4) was demonstrated using this computational method in combination with the Molecular Signatures Database thereby strengthening the evidence that the expression of hnRNP C and tpn was inversely correlated.
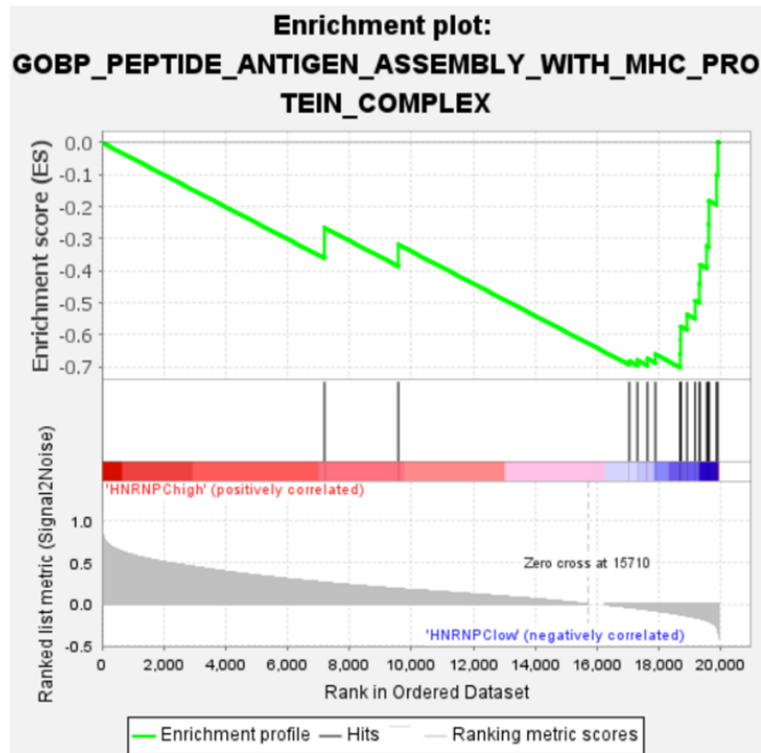
Figure 16 Enrichment plot for the correlation of the expression of hnRNP C mRNA and the MHC protein complex
The link of hnRNP C expression and MHC protein complex was analyzed in 67 metastatic melanoma cases from the TCGA-SKCM dataset via GSEA, https://www.gsea-msigdb.org/gsea/index.jsp) and presented as enrichment score.

Table 4 List of the MHC protein complex via GESA

	SYMBOL	TITLE	RANK IM GENE LIST	RANK METRIC SCORE	RUNNING ES	CORE ENRICHMENT
1	CALR	na	7192	0.260	-0.2660	No
2	PDIA3	na	9578	0.184	-0.3185	No
3	TAPBPL	na	17042	-0.031	-0.6820	Yes
4	B2M	na	17300	-0.042	-0.6795	Yes
5	HLA-DQA1	na	17627	-0.058	-0.6746	Yes
6	HLA-DQB1	na	17882	-0.072	-0.6609	Yes
7	TAPBP	na	18684	-0.116	-0.6588	Yes
8	HLA-DMB	na	18694	-0.117	-0.6165	Yes

9	HLA-DRB5	na	18698	-0.117	-0.5737	Yes
10	HLA-DRB1	na	18905	-0.132	-0.5357	Yes
11	HLA-DRA	na	19170	-0.152	-0.4933	Yes
12	HLA-DOB	na	19305	-0.163	-0.4403	Yes
13	HLA-DOA	na	19325	-0.165	-0.3810	Yes
14	HLA-DPA1	na	19540	-0.187	-0.3234	Yes
15	HLA-DPB1	na	19604	-0.197	-0.2545	Yes
16	HLA-DMA	na	19614	-0.199	-0.1820	Yes
17	HLA-DQB2	Na	19859	-0.255	-0.1009	Yes
18	HLA-DOA2	Na	19902	-0.286	0.0018	Yes

4.2.3 Upregulation of tpn expression by knock down of hnRNP C

Knockdown hnRNP C in two metastatic melanoma cell lines Buf1379 and Buf1402 to gain functional insights into the hnRNP C-mediated regulation of tpn. After the successful knockdown of hnRNP C (Figure 17 A), the tpn mRNA expression levels were significantly increased (Figure 17 B). Using q-PCR to investigate whether hnRNP C also affect other molecules of the antigen process and presentation pathway, after knockdown hnRNP C, the expression of TAP1, TAP2 and HLA-I associated molecules were tested. As shown in Figure 17 C to G, in negative control (NC) vs. hnRNPC knock down (siHNRNPC), the hnRNP C mRNA levels of TAP1, TAP2 and HLA-ABC were not comparable, while HLA-B and HLA-C expression was only slightly altered.
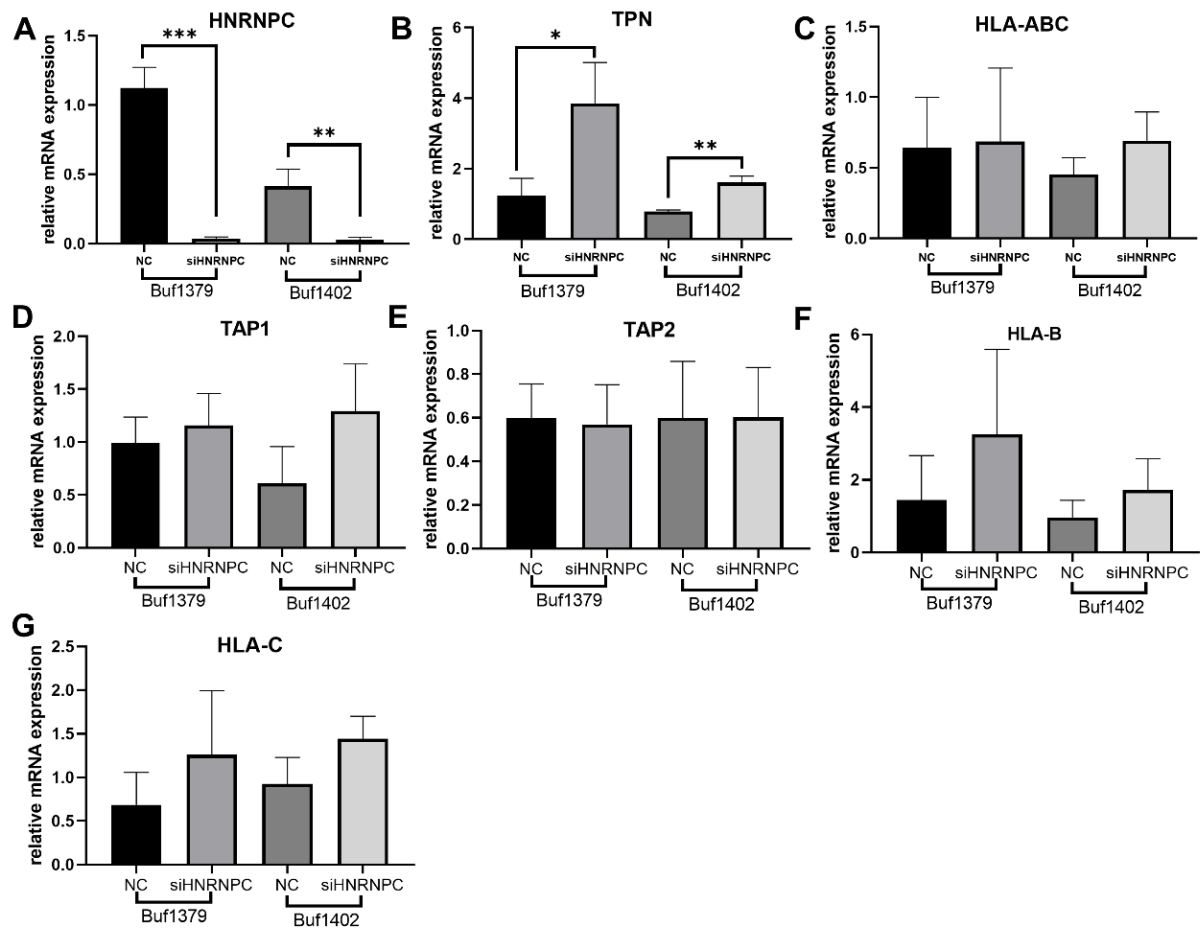
Figure 17 Upregulation of tpn mRNA levels by knock down of hnNRNP C
The mRNA expression levels of hnRNP C and tpn as well as other MHC-I-associated molecules in two metastatic melanoma cell lines 48 hrs after transfection with siHNRNPC or a negative control (NC) was determined via RT-qPCR. The data were normalized to parental cells and presented as mean of relative expression levels ± SD.

Furthermore, after hnRNP C knock down, tpn protein levels were 2-fold upregulated (Figure 18 A and B) in both cell lines, while the HLA-I heavy chain expression was slightly upregulated in Buf1379 (Figure 18 C and D). Immunoprecipitation demonstrated that hnRNP C could bind directly or indirectly to tpn in both melanoma cell lines (Figure 18 E), while the HC-10 Ab does not bind to tpn.
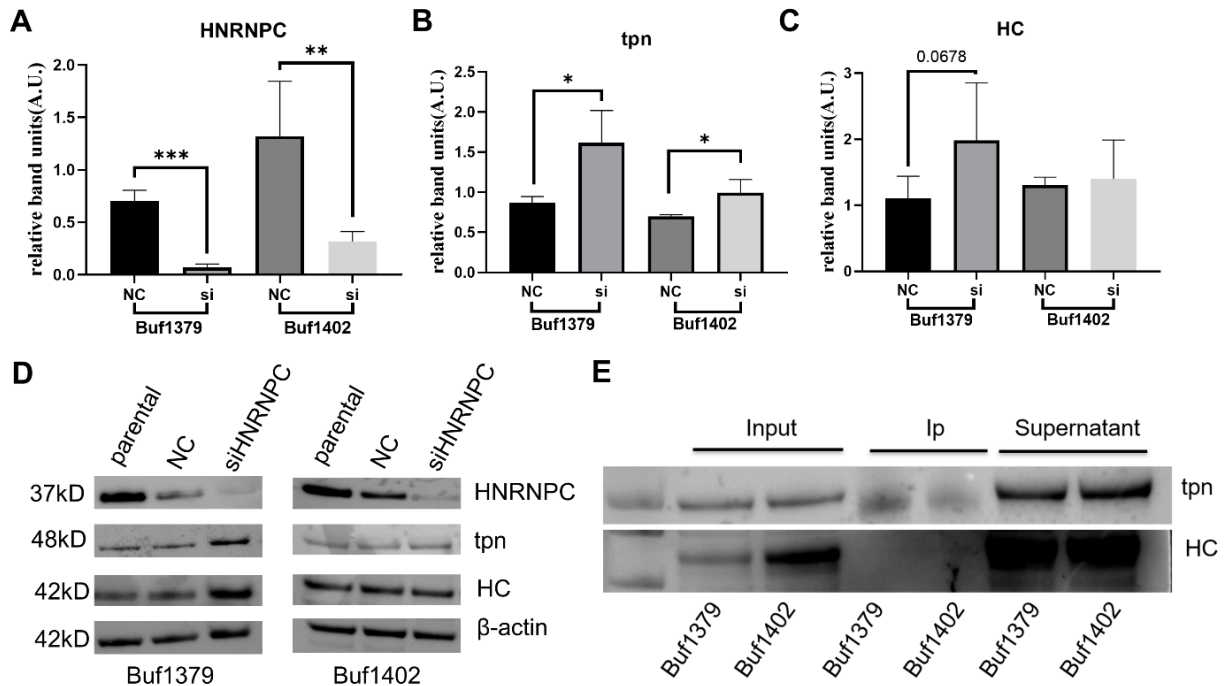
Figure 18 Upregulation of tpn protein levels by knock down of hnNRNP C
(A-D) The protein expression of hnRNP C, tpn marker was determined 48hrs after transfection of Buf1379 and Buf1402 cells with siHNRNPC or NC using Western blot analysis as described in Materials and Methods. The relative band intensities (A.U., arbitrary units) were compared to parental melanoma cells and normalized to staining with an anti-β-actin Ab (mean ± SD, n = 3 biological replicates). (E) Western blot analyses of immunoprecipitants were performed as described in Materials and Methods. *p < 0.05, **p < 0.01 and ***p < 0.001.

4.2.4 Association of hnRNP C and activation of HLA-I pathway with the immune cell infiltration

The expression of tpn mRNA and protein level after knockdown can be upregulate via hnRNP C, and HLA-I pathway associated molecules are also positively correlated to hnRNP C as determined by flow cytometry. HLA-ABC and HLA-BC are upregulated on the cell surface of Buf1379 cells after knockdown hnRNP C (Figure 19 A), while in Buf1402 cells, only HLA-BC was slightly upregulated (Figure 19 B), which correlated to the Western blot results of the HLA-I HC. Since it could be assumed that the HLA-I pathway activation after knock down hnRNP C might affect the immune cell infiltration including CD8^{+} T cells recognizing HLA class I surface antigens, 67 metastatic melanoma cases from the TCGA-SKCM dataset were investigated to determine the link between the immune cell infiltration and hnRNP C expression. Typically, CD8^{+} T cells recognize antigens presented by HLA-I[4]. As shown in Figure 19 C, CD8^{+} T cell infiltration has a significant negative link with the hnRNP C high group, which might be due to higher hnRNP C levels inversely associated with tpn thereby verifying the negative influence of hnRNP C expression on the HLA-I pathway.
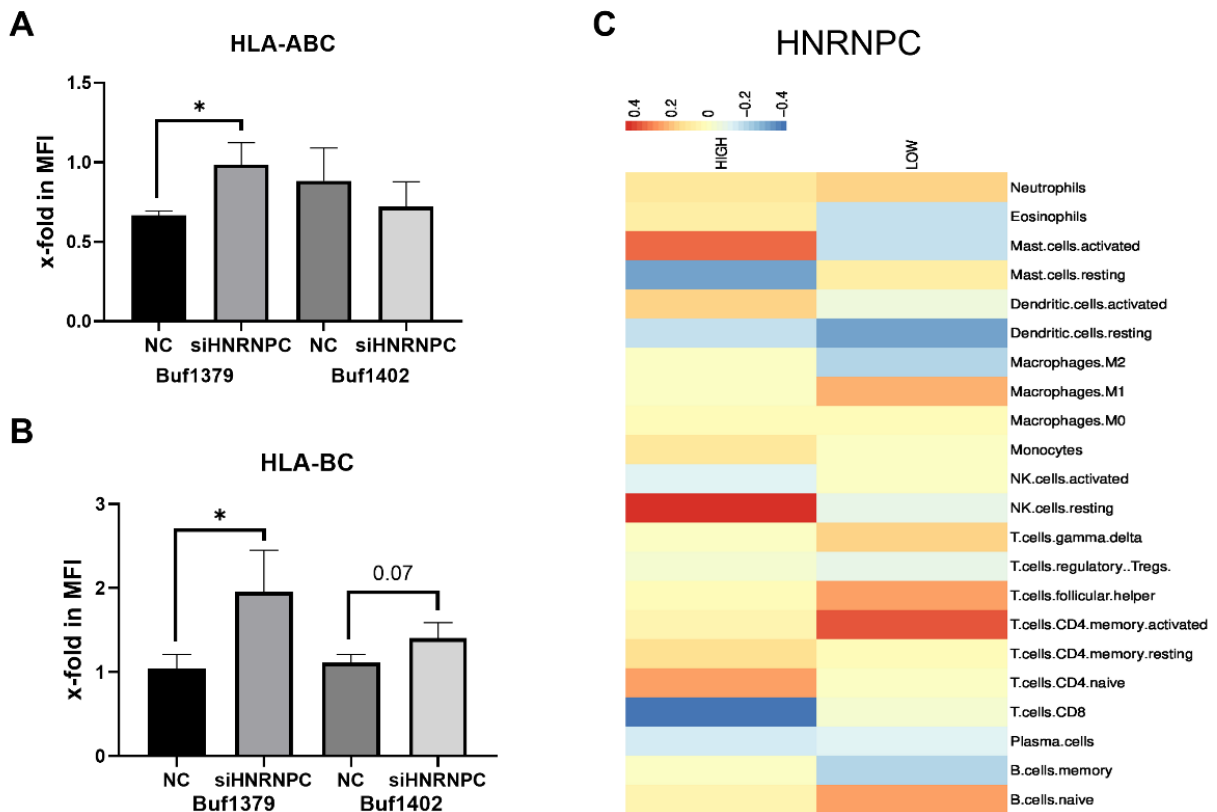
Figure 19 Effect of siRNA-mediated downregulation of hnRNP C on HLA-I cell surface expression and immune cell infiltration

(A-B) The HLA-I surfaces expression of melanoma cells upon transfection with si-HNRNPC and NC was determined by flow cytometry as described in Materials and Methods. Using HLA-ABC and HLA-BC antibodies to stain melanoma cells. The data were presented as x-fold change in the mean fluorescence intensity (MFI) to parental cells (mean ± SD, n = 3 biological replicates). (C) Using CIBERSORT of the TCGA SKMC dataset, the hnRNP C expression was correlated to the immune cell infiltration, and data are presented in a heat map. *p < 0.05.

4.3 Promotion of tumor metastasis via CXCR3-hnRNP C-MIF axis by the crosstalk between melanoma cells and tumor associated macrophages

4.3.1 hnRNP C-mediated induction of melanoma cell metastasis via EMT

Furthermore, the analysis of the clinical relevance of hnRNP C using the dataset "R2: Mixed Melanoma (metastasis) – Hynes – 83 – MAS5.0 – u133a" from R2 genomic analysis web tool. demonstrated that this protein is involved in metastatic progression of melanoma, since higher expression levels were found in metastases compared to primary melanoma lesions (Figure 20 A).
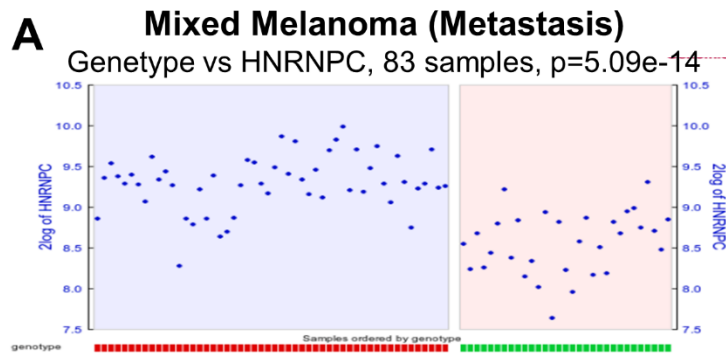
Figure 20 hnRNP C expression in metastasis melanoma and primary melanoma
(A) 83 cases of the melanoma dataset "R2: Mixed Melanoma (metastasis) – Hynes – 83 – MAS5.0 – u133a" from R2 genomic analysis web tool were analyzed for hnRNP C expression in primary (green group) and metastatic melanoma patients (red group).

To validate the database results, growth properties of two melanoma cell lines Buf1379 and Buf1402 transfected with si hnRNP or a control siRNA (NC) were determined. Scratch assays were performed for 48 hrs and 72 hrs after transfection. As shown in Figure 21 A-D, the migration ratio of the knock down hnNRP C group (siHNRNPC) is lower than that of the control group (NC). In both melanoma cell lines, a reduced migration and invasion were found after knock down of hnRNP C suggesting that hnRNP C expression alters their metastatic phenotype in this both melanoma cell lines (Figure 21 E and F).

To verify whether the effect of hnRNP C on melanoma migration and invasion is mediated by EMT in melanoma cells the snail2 and vimentin mRNA expression was determined by Using q-PCR. As shown in Figure 22 A-F, the mRNA expression levels of both genes were downregulated in the siHNRNPC group, but not other markers. Upon subsequent analysis of the protein level, only vimentin is downregulated after knock down hnRNP C (Figure 22 G-I), while snail2 protein levels were not detected. Nevertheless, these data suggest that hnRNP C is involved in melanoma cell metastasis by promoting EMT.
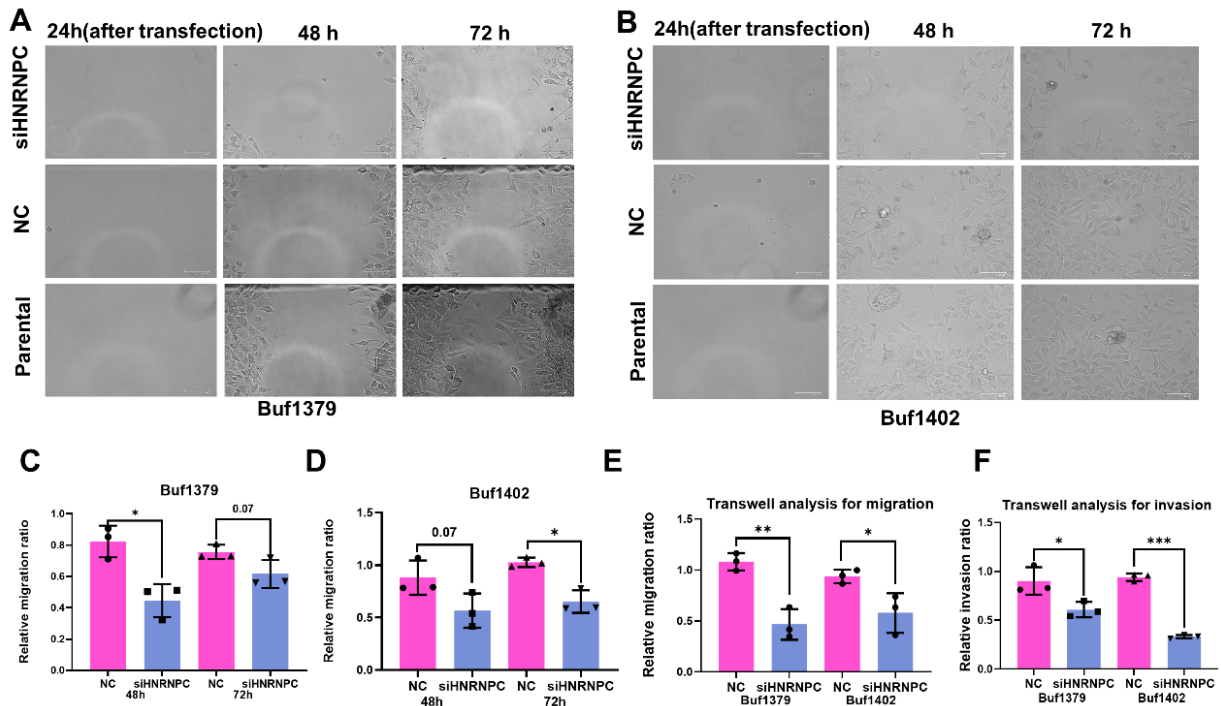
Figure 21 hnRNP C-mediated alteration of melanoma metastasis phenotype
(A-D) with si hnRNPC, si NC and parental groups, the healing wound analysis in melanoma cell lines after transfection 24 hrs, 48 hrs and 72 hrs. (E-F) Using the trans-well experiments, the migration and invasion was determined in melanoma cell lines (mean ± SD, n = 3 biological replicates). *$p < 0.05$, **$p < 0.01$ and ***$p < 0.001$.
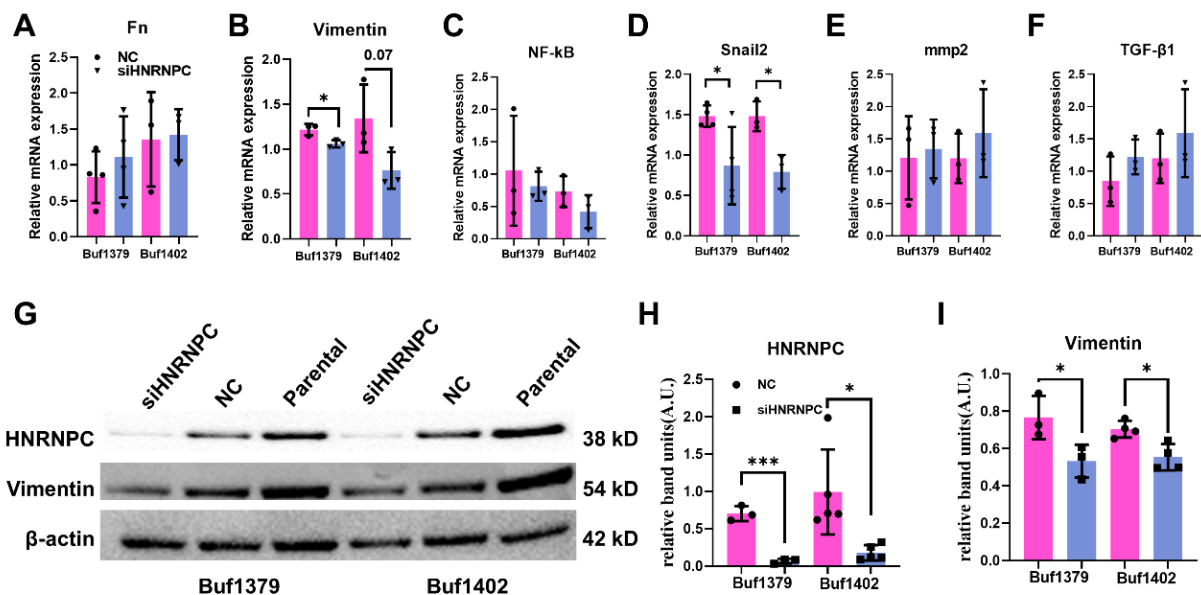

Figure 22 Alterations of EMT markers after knock down hnRNP C
(A-F) The mRNA expression of EMT markers were determined after transfection of si hnRNPC or negative control (NC) for 48 hrs in two melanoma cell lines by RT-qPCR (mean ± SD, n = 3 biological replicates). (G-I) The expression of hnRNP C and vimentin was explored after transfection with si hnRNPC or NC by Western blot analysis as described in Materials and Methods. The relative band intensities (A.U., arbitrary units) were normalized to the

49

corresponding β-actin and compared to parental melanoma cells (mean ± SD, n = 3 biological replicates). *p < 0.05.

4.3.2 TAM-mediated upregulation of tumor-derived hnRNP C and promotion of melanoma cell metastasis

Since the TME also can affect tumor metastasis as described in chapter 1.4, the data set "R2: Mixed Melanoma (metastasis) – Hynes – 83 – MAS5.0 – u133a" was used to explore the immune cell composition. Interestingly, macrophages are highly abundant in the TME of melanoma when compared to other immune cells (Figure 23) suggesting that macrophages, especially TAM, play an important role in tumor metastasis of this disease.
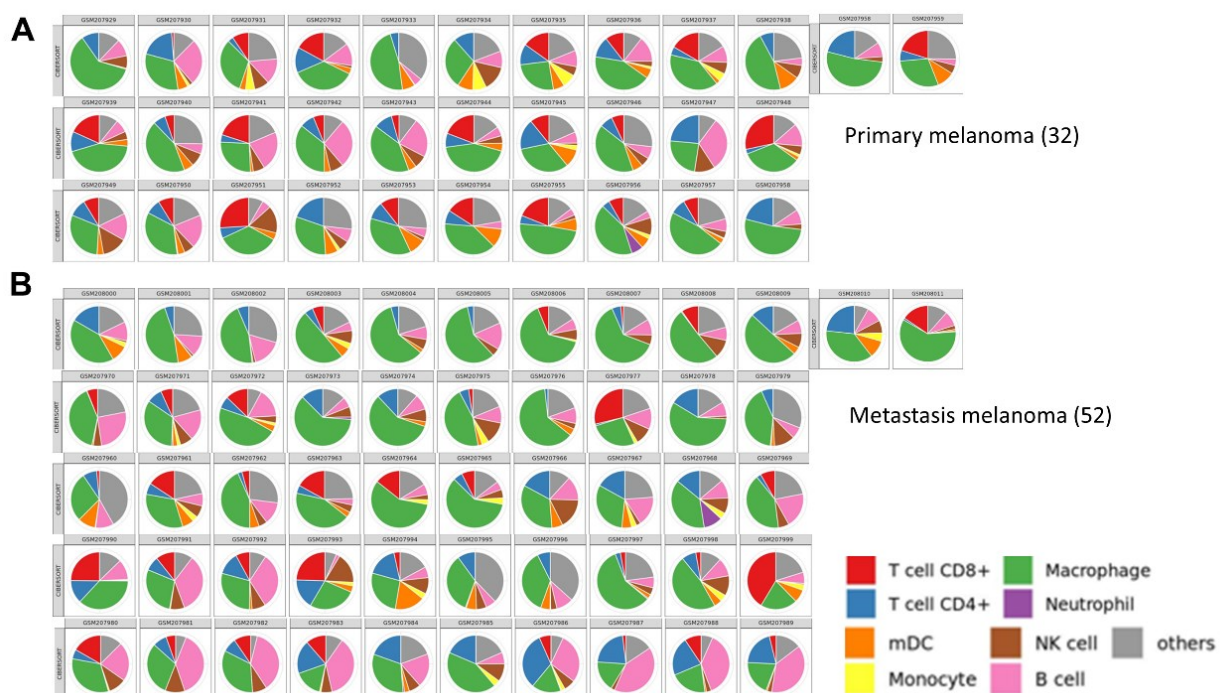
Figure 23 Immune cell infiltration in melanoma patients
In total, 83 cases of the melanoma dataset "R2: Mixed Melanoma (metastasis) – Hynes – 83 – MAS5.0 – u133a" from R2 genomic analysis web tool were analyzed regarding the repertoire of immune cell infiltrate in primary (A) and metastatic patients (B).

Based on this information, co-culture experiments were performed to link the role of macrophages on tumor cell metastasis of melanoma with the function of hnRNP C or not. M0 and TAM were co-cultured with melanoma cells Buf1379 and Buf1402, respectively (Figure 24 A). As shown in Figure 24 B-C, the melanoma cells migrate in TAM and M0 groups, but with a significant difference. While already two hours after scratching, migration changes were most pronounced in the TAM group, while the migration of the parental group remained almost unchanged. Since the two melanoma cells were not in direct contact with the macrophage subpopulation during the co-culture period, it is suggested that this short-term migration effect might be mediated by the exchange of small molecules.
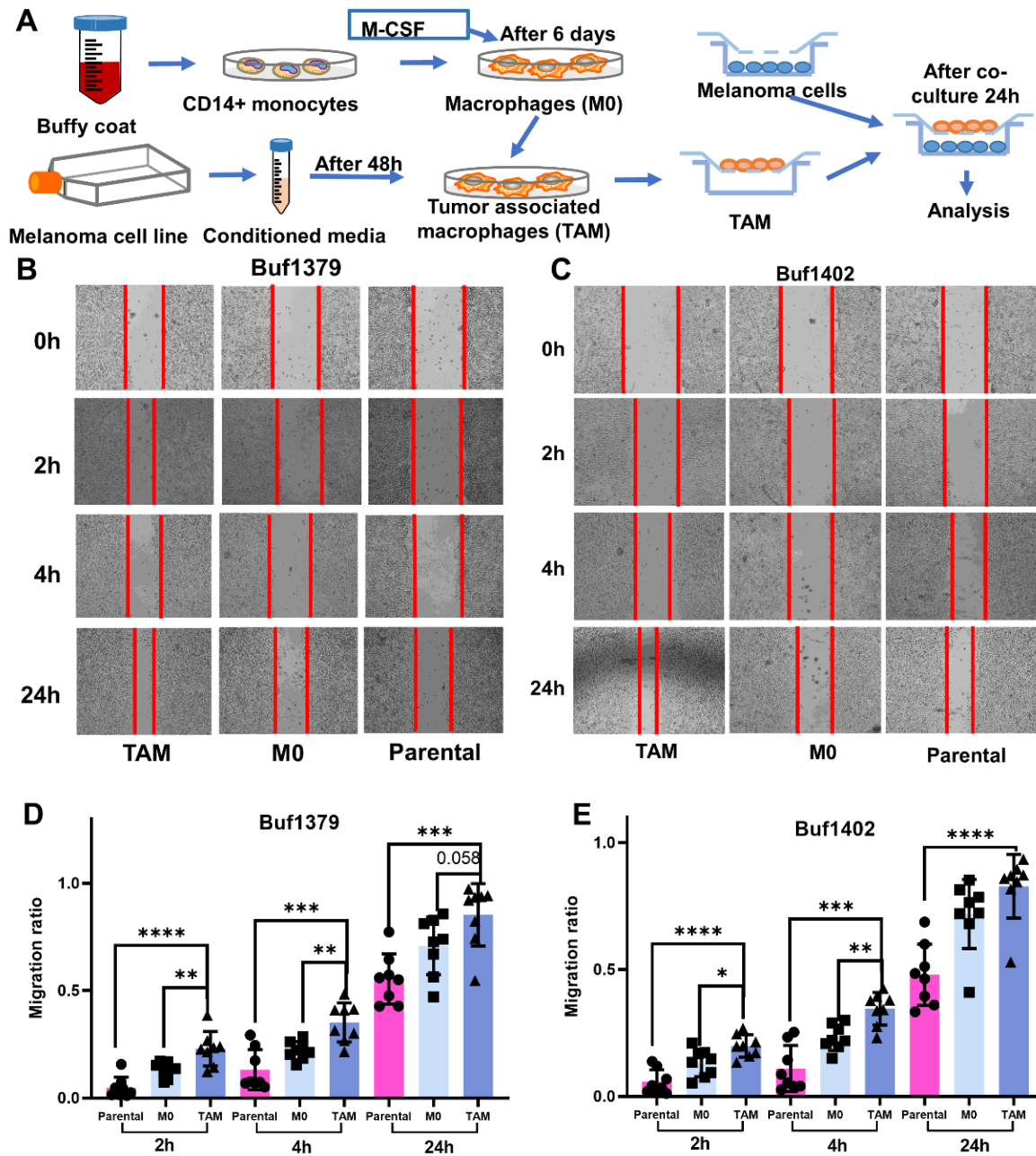
Figure 24 Promotion of melanoma cell migration by co-culture with TAM
Schematic diagram of macrophages isolation and co-culture between M0, TAM, and melanoma cells. (B-E) Using the scratch assay, melanoma cell migration was determined after co-culture with M0 and TAM 0 hrs, 2 hrs, 4 hrs and 24 hrs (mean ± SD, n = 3 biological replicates) and data are presented as migration rate. *p < 0.05, **p < 0.01, ***p < 0.001 and ****p < 0.0001.

After co-culture, qPCR was performed to determine the hnRNP C expression. Interestingly, hnRNP C expression in tumor cells was significantly increased at both the mRNA (Figure 25 A-D) and protein levels (Figure 25 E-F) after co-culture with TAM. This was accompanied by an increased expression of the EMT-related protein vimentin after co-culture (Figure 25 E and

51

G). These data suggest that the tumor metastasis formation caused by TAM might regulate the hnRNP C protein expression.
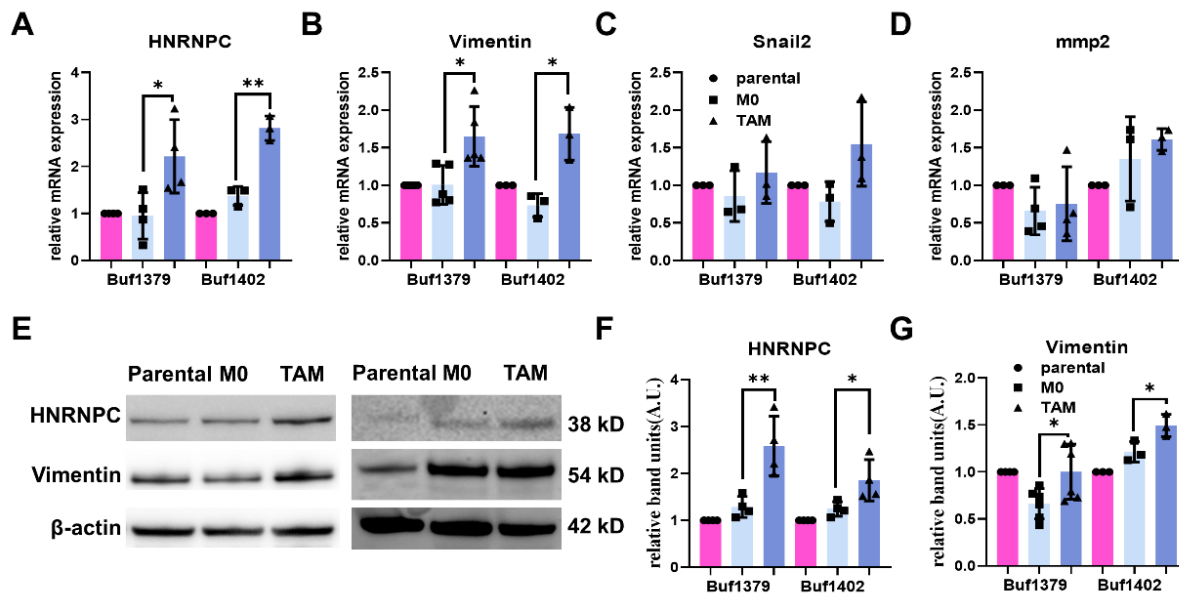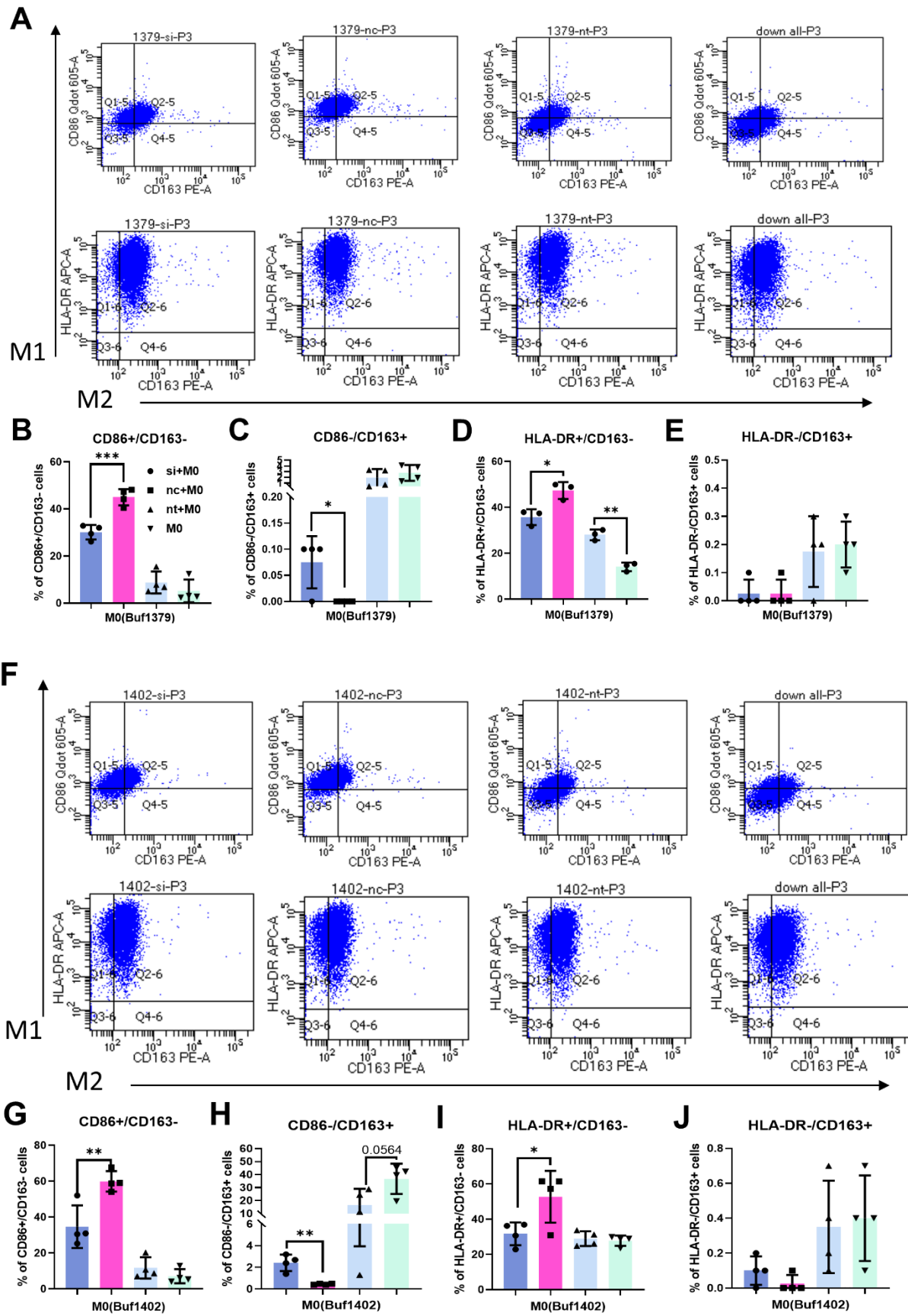

Figure 25 Expression of EMT markers in melanoma cells after co-culture with TAM and M0
(A-D) Using qPCR of as described in Materials and Methods, EMT markers and hnRNP C expression was analyzed in melanoma cells after co-culture with TAM and M0 for 24 hrs and data are presented as relative mRNA expression levels. (E-G) Using Western blot as described in Materials and Methods the protein expression of hnRNP C and vimentin was determined after co-culture. The relative band intensities (A.U., arbitrary units) were normalized same as describe above (mean ± SD, n = 3 biological replicates). *p < 0.05 and **p < 0.01.

In addition, due to the induction of M0 with hnRNP C-transfected culture medium for 48 hrs changes in the macrophage phenotype were observed (Figure 26 A and F). Treatment with the supernatant from hnRNP C-transfected melanoma cell lines decreased the expression of the M1 macrophage marker CD86 (Figure 26 B, G and Q), but increased the expression of the M2 marker CD163 (Figure 26 C and H) in M0 compared to the control group. Furthermore, treatment with melanoma culture medium (nt+M0) resulted in an increased CD86 expression, but a minor decrease of CD163 expression compared to the M0 group. Analysis of the M1 marker HLA-DR yielded the same results demonstrating that the melanoma cell line-induced TAMs favor the M1 phenotype, whereas knock down hnRNP C melanoma cells downregulates the M1 phenotype and upregulates the M2 phenotype. Next to the M1 markers, the M2 marker CD206 was also analyzed (Figure 26 K and P). In Buf1379 cells, the change in the M1 markers was not significant (Figure 26 L-O), while the similar conclusions were reached in the Buf1402 (Figure 26 Q-T).

K

M1
M2

L CD86+/CD206-

M CD86-/CD206+

N HLA-DR+/CD206-

O HLA-DR-/CD206+

P

M1
M2

Q CD86+/CD206-

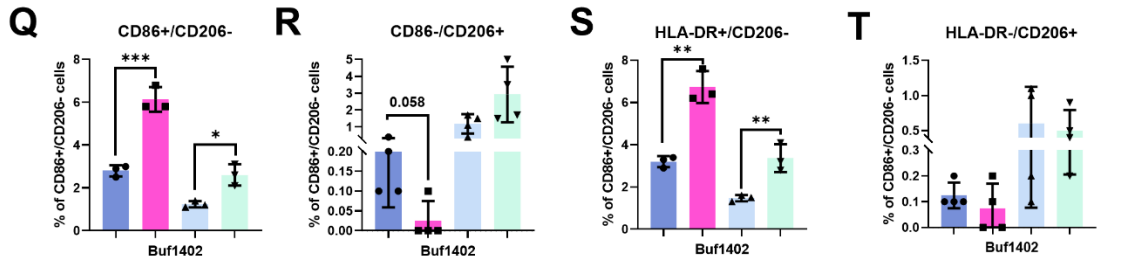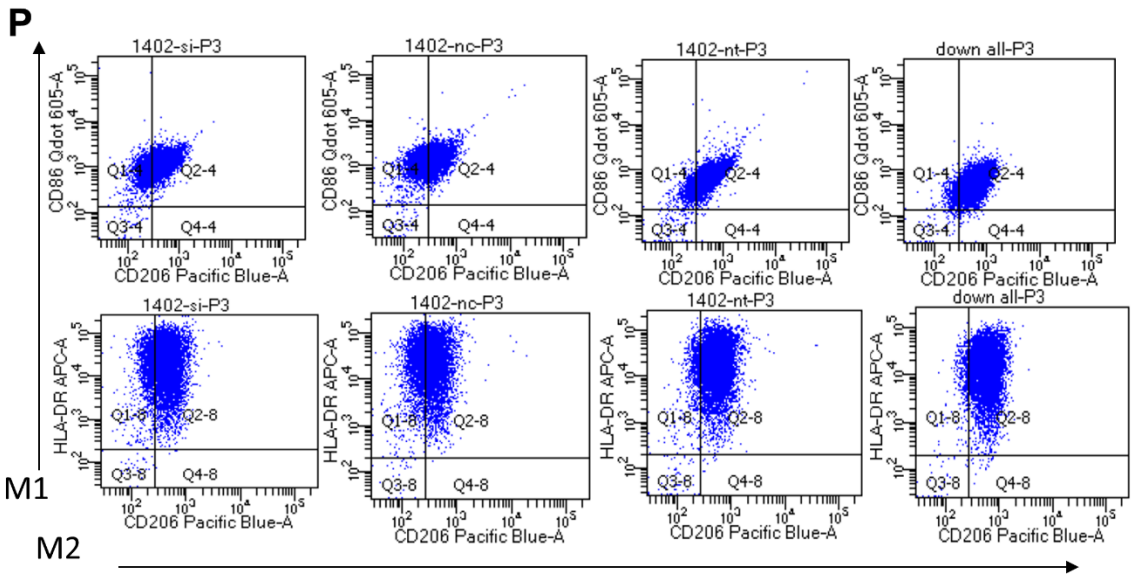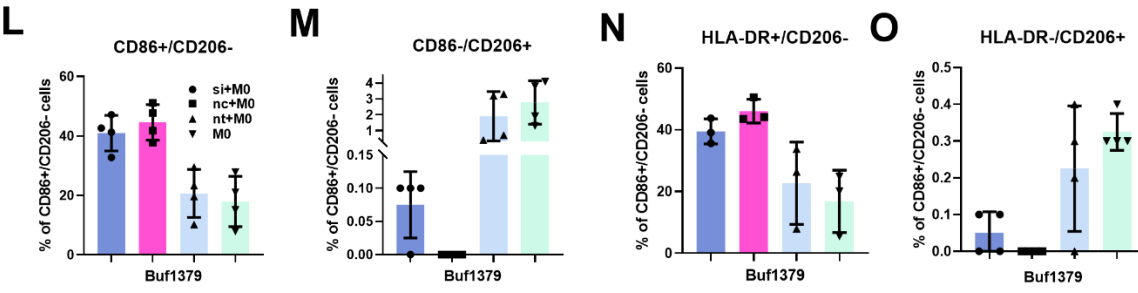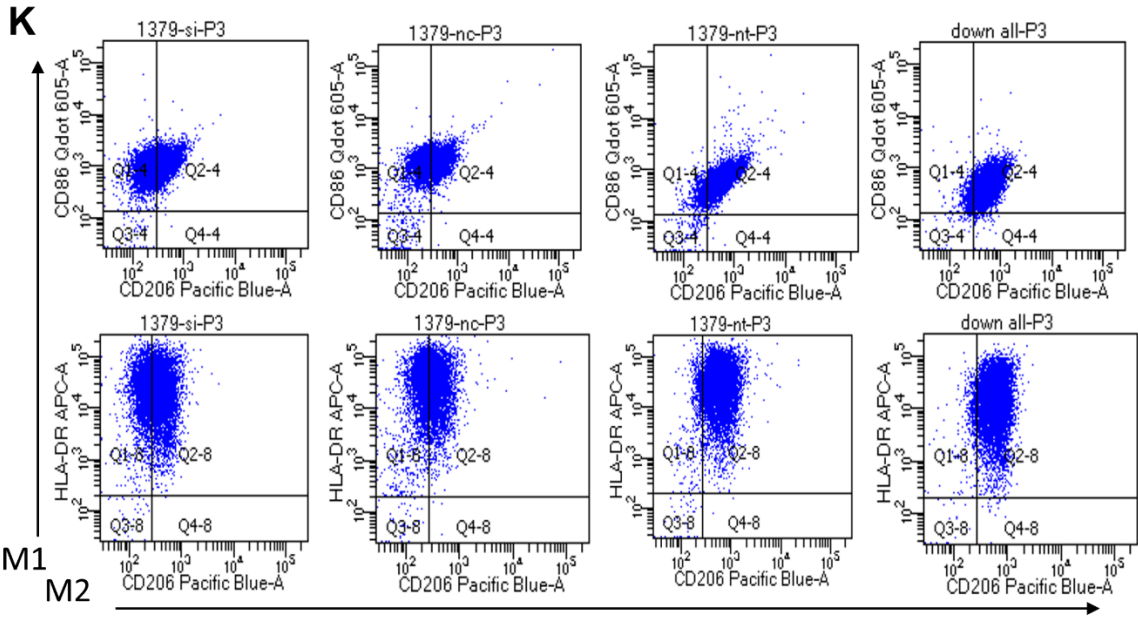**R** CD86-/CD206+

S HLA-DR+/CD206-

T HLA-DR-/CD206+

Figure 26 Expression of macrophage markers after incubation with melanoma conditioned medium

(A-E) The macrophage marker expression on cell surfaces was determined after incubation with Buf1379 melanoma conditioned medium including si hnRNPC, si NC and parental melanoma supernatant by multiple flow cytometry. Analysis of the M1-like macrophages markers CD86 and HLA-DR as well as M2-like macrophages CD163 as CD86+/CD163- (B), CD86-/CD163+ (C), HLA-DR+/CD163- (D) and HLA-DR-/CD163+ (E) in macrophages. (F-J) the same multiple flow cytometry analysis of macrophage marker expression after incubating with Buf1402 melanoma conditioned medium. (K-O) Analysis of macrophage marker expression on cell surfaces after the same induction for macrophages incubating with Buf1379 melanoma conditioned medium including si hnRNPC, si NC and parental melanoma supernatant by multiple flow cytometry. The analysis of M1-like macrophage markers CD86 and HLA-DR as well as M2-like macrophage markers CD206 as CD86+/CD206- (L), CD86-/CD206+ (M), HLA-DR+/CD206-(N) and HLA-DR-/CD206+ (O) in macrophages. (P-T) the same multiple flow cytometry analysis after incubation with Buf1402 melanoma conditioned medium. The data were presented as mean fluorescence intensities (MFI) to parental cells (mean ± SD, n = 3 biological replicates*$p < 0.05$, **$p < 0.01$ and ***$p < 0.001$.

4.3.3 Altered secretion of cytokines of TAM and melanoma cells upon co-culture

The cytokine analysis of the cell supernatants from the co-culture experiments was determined to investigate the underlying mechanism of the TAM-mediated upregulation of hnRNP C. As shown in Figure 27 A and B, a heterogenous cytokine release was found under the various conditions analyzed. The major tumor-derived cytokines were VEGF, IGFBP2 and MIF. Other cytokines, such as angiopoietin, are also highly variable after co-culture, and macrophages themselves secrete a lot of angiopoietins.
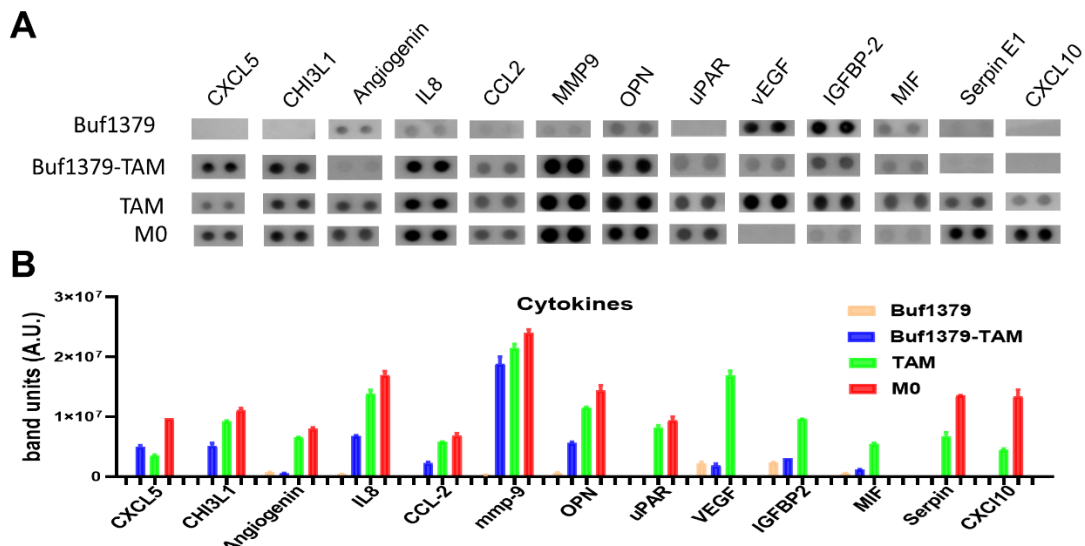

Figure 27 Analysis of the cytokine concentration in the supernatants after co-culture
(A-B) Using cytokine analysis kit the cytokine secretion into the supernatant of the different groups including the parental Buf1379 group, Buf1379 and TAM co-culture group, TAM incubation with Buf1379 parental conditioned medium group and the M0 group. The relative band intensities (A.U., arbitrary units) were normalized same as describe above (mean ± SD, n = 2 biological replicates).

To determine the link between the major tumor-derived cytokines VEGF, IGFBP2 and MIF, the mRNA expression levels upon knock down of hnRNP C or co-culture with macrophages were determined. As shown in Figure 28 A-C, MIF was significantly downregulated when hnRNP C was decreased, while VEGF and IGFBP2 were only minor affected. Vice versa, MIF expression was found significantly upregulated when hnRNP C was increased, but VEGF and IGFBP2 not (Figure 28 D-F). Based on these data, the two cytokines MIF and VEGF were selected for ELISA. From M0 to TAM groups, MIF concentration in the supernatant is gradual higher than parental group suggesting MIF is downstream of hnRNP C (Figure 28 I-J).
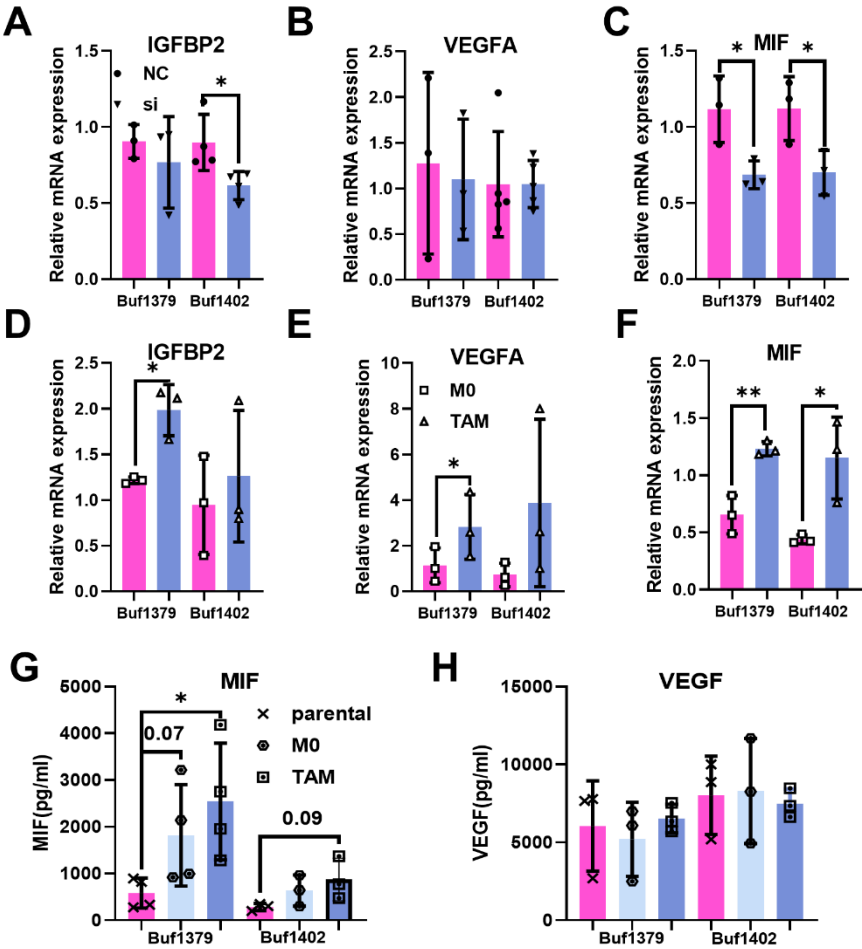

Figure 28 Melanoma-derived cytokines analysis for supernatant after co-culture
(A-C) The mRNA expression of MIF, VEGFA and IGFBP2 was determined after knock down of hnRNPC in two melanoma cell lines and (D-F) after co-culture of melanoma cells with TAM and M0 by qPCR and presented as relative mRNA expression levels, while (I and J) theMIF and VEGF secretion was analyzed after co-culture of two melanoma cell lines with TAM and M0 by ELISA (mean ± SD, n = 3 biological replicates) and presented as a bar chart in pg/ml. *p < 0.05 and **p < 0.01.

As already shown, the expression of markers associated with the M1 phenotype increased after co-culture of macrophages with melanoma cells. Using a CIBERSORT analysis of a TCGA-SKCM dataset, the cytokine with the highest correlation to the M1 phenotype of

macrophages was CXCL10 (Figure 29). This is in line with our cytokine analyses, which also identified CXCL10 and some other macrophage-derived cytokines to be significantly altered (Figure 27 B).
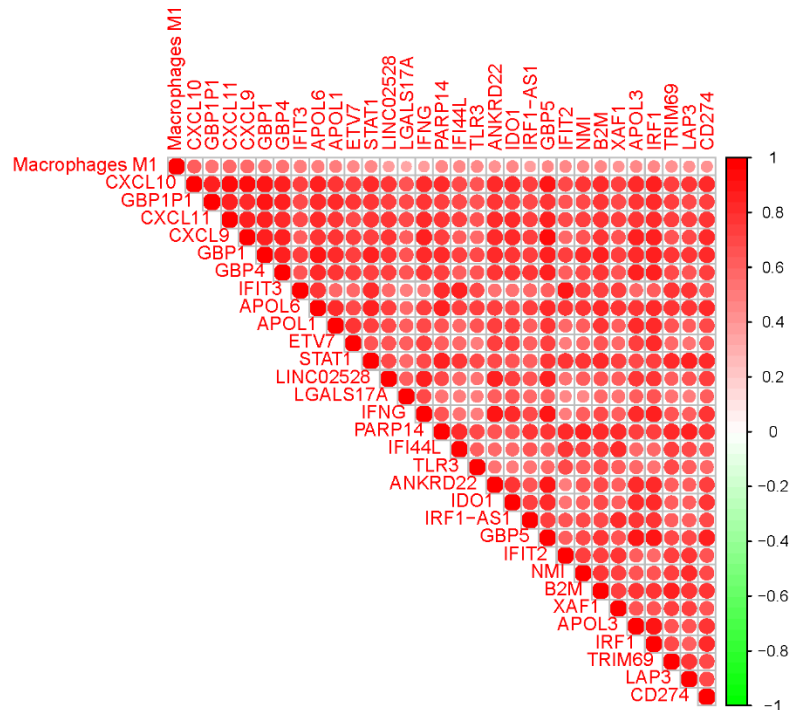

Figure 29 Correlation of cytokine expression with the M1-like macrophage phenotype in melanoma patients
The relevance of cytokines and M1-like macrophages was determined via the CIBERSORT website and R language using the TCGA-SKCM dataset. Green dots represent a negative correlation, red dots a positive correlation.

Subsequently, CXCL10, IL8 and CCL2 were selected for further explore these data and the relevance to macrophages. The concentration of CXCL10 gradually increased from parental group to the TAM group in the two melanoma cell lines as determined by ELISA (Figure 30 A), while IL8 and CCL2 directly increased after co-cultivation and did not show a gradual increase (Figure 30 B and C). Comparison of M0 and post-induction macrophages demonstrated an increased concentration of CXCL10 after induction (Figure 30 D). In contrast, no increase in the CCL2 and IL8 concentrations was detected in the melanoma cell supernatants (Figure 30 E and F) suggesting a possible interaction of CXCL10 with melanoma cells.

Finally, neutralizing Abs to inhibit CXCL10 and its receptor were employed to verify whether CXCL10 is an intermediate mediator of the upregulation of hnRNP C, while other receptors served as a control. As shown in Figure 31 A, the TAM-mediated upregulation of hnRNP C of the two melanoma cell lines Buf1379 and Buf1402 was inhibited by treatment with the anti-CXCR3 Ab, while others are not (Figure 31 A-C) suggesting that TAMs upregulate hnRNP C via CXCR3.
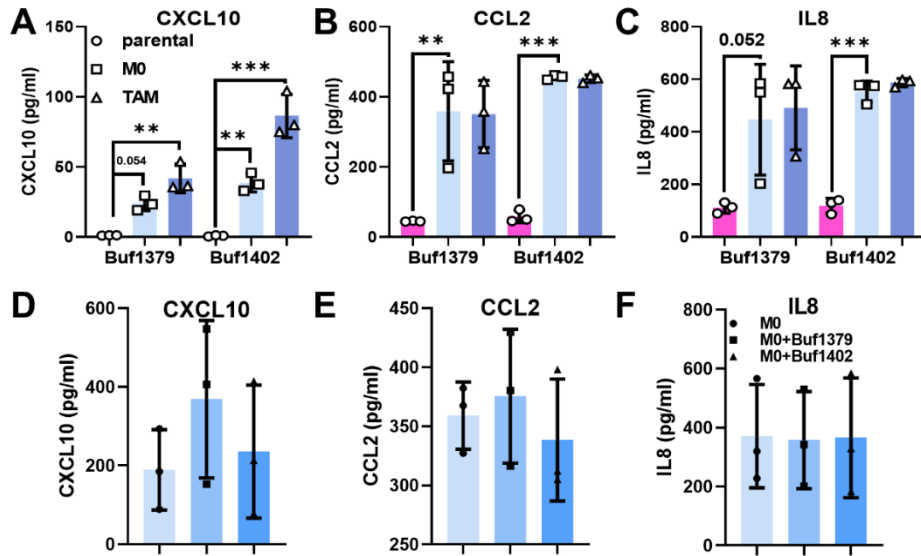
Figure 30 Macrophage-derived cytokine analysis in the supernatant after co-culture
(A-C) The concentration of CXCL10, IL8 and CCL2 in different supernatant groups after co-culture with two melanoma cell lines was explored via ELISA and the results were presented in bar graphs in pg/ml of the respective cytokine. (D-F) The concentration of CXCL10, IL8 and CCL2 in M0, supernatants from M0 co-cultured with Buf1379 and Buf1402, respectively (mean ± SD, n = 3 biological replicates) was determined by ELISA and the results are presented as bar charts in pg/ml of the respective cytokine. **p < 0.051 and ***p < 0.001.
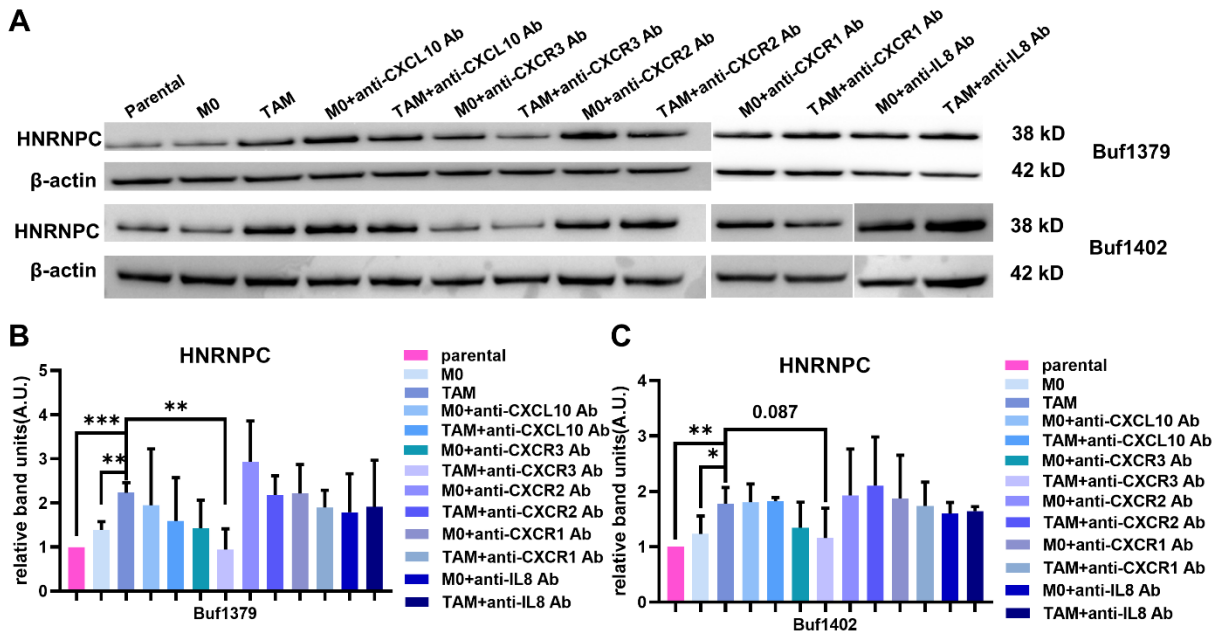

Figure 31 Effect of cytokines and their receptors on hnRNP C expression in different co-culture conditions
(A-C) Using Western Blot the hnRNP C expression was analyzed after antibody neutralization including anti-CXCL10, anti-CXCR1, anti-CXCR2, anti-CXCR3 and anti-IL8 Ab in M0 and TAM as well as parental groups with two melanoma cell lines Buf1379 and Buf1402 (mean ± SD, n = 3 biological replicates). **p < 0.01 and ***p < 0.001. The relative band intensities (A.U., arbitrary units) were normalized same as describe above (mean ± SD, n = 3 biological replicates).

5 Discussion

The aim of this thesis is to study the effect of posttranscriptional regulation of the HLA-I APM component tpn and its effect on the HLA-I antigen processing and presentation pathway and CD8^{+}T cell infiltration in melanoma. Own published data and this study have demonstrated that one major tumor immune escape mechanism is the deficient expression of HLA-associated molecules in tumors[56 118 119]. This abnormality can be caused by genetic abnormalities or downregulation of the e.g. HLA-I HC[120]. In addition, epigenetic or post-transcriptional regulation can also control the HLA-I associated molecule expression[33 47]. These different causes gave rise to the same result: HLA class I defects and tumor immune escape. Furthermore, the low expression of HLA-I APM components, like e.g. TAP1, tpn, LMP2, HLA-A and HLA-B, correlated with a poor patients' survival in several cancers, including melanoma[19 34 121 122]. Tpn as a part of peptide loading complex, is a major component in the antigen processing and presentation pathway involved in the immune evasion of tumors due to its downregulation[17]. Our *in silico* analyses demonstrated that patients with a high expression of tpn have a better OS, while tpn loss was found in metastatic melanoma leading to a worse patients' outcome.

MiRNAs, a family of approximately 20nt small single-stranded non-coding RNAs, are very powerful regulators of the post-transcriptional gene expression[41]. We have identified miR-155-5p to target tpn, but this targeting did not lead to the conventional negative regulation of tpn expression. Several studies have revealed that, like most miRNAs, miR-155-5p down-regulates target proteins thereby affecting cell proliferation, expression of immune modulatory molecules, like PD-L1, and the extracellular microenvironment in different cancers including melanoma as well as in other diseases[31 110 123 124]. We also identified that miR-155-5p downregulated PD-L1 in MZ-Mel2 melanoma cell line. However, in contrast to these negative effects, our results demonstrated a new miR-155-5p function leading to an upregulation of tpn via binding with a silencer directly. Since proper HLA-I surface expression on melanoma is required for recognition by CD8+ cytotoxic T lymphocytes (CTL), the CIBERSORT web tool was used to determine the effect of miR-155 on tpn and consequently on the HLA-I signaling pathway, which might alter the interaction between melanoma cells and immune cells[4]. The CD107a degranulation assay demonstrated that the higher HLA-I surface expression via miR-155-5p-mediated enhanced tpn levels was accompanied by a reduced NK cell recognition. Thus, since miR-155-5p directly binds to tpn 3'UTR, the tpn mRNA expression and stability was upregulated thereby affecting its protein level. Most importantly, the increased tpn protein

levels enhanced the antigen processing and presentation pathway resulting in increased HLA-I surface expression of human melanoma cells (Figure 32).
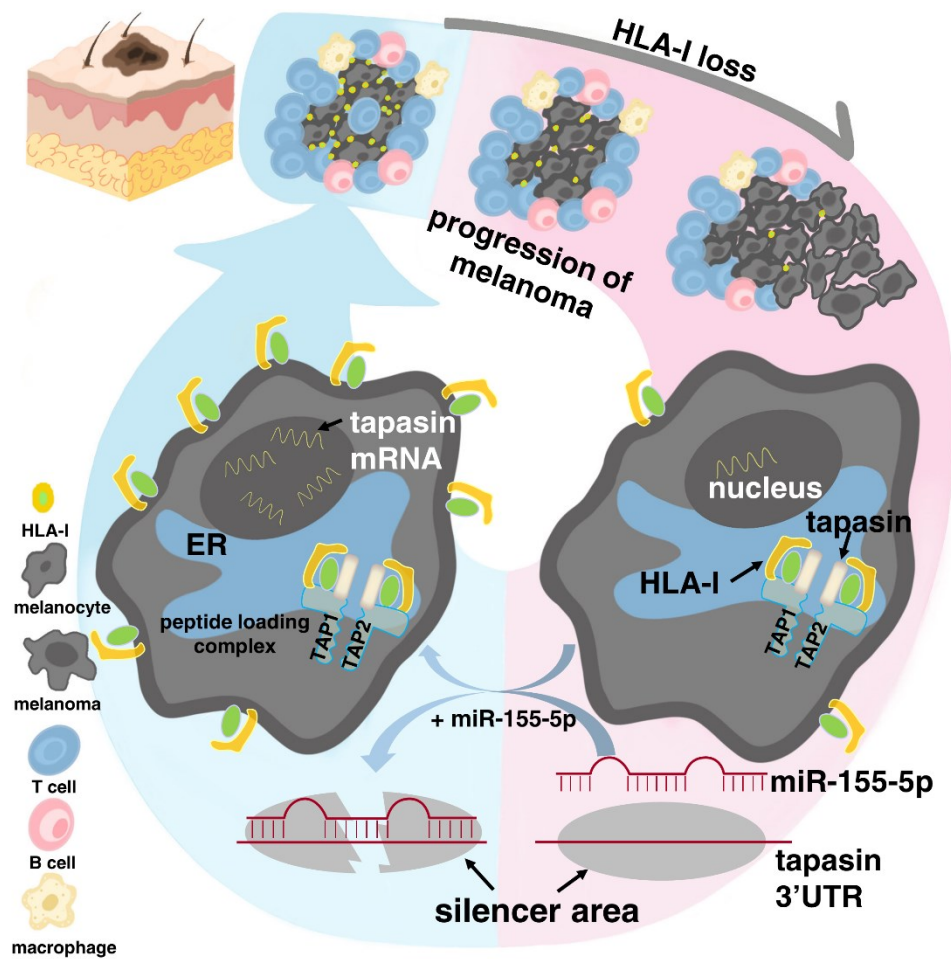

Figure 32 miR-155-5p-mediated inhibition of the silencer area and activation of the antigen processing and presentation pathway

So far, miRNAs unconventional functions are mainly classified into three categories: (i) competitive binding with some inhibitory proteins, (ii) direct interaction with some functional components and (iii) unconventional regulation directly in the nucleus [51]. So far, miR-155-5p has been reported to positively control colon cancer cell migration via direct binding to an AU-rich element present in the HuR 3'UTR[125] suggesting a miRNA-mediated RNA activation, but this mechanism is different as the one described in the thesis. Intriguing, this kind of miRNA-mediated RNA activation always occurs on the specific binding sequences, like AU-rich elements and the silencer identified in this work. Figure created independently with PowerPoint and Procreate.

To date, silencers, important genomic regulatory elements in homeostasis and disease, have not yet been explored in detail and the knowledge of the silencer characteristics are not

abundant and uniform according to the latest literature[76 83 84]. Using luciferase assays and CRISPR/Cas9 the sequence, which was suggested as a silencer from database and other publication[85],was verified. So far, the role of silencers in the expression of genes involved in the immunogenicity of tumors and/or anti-tumoral immune responses had not yet been analyzed and characterized by others. Our study identified for the first time a direct upregulation of tpn mRNA by miR-155-5p, which was associated with its binding to a silencer. This process resulted in increased HLA-I surface antigens leading to an increased recognition by CD8+ CTL, but a reduced NK cell cytotoxicity (Figure 32). Thus, due to the interaction between miRNA and a directly bound silencer, we provide evidence of a novel mechanism leading to an upregulation of the immune modulatory tpn expression, which might have also an impact on T cell-based immunotherapies.

During progression of melanoma, HLA-I surface expression is gradually lost and the expression of tpn decreases[126]. Upon transfection into melanoma cell lines, miR-155-5p binding to a silencer sequence in the tpn 3'UTR disrupts the function of the silencer and promotes the transcription of the tpn mRNA. The upregulation of tpn enhances the antigen processing and presentation pathway thereby leading to increased HLA-I surface antigens for immune cell recognition.

In addition, our study identified RNA binding proteins on 3'UTR of tpn. Mass spectrometry and *in silico* analysis as well as molecular biology experiments showed that hnRNP C binds to the tpn 3'UTR and down-regulation of hnRNP C significantly increases the expression of tpn thereby improving the expression of HLA-I on the surface of melanoma cells (Figure 33). HnRNP C is a member of the subfamily of ubiquitously expressed hnRNPs, while the mechanisms of action in tumors have not yet been well defined when a high expression in tumors was described[127]. During the last few years, hnRNP C and tumor-associated studies were mainly correlated with tumor phenotypes like proliferation and migration[70 127-131], which affected the survival of patients[72 132], while the tumor immune escape has not been addressed. So far, only little information is available about the impact of miRNAs on the HLA class I molecules[34 119] and the effects of RBPs on these molecules are mainly unexplored.
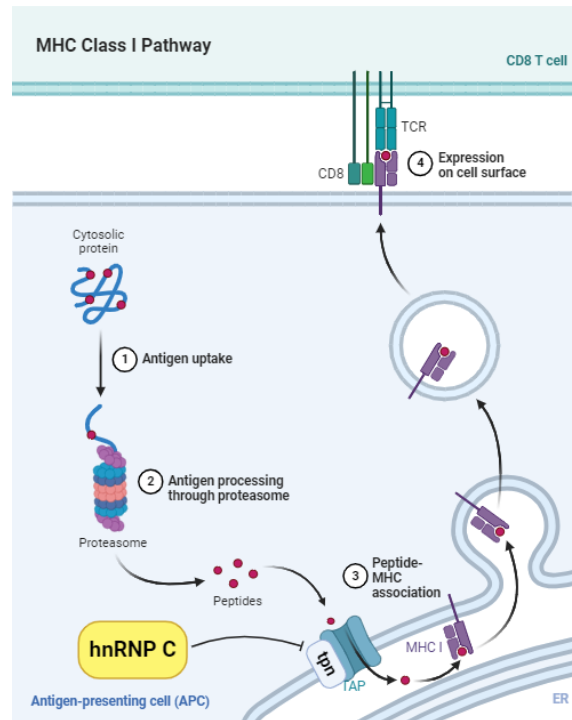
Figure 33 hnRNP C targets TAP-associated glycoprotein tapasin in melanoma and inhibition HLA-I pathway. (Created with BioRender.com).

Our finding is in accordance with recent studies indicating that lower expression of hnRNP C is associated with a better outcome of patients with many different cancer types. Two datasets about melanoma patients revealed that the expression of hnRNP C is usually associated with the patients' outcome. In addition, the expression of hnRNP C is different in paired tumor and normal tissues. Our analysis data also match these observed in earlier studies[133][134] that almost all the cancer types from TCGA dataset showed higher hnRNP C transcript levels in tumors. As shown in this study, both hnRNP C and tpn have a clinical relevance due to hnRNP C has a strong negative correlation with tpn in many cancer types. In our previous work, hnRNP C has been identified to bind to the tpn 3'UTR. Subsequently, more *in silico* analysis and co-immunoprecipitation experiments were performed and confirmed our results. HnRNP C even has a powerful negative link with components of the APM, which might be due to the binding of hnRNP C to tpn.

In eukaryotes, genes are also subjected to processing, translocation, and stabilization prior to translation, and the transcriptional process and post-transcriptional co-regulation is strictly controlled by RBPs, which bind to the 3'UTR of respective mRNAs[135] leading to negative regulatory effects[136][137]. Dependent on these findings, our results also reveal that at the mRNA and protein level, hnRNP C can negatively regulate tpn expression. In addition, the mRNA levels of other molecules, such as HLA-B and HLA-C as well as the HLA-I HC, were also

upregulated upon hnRNP C knockdown. One possible explanation might be that hnRNP C also bind to the HLA-I 3'UTR. However, the immunoprecipitation demonstrated that hnRNP C only interact with tpn, not with HLA-I. Furthermore, after hnRNP C knock down, HLA-ABC and HLA-BC levels on cell surface were altered, which was accompanied by a reduced tumor infiltration with CD8^{+} T cells illustrating the role of hnRNP C on tpn and the HLA class I pathway.

In addition, our study also found that hnRNP C expression was much higher in melanoma metastases than in primary tumors. Analysis of the role of hnRNP C in melanoma metastasis demonstrated an upregulation of hnRNP in melanoma metastasis via modulating the expression of the EMT marker vimentin confirming previous studies in other tumor entities[72 74].

Since TAMs play an important role in tumor metastasis formation[119 138-141]., we determined the role of TAMs in our melanoma models. Our data demonstrated an accelerated metastatic phenotype of melanoma cells after co-culture with TAMs, a correlation between hnRNP C and macrophages in melanoma metastasis formation has not yet been analyzed. Interestingly, as hypothesized, co-culture with M0 macrophages and TAMs can upregulate hnRNP C and vimentin suggesting that TAMs led to metastasis, which might be partially mediated by the regulation of hnRNP C. One must guess that the two types of cells that are not in contact are interacting with each other via cytokines.

In the TME, many different types of cells transmit information and interact with each other through cytokines[142]. To date, there exist only a few studies on TAM-related cytokines, like the CCL2/CCR2 axis, which recruit large numbers of macrophages to condition immune suppression in multiple tumors[143 144] and are mainly expressed on macrophages of the M2-like immune-stimulatory phenotype. The difference between the M2 type and the M1-like immune-stimulatory phenotype is the secretion of CXCL10 in tumors[145]. This was confirmed in our study, since the TAM also secreted more CXCl10, but the TAMs induced by melanoma cells were mainly of the M1, rather than the M2 phenotype reported in most publications[146 147]. Our *in silico* analysis and experimental data as well as the data from Luo and co-authors support that CXCL10 could be secreted from M1 phenotype macrophages. It is noteworthy that based on single cell sequencing, TAMs were no longer only categorized into the M1 and M2 phenotype, but rather classified into multiple categories based on their location, function and cytokine release[148 149]. According to their classification, the TAMs in our study favored the IFN-TAM phenotype characterized by secretion of more CXCL10 and the expression of the M1-like markers CD86 and MHC-II[148]. In our study, the M0 group can be regarded as the group that progresses to TAMs with a gradually increase of CXCL10 expression from M0 to TAMs suggesting that CXCL10 plays a role in the progressive induction of TAMs. The function of

CXCL10 is the upregulation of hnRNP C, which was confirmed after blockade of its receptor CXCR3 using a neutralizing Ab. However, it is puzzling that blockade of CXCL 10 did not very significantly inhibit the upregulation of hnRNP C. At the same time, analysis of tumor-derived cytokines also pointed to MIF as a downstream molecule that might be the primary molecule inducing macrophages to become IFN-TAM (Figure 34). This has also recently described by Zhao and co-workers demonstrating that MIF is capable of inducing and reprogramming the macrophage phenotypes[150].
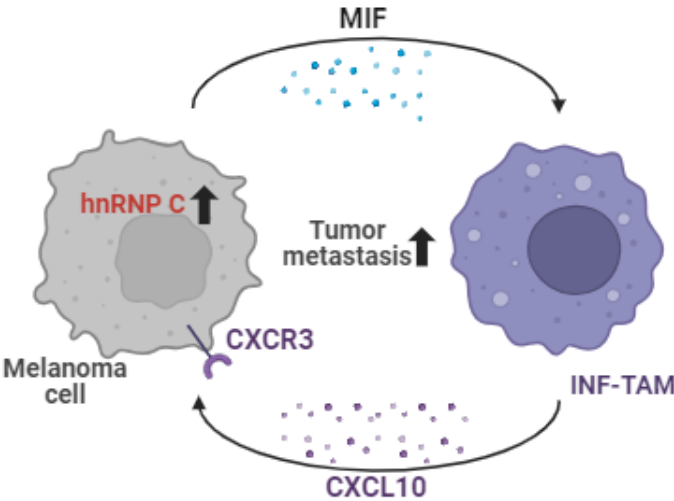

Figure 34 Tumor metastasis by the crosstalk between melanoma cells and TAM via CXCR3-hnRNP C-MIF axis. (Created with BioRender.com).

6 Conclusion

Tumor immunotherapy and an available strategy for combinations of immunotherapy have not been extensively explored. In this study, we identified that miR-155-5p and hnRNP C can bind to the 3'UTR of tpn. For miR-155-5p, a new unconventional function of miRNAs was found that lead to an upregulation of its target protein tpn by binding to a silencer. In detail, overexpression of miR-155-5p upregulated the expression of tpn in different human melanoma cell lines, which resulted in an increased HLA-I surface expression thereby enhancing the antigen processing and presentation pathway. Moreover, some characteristics of silencers were present as in the miR-155-5p binding sequence in the 3'UTR of tpn, such as an overlap with DNase I hypersensitivity sites, a high GC content and methylated histones H3K27me3. The intrinsic suppressive activity of this sequence was confirmed after deletion of the miR-155-5p binding sequence in the 3'UTR of tpn in the reporter plasmid as well as within the genome of the melanoma cell line FM3. This is the first report (i) identifying a silencer in the 3'UTR of tpn, (ii) which directly interacts with a non-coding RNA and (iii) has clinical relevance. These data extend the function of miRNAs and add new insights to our knowledge of silencers, which might have implications for immunotherapy in the future.

For hnRNP C, one of the most important members of the hnRNPs family, which has been associated with tumor progression[72 131 151 152]. In this study, hnRNP C led to an inhibition of tpn expression, while the knock down of hnRNP C can upregulate tpn expression thereby enhancing HLA-I surface expression and CD8^{+} T cell recognition. At the same time, we also explored melanoma cells and macrophages interaction with each other through the CXCR3-hnRNP C-MIF axis to promote tumor cell metastasis, providing a deeper understanding of the phenotypic diversity of TAM. These results suggest that hnRNP C is a potential biomarker of melanoma metastasis and provide a new perspective to further elucidate cellular interactions within the TME, which has an important implication for the implementation of T cell-based immunotherapies.

7 References

1. Bukur J, Jasinski S, Seliger B. The role of classical and non-classical HLA class I antigens in human tumors. *Semin Cancer Biol* 2012;22(4):350-8. doi: 10.1016/j.semcancer.2012.03.003 [published Online First: 20120324]

2. Hulpke S, Tampe R. The MHC I loading complex: a multitasking machinery in adaptive immunity. *Trends Biochem Sci* 2013;38(8):412-20. doi: 10.1016/j.tibs.2013.06.003 [published Online First: 20130710]

3. Leone P, Shin EC, Perosa F, et al. MHC class I antigen processing and presenting machinery: organization, function, and defects in tumor cells. *J Natl Cancer Inst* 2013;105(16):1172-87. doi: 10.1093/jnci/djt184 [published Online First: 20130712]

4. Wang Y, Jasinski-Bergner S, Wickenhauser C, et al. Cancer Immunology: Immune Escape of Tumors-Expression and Regulation of HLA Class I Molecules and Its Role in Immunotherapies. *Adv Anat Pathol* 2023;30(3):148-59. doi: 10.1097/PAP.0000000000000389 [published Online First: 20221215]

5. Baker DJ, Arany Z, Baur JA, et al. CAR T therapy beyond cancer: the evolution of a living drug. *Nature* 2023;619(7971):707-15. doi: 10.1038/s41586-023-06243-w [published Online First: 20230726]

6. Hormuth DA, 2nd, Farhat M, Christenson C, et al. Opportunities for improving brain cancer treatment outcomes through imaging-based mathematical modeling of the delivery of radiotherapy and immunotherapy. *Adv Drug Deliv Rev* 2022;187:114367. doi: 10.1016/j.addr.2022.114367 [published Online First: 20220530]

7. Lybaert L, Vermaelen K, De Geest BG, et al. Immunoengineering through cancer vaccines - A personalized and multi-step vaccine approach towards precise cancer immunity. *J Control Release* 2018;289:125-45. doi: 10.1016/j.jconrel.2018.09.009 [published Online First: 20180914]

8. Jang A, Lichterman JN, Zhong JY, et al. Immune approaches beyond traditional immune checkpoint inhibitors for advanced renal cell carcinoma. *Hum Vaccin Immunother* 2023;19(3):2276629. doi: 10.1080/21645515.2023.2276629 [published Online First: 20231110]

9. Dersh D, Holly J, Yewdell JW. A few good peptides: MHC class I-based cancer immunosurveillance and immunoevasion. *Nat Rev Immunol* 2021;21(2):116-28. doi: 10.1038/s41577-020-0390-6 [published Online First: 20200820]

10. Ruffin AT, Li H, Vujanovic L, et al. Improving head and neck cancer therapies by immunomodulation of the tumour microenvironment. *Nat Rev Cancer* 2023;23(3):173-88. doi: 10.1038/s41568-022-00531-9 [published Online First: 20221201]

11. Wu J, Wu W, Zhou B, et al. Chimeric antigen receptor therapy meets mRNA technology. *Trends Biotechnol* 2024;42(2):228-40. doi: 10.1016/j.tibtech.2023.08.005 [published Online First: 20230921]

12. Boelaars K, van Kooyk Y. Targeting myeloid cells for cancer immunotherapy: Siglec-7/9/10/15 and their ligands. *Trends Cancer* 2023 doi: 10.1016/j.trecan.2023.11.009 [published Online First: 20231229]

13. Garrido F, Aptsiauri N. Cancer immune escape: MHC expression in primary tumours versus metastases. *Immunology* 2019;158(4):255-66. doi: 10.1111/imm.13114 [published Online First: 20191001]

14. Garrido F, Perea F, Bernal M, et al. The Escape of Cancer from T Cell-Mediated Immune Surveillance: HLA Class I Loss and Tumor Tissue Architecture. *Vaccines (Basel)* 2017;5(1) doi: 10.3390/vaccines5010007 [published Online First: 20170227]

15. Garrido F. HLA Class-I Expression and Cancer Immunotherapy. *Adv Exp Med Biol* 2019;1151:79-90. doi: 10.1007/978-3-030-17864-2_3

16. Wu X, Li T, Jiang R, et al. Targeting MHC-I molecules for cancer: function, mechanism, and therapeutic prospects. *Mol Cancer* 2023;22(1):194. doi: 10.1186/s12943-023-01899-4 [published Online First: 20231202]

17. Dhatchinamoorthy K, Colbert JD, Rock KL. Cancer Immune Evasion Through Loss of MHC Class I Antigen Presentation. *Front Immunol* 2021;12:636568. doi: 10.3389/fimmu.2021.636568 [published Online First: 20210309]

18. Sari G, Rock KL. Tumor immune evasion through loss of MHC class-I antigen presentation. *Curr Opin Immunol* 2023;83:102329. doi: 10.1016/j.coi.2023.102329 [published Online First: 20230430]

19. Maggs L, Sadagopan A, Moghaddam AS, et al. HLA class I antigen processing machinery defects in antitumor immunity and immunotherapy. *Trends Cancer* 2021;7(12):1089-101. doi: 10.1016/j.trecan.2021.07.006 [published Online First: 20210903]

20. Aptsiauri N, Ruiz-Cabello F, Garrido F. The transition from HLA-I positive to HLA-I negative primary tumors: the road to escape from T-cell responses. *Curr Opin Immunol* 2018;51:123-32. doi: 10.1016/j.coi.2018.03.006 [published Online First: 20180319]

21. McGranahan N, Rosenthal R, Hiley CT, et al. Allele-Specific HLA Loss and Immune Escape in Lung Cancer Evolution. *Cell* 2017;171(6):1259-71 e11. doi: 10.1016/j.cell.2017.10.001 [published Online First: 20171026]

22. Del Campo AB, Carretero J, Munoz JA, et al. Adenovirus expressing beta2-microglobulin recovers HLA class I expression and antitumor immunity by increasing T-cell recognition. *Cancer Gene Ther* 2014;21(8):317-32. doi: 10.1038/cgt.2014.32 [published Online First: 20140627]

23. Lin H, Zhang R, Wu W, et al. Comprehensive network analysis of the molecular mechanisms associated with sorafenib resistance in hepatocellular carcinoma. *Cancer Genet* 2020;245:27-34. doi: 10.1016/j.cancergen.2020.04.076 [published Online First: 20200517]

24. Stifter K, Krieger J, Ruths L, et al. IFN-gamma treatment protocol for MHC-I(lo)/PD-L1(+) pancreatic tumor cells selectively restores their TAP-mediated presentation competence

and CD8 T-cell priming potential. *J Immunother Cancer* 2020;8(2) doi: 10.1136/jitc-2020-000692

25. Attaran N, Gu X, Coates PJ, et al. Downregulation of TAP1 in Tumor-Free Tongue Contralateral to Squamous Cell Carcinoma of the Oral Tongue, an Indicator of Better Survival. *Int J Mol Sci* 2020;21(17) doi: 10.3390/ijms21176220 [published Online First: 20200827]

26. Dubois A, Furstoss N, Calleja A, et al. Retraction Note: LAMP2 expression dictates azacytidine response and prognosis in MDS/AML. *Leukemia* 2020;34(9):2544. doi: 10.1038/s41375-020-0969-8

27. Stewart TJ, Smyth MJ. Improving cancer immunotherapy by targeting tumor-induced immune suppression. *Cancer Metastasis Rev* 2011;30(1):125-40. doi: 10.1007/s10555-011-9280-5

28. Mehta AM, Jordanova ES, Kenter GG, et al. Association of antigen processing machinery and HLA class I defects with clinicopathological outcome in cervical carcinoma. *Cancer Immunol Immunother* 2008;57(2):197-206. doi: 10.1007/s00262-007-0362-8 [published Online First: 20070712]

29. Hirata T, Yamamoto H, Taniguchi H, et al. Characterization of the immune escape phenotype of human gastric cancers with and without high-frequency microsatellite instability. *J Pathol* 2007;211(5):516-23. doi: 10.1002/path.2142

30. Gobbi G, Mirandola P, Micheloni C, et al. Expression of HLA class I antigen and proteasome subunits LMP-2 and LMP-10 in primary vs. metastatic breast carcinoma lesions. *International Journal of Oncology* 2004 doi: 10.3892/ijo.25.6.1625

31. Zhou X, Yan T, Huang C, et al. Melanoma cell-secreted exosomal miR-155-5p induce proangiogenic switch of cancer-associated fibroblasts via SOCS1/JAK2/STAT3 signaling pathway. *J Exp Clin Cancer Res* 2018;37(1):242. doi: 10.1186/s13046-018-0911-3 [published Online First: 20181003]

32. Rene C, Lozano C, Eliaou JF. Expression of classical HLA class I molecules: regulation and clinical impacts: Julia Bodmer Award Review 2015. *HLA* 2016;87(5):338-49. doi: 10.1111/tan.12787 [published Online First: 20160406]

33. Campoli M, Ferrone S. HLA antigen changes in malignant cells: epigenetic mechanisms and biologic significance. *Oncogene* 2008;27(45):5869-85. doi: 10.1038/onc.2008.273

34. Lazaridou M-F, Gonschorek E, Massa C, et al. Identification of miR-200a-5p targeting the peptide transporter TAP1 and its association with the clinical outcome of melanoma patients. *OncoImmunology* 2020;9(1):1774323. doi: 10.1080/2162402X.2020.1774323

35. Mari L, Hoefnagel SJM, Zito D, et al. microRNA 125a Regulates MHC-I Expression on Esophageal Adenocarcinoma Cells, Associated With Suppression of Antitumor Immune Response and Poor Outcomes of Patients. *Gastroenterology* 2018;155(3):784-98. doi: 10.1053/j.gastro.2018.06.030 [published Online First: 20180607]

36. Huang L, Malu S, McKenzie JA, et al. The RNA-binding Protein MEX3B Mediates Resistance to Cancer Immunotherapy by Downregulating HLA-A Expression. *Clin Cancer Res* 2018;24(14):3366-76. doi: 10.1158/1078-0432.CCR-17-2483 [published Online First: 20180301]

37. Chen JF, Mandel EM, Thomson JM, et al. The role of microRNA-1 and microRNA-133 in skeletal muscle proliferation and differentiation. *Nat Genet* 2006;38(2):228-33. doi: 10.1038/ng1725 [published Online First: 20051225]

38. Chen X, Ba Y, Ma L, et al. Characterization of microRNAs in serum: a novel class of biomarkers for diagnosis of cancer and other diseases. *Cell Res* 2008;18(10):997-1006. doi: 10.1038/cr.2008.282

39. Williams AH, Valdez G, Moresi V, et al. MicroRNA-206 delays ALS progression and promotes regeneration of neuromuscular synapses in mice. *Science* 2009;326(5959):1549-54. doi: 10.1126/science.1181046

40. Zhao Z, Xue L, Zheng L, et al. Tumor-derived miR-20b-5p promotes lymphatic metastasis of esophageal squamous cell carcinoma by remodeling the tumor microenvironment. *Signal Transduct Target Ther* 2023;8(1):29. doi: 10.1038/s41392-022-01242-1 [published Online First: 20230125]

41. Diener C, Keller A, Meese E. Emerging concepts of miRNA therapeutics: from cells to clinic. *Trends Genet* 2022;38(6):613-26. doi: 10.1016/j.tig.2022.02.006 [published Online First: 20220315]

42. Gao F, Zhao ZL, Zhao WT, et al. miR-9 modulates the expression of interferon-regulated genes and MHC class I molecules in human nasopharyngeal carcinoma cells. *Biochem Biophys Res Commun* 2013;431(3):610-6. doi: 10.1016/j.bbrc.2012.12.097 [published Online First: 20130104]

43. Li J, Lin TY, Chen L, et al. miR-19 regulates the expression of interferon-induced genes and MHC class I genes in human cancer cells. *Int J Med Sci* 2020;17(7):953-64. doi: 10.7150/ijms.44377 [published Online First: 20200406]

44. O'Huigin C, Kulkarni S, Xu Y, et al. The molecular origin and consequences of escape from miRNA regulation by HLA-C alleles. *Am J Hum Genet* 2011;89(3):424-31. doi: 10.1016/j.ajhg.2011.07.024

45. Manaster I, Goldman-Wohl D, Greenfield C, et al. MiRNA-mediated control of HLA-G expression and function. *PLoS One* 2012;7(3):e33395. doi: 10.1371/journal.pone.0033395 [published Online First: 20120316]

46. Mori A, Nishi H, Sasaki T, et al. HLA-G expression is regulated by miR-365 in trophoblasts under hypoxic conditions. *Placenta* 2016;45:37-41. doi: 10.1016/j.placenta.2016.07.004 [published Online First: 20160721]

47. Jongsma MLM, Guarda G, Spaapen RM. The regulatory network behind MHC class I expression. *Mol Immunol* 2019;113:16-21. doi: 10.1016/j.molimm.2017.12.005 [published Online First: 20171208]

48. Lazaridou MF, Gonschorek E, Massa C, et al. Identification of miR-200a-5p targeting the peptide transporter TAP1 and its association with the clinical outcome of melanoma patients. *Oncoimmunology* 2020;9(1):1774323. doi: 10.1080/2162402X.2020.1774323 [published Online First: 20200603]

49. Lazaridou MF, Massa C, Handke D, et al. Identification of microRNAs Targeting the Transporter Associated with Antigen Processing TAP1 in Melanoma. *J Clin Med* 2020;9(9) doi: 10.3390/jcm9092690 [published Online First: 20200820]

50. Dragomir MP, Knutsen E, Calin GA. Classical and noncanonical functions of miRNAs in cancers. *Trends Genet* 2022;38(4):379-94. doi: 10.1016/j.tig.2021.10.002 [published Online First: 20211030]

51. Dragomir MP, Knutsen E, Calin GA. SnapShot: Unconventional miRNA Functions. *Cell* 2018;174(4):1038-38 e1. doi: 10.1016/j.cell.2018.07.040

52. Bosisio D, Gaudenzi C, Sozzani S, et al. Unconventional functions of miRNAs. In: Xiao J, ed. MicroRNA: From Bench to Bedside: Academic Press 2022:181-214.

53. Eiring AM, Harb JG, Neviani P, et al. miR-328 functions as an RNA decoy to modulate hnRNP E2 regulation of mRNA translation in leukemic blasts. *Cell* 2010;140(5):652-65. doi: 10.1016/j.cell.2010.01.007

54. Tang R, Li L, Zhu D, et al. Mouse miRNA-709 directly regulates miRNA-15a/16-1 biogenesis at the posttranscriptional level in the nucleus: evidence for a microRNA hierarchy system. *Cell Res* 2012;22(3):504-15. doi: 10.1038/cr.2011.137 [published Online First: 20110823]

55. Vasudevan S, Tong Y, Steitz JA. Switching from repression to activation: microRNAs can up-regulate translation. *Science* 2007;318(5858):1931-4. doi: 10.1126/science.1149460 [published Online First: 20071129]

56. Friedrich M, Vaxevanis CK, Biehl K, et al. Targeting the coding sequence: opposing roles in regulating classical and non-classical MHC class I molecules by miR-16 and miR-744. *J Immunother Cancer* 2020;8(1):e000396. doi: 10.1136/jitc-2019-000396

57. Ramchandran R, Chaluvally-Raghavan P. miRNA-Mediated RNA Activation in Mammalian Cells. *Adv Exp Med Biol* 2017;983:81-89. doi: 10.1007/978-981-10-4310-9_6

58. Lunde BM, Moore C, Varani G. RNA-binding proteins: modular design for efficient function. *Nat Rev Mol Cell Biol* 2007;8(6):479-90. doi: 10.1038/nrm2178

59. Glisovic T, Bachorik JL, Yong J, et al. RNA-binding proteins and post-transcriptional gene regulation. *FEBS Lett* 2008;582(14):1977-86. doi: 10.1016/j.febslet.2008.03.004 [published Online First: 20080313]

60. Ariyachet C, Solis NV, Liu Y, et al. SR-like RNA-binding protein Slr1 affects Candida albicans filamentation and virulence. *Infect Immun* 2013;81(4):1267-76. doi: 10.1128/IAI.00864-12 [published Online First: 20130204]

61. Brochu C, Cabrita MA, Melanson BD, et al. NF-kappaB-dependent role for cold-inducible RNA binding protein in regulating interleukin 1beta. *PLoS One* 2013;8(2):e57426. doi: 10.1371/journal.pone.0057426 [published Online First: 20130221]

62. Wang ZL, Li B, Luo YX, et al. Comprehensive Genomic Characterization of RNA-Binding Proteins across Human Cancers. *Cell Rep* 2018;22(1):286-98. doi: 10.1016/j.celrep.2017.12.035

63. Friedrich M, Jasinski-Bergner S, Lazaridou MF, et al. Tumor-induced escape mechanisms and their association with resistance to checkpoint inhibitor therapy. *Cancer Immunol Immunother* 2019;68(10):1689-700. doi: 10.1007/s00262-019-02373-1 [published Online First: 20190803]

64. Kulkarni S, Ramsuran V, Rucevic M, et al. Posttranscriptional Regulation of HLA-A Protein Expression by Alternative Polyadenylation Signals Involving the RNA-Binding Protein Syncrip. *J Immunol* 2017;199(11):3892-99. doi: 10.4049/jimmunol.1700697 [published Online First: 20171020]

65. Chida S, Hohjoh H, Tokunaga K. Molecular analyses of the possible RNA-binding protein gene located in the human leukocyte antigen (HLA)--DR subregion. *Gene* 1999;240(1):125-32. doi: 10.1016/s0378-1119(99)00422-9

66. Streitfeld WS, Dalton AC, Howley BV, et al. PCBP1 regulates LIFR through FAM3C to maintain breast cancer stem cell self-renewal and invasiveness. *Cancer Biol Ther* 2023;24(1):2271638. doi: 10.1080/15384047.2023.2271638 [published Online First: 20231106]

67. Jung M, Ji E, Kang H, et al. The microRNA-195-5p/hnRNP A1 axis contributes to the progression of hepatocellular carcinoma by regulating the migration of cancer cells. *Biochem Biophys Res Commun* 2023;686:149183. doi: 10.1016/j.bbrc.2023.149183 [published Online First: 20231030]

68. Lu Y, Bi T, Zhou S, et al. MEX3A promotes angiogenesis in colorectal cancer via glycolysis. *Libyan J Med* 2023;18(1):2202446. doi: 10.1080/19932820.2023.2202446

69. Konig J, Zarnack K, Rot G, et al. iCLIP reveals the function of hnRNP particles in splicing at individual nucleotide resolution. *Nat Struct Mol Biol* 2010;17(7):909-15. doi: 10.1038/nsmb.1838 [published Online First: 20100704]

70. Cheng Y, Li L, Wei X, et al. HNRNPC suppresses tumor immune microenvironment by activating Treg cells promoting the progression of prostate cancer. *Cancer Sci* 2023;114(5):1830-45. doi: 10.1111/cas.15745 [published Online First: 20230213]

71. Zheng J, Wu S, Tang M, et al. USP39 promotes hepatocellular carcinogenesis through regulating alternative splicing in cooperation with SRSF6/HNRNPC. *Cell Death Dis* 2023;14(10):670. doi: 10.1038/s41419-023-06210-3 [published Online First: 20231011]

72. Liu D, Luo X, Xie M, et al. HNRNPC downregulation inhibits IL-6/STAT3-mediated HCC metastasis by decreasing HIF1A expression. *Cancer Sci* 2022;113(10):3347-61. doi: 10.1111/cas.15494 [published Online First: 20220812]

73. He Q, Yang C, Xiang Z, et al. LINC00924-induced fatty acid metabolic reprogramming facilitates gastric cancer peritoneal metastasis via hnRNPC-regulated alternative splicing of Mnk2. *Cell Death Dis* 2022;13(11):987. doi: 10.1038/s41419-022-05436-x [published Online First: 20221123]

74. Hwang SJ, Seol HJ, Park YM, et al. MicroRNA-146a suppresses metastatic activity in brain metastasis. *Mol Cells* 2012;34(3):329-34. doi: 10.1007/s10059-012-0171-6 [published Online First: 20120903]

75. Cholewa BD, Pellitteri-Hahn MC, Scarlett CO, et al. Large-scale label-free comparative proteomics analysis of polo-like kinase 1 inhibition via the small-molecule inhibitor BI 6727 (Volasertib) in BRAF(V600E) mutant melanoma cells. *J Proteome Res* 2014;13(11):5041-50. doi: 10.1021/pr5002516 [published Online First: 20140609]

76. Pang B, van Weerd JH, Hamoen FL, et al. Identification of non-coding silencer elements and their regulation of gene expression. *Nat Rev Mol Cell Biol* 2023;24(6):383-95. doi: 10.1038/s41580-022-00549-9 [published Online First: 20221107]

77. Segert JA, Gisselbrecht SS, Bulyk ML. Transcriptional Silencers: Driving Gene Expression with the Brakes On. *Trends Genet* 2021;37(6):514-27. doi: 10.1016/j.tig.2021.02.002 [published Online First: 20210309]

78. Brand AH, Breeden L, Abraham J, et al. Characterization of a "silencer" in yeast: a DNA sequence with properties opposite to those of a transcriptional enhancer. *Cell* 1985;41(1):41-8. doi: 10.1016/0092-8674(85)90059-5

79. Ngan CY, Wong CH, Tjong H, et al. Chromatin interaction analyses elucidate the roles of PRC2-bound silencers in mouse development. *Nat Genet* 2020;52(3):264-72. doi: 10.1038/s41588-020-0581-x [published Online First: 20200224]

80. Zeng W, Chen S, Cui X, et al. SilencerDB: a comprehensive database of silencers. *Nucleic Acids Res* 2021;49(D1):D221-D28. doi: 10.1093/nar/gkaa839

81. Hussain S, Sadouni N, van Essen D, et al. Short tandem repeats are important contributors to silencer elements in T cells. *Nucleic Acids Res* 2023;51(10):4845-66. doi: 10.1093/nar/gkad187

82. Cui K, Chen Z, Cao Y, et al. Restraint of IFN-gamma expression through a distal silencer CNS-28 for tissue homeostasis. *Immunity* 2023;56(5):944-58 e6. doi: 10.1016/j.immuni.2023.03.006 [published Online First: 20230410]

83. Huang D, Petrykowska HM, Miller BF, et al. Identification of human silencers by correlating cross-tissue epigenetic profiles and gene expression. *Genome Res* 2019;29(4):657-67. doi: 10.1101/gr.247007.118 [published Online First: 20190318]

84. Cai Y, Zhang Y, Loh YP, et al. H3K27me3-rich genomic regions can function as silencers to repress gene expression via chromatin interactions. *Nat Commun* 2021;12(1):719. doi: 10.1038/s41467-021-20940-y [published Online First: 20210129]

85. Pang B, Snyder MP. Systematic identification of silencers in human cells. *Nat Genet* 2020;52(3):254-63. doi: 10.1038/s41588-020-0578-5 [published Online First: 20200224]

86. Ogbourne S, Antalis TM. Transcriptional control and the role of silencers in transcriptional regulation in eukaryotes. *Biochem J* 1998;331 (Pt 1)(Pt 1):1-14. doi: 10.1042/bj3310001

87. Cam A, Legraverend C. Transcriptional Repression, a Novel Function for 3' Untranslated Regions. *Eur J Biochem* 1995;231(3):620-27. doi: 10.1111/j.1432-1033.1995.0620d.x

88. Yan ZJ, Jiang C, Qian RL. Trans-acting factors from the human fetal liver binding to the human epsilon-globin gene silencer. *Cell Res* 1997;7(2):151-9. doi: 10.1038/cr.1997.16

89. Xiao Y, Yu D. Tumor microenvironment as a therapeutic target in cancer. *Pharmacol Ther* 2021;221:107753. doi: 10.1016/j.pharmthera.2020.107753 [published Online First: 20201128]

90. Wculek SK, Cueto FJ, Mujal AM, et al. Dendritic cells in cancer immunology and immunotherapy. *Nat Rev Immunol* 2020;20(1):7-24. doi: 10.1038/s41577-019-0210-z [published Online First: 20190829]

91. Hartupee C, Nagalo BM, Chabu CY, et al. Pancreatic cancer tumor microenvironment is a major therapeutic barrier and target. *Front Immunol* 2024;15:1287459. doi: 10.3389/fimmu.2024.1287459 [published Online First: 20240201]

92. Biffi G, Tuveson DA. Diversity and Biology of Cancer-Associated Fibroblasts. *Physiol Rev* 2021;101(1):147-76. doi: 10.1152/physrev.00048.2019 [published Online First: 20200528]

93. Song M, He J, Pan QZ, et al. Cancer-Associated Fibroblast-Mediated Cellular Crosstalk Supports Hepatocellular Carcinoma Progression. *Hepatology* 2021;73(5):1717-35. doi: 10.1002/hep.31792

94. Tang F, Li J, Qi L, et al. A pan-cancer single-cell panorama of human natural killer cells. *Cell* 2023;186(19):4235-51 e20. doi: 10.1016/j.cell.2023.07.034 [published Online First: 20230821]

95. Vitale I, Manic G, Coussens LM, et al. Macrophages and Metabolism in the Tumor Microenvironment. *Cell Metab* 2019;30(1):36-50. doi: 10.1016/j.cmet.2019.06.001

96. Chen Y, Song Y, Du W, et al. Tumor-associated macrophages: an accomplice in solid tumor progression. *J Biomed Sci* 2019;26(1):78. doi: 10.1186/s12929-019-0568-z [published Online First: 20191020]

97. Yin Y, Liu B, Cao Y, et al. Colorectal Cancer-Derived Small Extracellular Vesicles Promote Tumor Immune Evasion by Upregulating PD-L1 Expression in Tumor-Associated Macrophages. *Adv Sci (Weinh)* 2022;9(9):2102620. doi: 10.1002/advs.202102620 [published Online First: 20220117]

98. Song M, Yeku OO, Rafiq S, et al. Tumor derived UBR5 promotes ovarian cancer growth and metastasis through inducing immunosuppressive macrophages. *Nat Commun* 2020;11(1):6298. doi: 10.1038/s41467-020-20140-0 [published Online First: 20201208]

99. Zhong Q, Fang Y, Lai Q, et al. CPEB3 inhibits epithelial-mesenchymal transition by disrupting the crosstalk between colorectal cancer cells and tumor-associated macrophages

via IL-6R/STAT3 signaling. *J Exp Clin Cancer Res* 2020;39(1):132. doi: 10.1186/s13046-020-01637-4 [published Online First: 20200711]

100. Chesney JA, Mitchell RA. 25 Years On: A Retrospective on Migration Inhibitory Factor in Tumor Angiogenesis. *Mol Med* 2015;21 Suppl 1(Suppl 1):S19-24. doi: 10.2119/molmed.2015.00055 [published Online First: 20151027]

101. Okikawa S, Morine Y, Saito Y, et al. Inhibition of the VEGF signaling pathway attenuates tumor-associated macrophage activity in liver cancer. *Oncol Rep* 2022;47(4) doi: 10.3892/or.2022.8282 [published Online First: 20220216]

102. Sun L, Zhang X, Song Q, et al. IGFBP2 promotes tumor progression by inducing alternative polarization of macrophages in pancreatic ductal adenocarcinoma through the STAT3 pathway. *Cancer Lett* 2021;500:132-46. doi: 10.1016/j.canlet.2020.12.008 [published Online First: 20201210]

103. Yarmarkovich M, Maris JM. When Cold Is Hot: Immune Checkpoint Inhibition Therapy for Rhabdoid Tumors. *Cancer Cell* 2019;36(6):575-76. doi: 10.1016/j.ccell.2019.11.006

104. Vaxevanis CK, Friedrich M, Tretbar SU, et al. Identification and characterization of novel CD274 (PD-L1) regulating microRNAs and their functional relevance in melanoma. *Clin Transl Med* 2022;12(7):e934. doi: 10.1002/ctm2.934

105. Hammerle M, Gutschner T, Uckelmann H, et al. Posttranscriptional destabilization of the liver-specific long noncoding RNA HULC by the IGF2 mRNA-binding protein 1 (IGF2BP1). *Hepatol* 2013;58(5):1703-12. doi: 10.1002/hep.26537 [published Online First: 20130807]

106. Chen C, Ridzon DA, Broomer AJ, et al. Real-time quantification of microRNAs by stem-loop RT-PCR. *Nucleic Acids Res* 2005;33(20):e179. doi: 10.1093/nar/gni178 [published Online First: 20051127]

107. Schneider CA, Rasband WS, Eliceiri KW. NIH Image to ImageJ: 25 years of image analysis. *Nat Methods* 2012;9(7):671-5. doi: 10.1038/nmeth.2089

108. Mootha VK, Lindgren CM, Eriksson KF, et al. PGC-1alpha-responsive genes involved in oxidative phosphorylation are coordinately downregulated in human diabetes. *Nat Genet* 2003;34(3):267-73. doi: 10.1038/ng1180

109. Braun J, Misiak D, Busch B, et al. Rapid identification of regulatory microRNAs by miTRAP (miRNA trapping by RNA in vitro affinity purification). *Nucleic Acids Res* 2014;42(8):e66. doi: 10.1093/nar/gku127 [published Online First: 20140207]

110. Li X, Wang S, Mu W, et al. Reactive oxygen species reprogram macrophages to suppress antitumor immune response through the exosomal miR-155-5p/PD-L1 pathway. *J Exp Clin Cancer Res* 2022;41(1):41. doi: 10.1186/s13046-022-02244-1 [published Online First: 20220127]

111. Alter G, Malenfant JM, Altfeld M. CD107a as a functional marker for the identification of natural killer cell activity. *J Immunol Methods* 2004;294(1-2):15-22. doi: 10.1016/j.jim.2004.08.008

112. Elton TS, Selemon H, Elton SM, et al. Regulation of the MIR155 host gene in physiological and pathological processes. *Gene* 2013;532(1):1-12. doi: 10.1016/j.gene.2012.12.009 [published Online First: 20121214]

113. Consortium EP. An integrated encyclopedia of DNA elements in the human genome. *Nature* 2012;489(7414):57-74. doi: 10.1038/nature11247

114. Imamachi N, Salam KA, Suzuki Y, et al. A GC-rich sequence feature in the 3' UTR directs UPF1-dependent mRNA decay in mammalian cells. *Genome Res* 2017;27(3):407-18. doi: 10.1101/gr.206060.116 [published Online First: 20161209]

115. Courel M, Clement Y, Bossevain C, et al. GC content shapes mRNA storage and decay in human cells. *Elife* 2019;8:e49708. doi: 10.7554/eLife.49708 [published Online First: 20191219]

116. Fallmann J, Sedlyarov V, Tanzer A, et al. AREsite2: an enhanced database for the comprehensive investigation of AU/GU/U-rich elements. *Nucleic Acids Res* 2016;44(D1):D90-5. doi: 10.1093/nar/gkv1238 [published Online First: 20151123]

117. Ran FA, Hsu PD, Wright J, et al. Genome engineering using the CRISPR-Cas9 system. *Nat Protoc* 2013;8(11):2281-308. doi: 10.1038/nprot.2013.143 [published Online First: 20131024]

118. Bao Y, Qiao Y, Choi JE, et al. Targeting the lipid kinase PIKfyve upregulates surface expression of MHC class I to augment cancer immunotherapy. *Proc Natl Acad Sci U S A* 2023;120(49):e2314416120. doi: 10.1073/pnas.2314416120 [published Online First: 20231127]

119. Lazaridou MF, Massa C, Handke D, et al. Identification of microRNAs Targeting the Transporter Associated with Antigen Processing TAP1 in Melanoma. *J Clin Med* 2020;9(9) doi: 10.3390/jcm9092690 [published Online First: 20200820]

120. Matsui M, Kawano M, Matsushita S, et al. Introduction of a point mutation into an HLA class I single-chain trimer induces enhancement of CTL priming and antitumor immunity. *Mol Ther Methods Clin Dev* 2014;1:14027. doi: 10.1038/mtm.2014.27 [published Online First: 20140702]

121. Anderson P, Aptsiauri N, Ruiz-Cabello F, et al. HLA class I loss in colorectal cancer: implications for immune escape and immunotherapy. *Cell Mol Immunol* 2021;18(3):556-65. doi: 10.1038/s41423-021-00634-7 [published Online First: 20210120]

122. Eichmuller SB, Osen W, Mandelboim O, et al. Immune Modulatory microRNAs Involved in Tumor Attack and Tumor Immune Escape. *J Natl Cancer Inst* 2017;109(10) doi: 10.1093/jnci/djx034

123. Wang D, Wang X, Song Y, et al. Exosomal miR-146a-5p and miR-155-5p promote CXCL12/CXCR7-induced metastasis of colorectal cancer by crosstalk with cancer-associated fibroblasts. *Cell Death Dis* 2022;13(4):380. doi: 10.1038/s41419-022-04825-6 [published Online First: 20220420]

124. Ren XS, Tong Y, Qiu Y, et al. MiR155-5p in adventitial fibroblasts-derived extracellular vesicles inhibits vascular smooth muscle cell proliferation via suppressing angiotensin-converting enzyme expression. *J Extracell Vesicles* 2020;9(1):1698795. doi: 10.1080/20013078.2019.1698795 [published Online First: 20191202]

125. Al-Haidari A, Algaber A, Madhi R, et al. MiR-155-5p controls colon cancer cell migration via post-transcriptional regulation of Human Antigen R (HuR). *Cancer Lett* 2018;421:145-51. doi: 10.1016/j.canlet.2018.02.026 [published Online First: 20180220]

126. Dhatchinamoorthy K, Colbert JD, Rock KL. Cancer Immune Evasion Through Loss of MHC Class I Antigen Presentation. *Front Immunol* 2021;12:636568. doi: 10.3389/fimmu.2021.636568 [published Online First: 20210309]

127. Wu Y, Zhao W, Liu Y, et al. Function of HNRNPC in breast cancer cells by controlling the dsRNA-induced interferon response. *EMBO J* 2018;37(23) doi: 10.15252/embj.201899017 [published Online First: 20180829]

128. Cai Y, Lyu T, Li H, et al. LncRNA CEBPA-DT promotes liver cancer metastasis through DDR2/beta-catenin activation via interacting with hnRNPC. *J Exp Clin Cancer Res* 2022;41(1):335. doi: 10.1186/s13046-022-02544-6 [published Online First: 20221206]

129. Wu Z, Zuo X, Zhang W, et al. m6A-Modified circTET2 Interacting with HNRNPC Regulates Fatty Acid Oxidation to Promote the Proliferation of Chronic Lymphocytic Leukemia. *Adv Sci (Weinh)* 2023;10(34):e2304895. doi: 10.1002/advs.202304895 [published Online First: 20231011]

130. Shi S, Wu T, Ma Z, et al. Serum-derived extracellular vesicles promote the growth and metastasis of non-small cell lung cancer by delivering the m6A methylation regulator HNRNPC through the regulation of DLGAP5. *J Cancer Res Clin Oncol* 2023;149(8):4639-51. doi: 10.1007/s00432-022-04375-6 [published Online First: 20220929]

131. Fischl H, Neve J, Wang Z, et al. hnRNPC regulates cancer-specific alternative cleavage and polyadenylation profiles. *Nucleic Acids Res* 2019;47(14):7580-91. doi: 10.1093/nar/gkz461

132. Gu Z, Yang Y, Ma Q, et al. HNRNPC, a predictor of prognosis and immunotherapy response based on bioinformatics analysis, is related to proliferation and invasion of NSCLC cells. *Respir Res* 2022;23(1):362. doi: 10.1186/s12931-022-02227-y [published Online First: 20221219]

133. Xia N, Yang N, Shan Q, et al. HNRNPC regulates RhoA to induce DNA damage repair and cancer-associated fibroblast activation causing radiation resistance in pancreatic cancer. *J Cell Mol Med* 2022;26(8):2322-36. doi: 10.1111/jcmm.17254 [published Online First: 20220311]

134. Huang GZ, Wu QQ, Zheng ZN, et al. M6A-related bioinformatics analysis reveals that HNRNPC facilitates progression of OSCC via EMT. *Aging (Albany NY)* 2020;12(12):11667-84. doi: 10.18632/aging.103333 [published Online First: 20200611]

135. Kattan FG, Koukouraki P, Anagnostopoulos AK, et al. RNA binding protein AUF1/HNRNPD regulates nuclear export, stability and translation of SNCA transcripts.

Open Biol 2023;13(11):230158. doi: 10.1098/rsob.230158 [published Online First: 20231122]

136. Chen Z, Pi H, Zheng W, et al. The 3' Non-Coding Sequence Negatively Regulates PD-L1 Expression, and Its Regulators Are Systematically Identified in Pan-Cancer. *Genes (Basel)* 2023;14(8) doi: 10.3390/genes14081620 [published Online First: 20230813]

137. Yang YC, Lin YW, Lee WJ, et al. The RNA-binding protein KSRP aggravates malignant progression of clear cell renal cell carcinoma through transcriptional inhibition and post-transcriptional destabilization of the NEDD4L ubiquitin ligase. *J Biomed Sci* 2023;30(1):68. doi: 10.1186/s12929-023-00949-9 [published Online First: 20230814]

138. Zheng J, Dou R, Zhang X, et al. LINC00543 promotes colorectal cancer metastasis by driving EMT and inducing the M2 polarization of tumor associated macrophages. *J Transl Med* 2023;21(1):153. doi: 10.1186/s12967-023-04009-6 [published Online First: 20230225]

139. Zhang G, Gao Z, Guo X, et al. CAP2 promotes gastric cancer metastasis by mediating the interaction between tumor cells and tumor-associated macrophages. *J Clin Invest* 2023;133(21) doi: 10.1172/JCI166224 [published Online First: 20231101]

140. Banerjee K, Kerzel T, Bekkhus T, et al. VEGF-C-expressing TAMs rewire the metastatic fate of breast cancer cells. *Cell Rep* 2023;42(12):113507. doi: 10.1016/j.celrep.2023.113507 [published Online First: 20231201]

141. Lee C, Kim S, Jeong C, et al. TAMpepK Suppresses Metastasis through the Elimination of M2-Like Tumor-Associated Macrophages in Triple-Negative Breast Cancer. *Int J Mol Sci* 2022;23(4) doi: 10.3390/ijms23042157 [published Online First: 20220215]

142. Mempel TR, Lill JK, Altenburger LM. How chemokines organize the tumour microenvironment. *Nat Rev Cancer* 2024;24(1):28-50. doi: 10.1038/s41568-023-00635-w [published Online First: 20231208]

143. Lee S, Lee E, Ko E, et al. Tumor-associated macrophages secrete CCL2 and induce the invasive phenotype of human breast epithelial cells through upregulation of ERO1-alpha and MMP-9. *Cancer Lett* 2018;437:25-34. doi: 10.1016/j.canlet.2018.08.025 [published Online First: 20180827]

144. Yang H, Zhang QN, Xu M, et al. CCL2-CCR2 axis recruits tumor associated macrophages to induce immune evasion through PD-1 signaling in esophageal carcinogenesis. *Molecular Cancer* 2020;19(1) doi: ARTN 41

10.1186/s12943-020-01165-x

145. Luo F, Li H, Ma W, et al. The BCL-2 inhibitor APG-2575 resets tumor-associated macrophages toward the M1 phenotype, promoting a favorable response to anti-PD-1 therapy via NLRP3 activation. *Cell Mol Immunol* 2024;21(1):60-79. doi: 10.1038/s41423-023-01112-y [published Online First: 20231207]

146. Nasir I, McGuinness C, Poh AR, et al. Tumor macrophage functional heterogeneity can inform the development of novel cancer therapies. *Trends Immunol* 2023;44(12):971-85. doi: 10.1016/j.it.2023.10.007

147. Liu Y, Zhang D, Zhang Z, et al. Multifunctional nanoparticles inhibit tumor and tumor-associated macrophages for triple-negative breast cancer therapy. *J Colloid Interface Sci* 2024;657:598-610. doi: 10.1016/j.jcis.2023.11.156 [published Online First: 20231129]

148. Ma RY, Black A, Qian BZ. Macrophage diversity in cancer revisited in the era of single-cell omics. *Trends Immunol* 2022;43(7):546-63. doi: 10.1016/j.it.2022.04.008 [published Online First: 20220609]

149. Mulder K, Patel AA, Kong WT, et al. Cross-tissue single-cell landscape of human monocytes and macrophages in health and disease. *Immunity* 2021;54(8):1883-900 e5. doi: 10.1016/j.immuni.2021.07.007 [published Online First: 20210730]

150. Zhao J, Li H, Zhao S, et al. Epigenetic silencing of miR-144/451a cluster contributes to HCC progression via paracrine HGF/MIF-mediated TAM remodeling. *Mol Cancer* 2021;20(1):46. doi: 10.1186/s12943-021-01343-5 [published Online First: 20210303]

151. Sarbanes SL, Le Pen J, Rice CM. Friend and foe, HNRNPC takes on immunostimulatory RNAs in breast cancer cells. *EMBO J* 2018;37(23) doi: 10.15252/embj.2018100923 [published Online First: 20181102]

152. Yan M, Sun L, Li J, et al. RNA-binding protein KHSRP promotes tumor growth and metastasis in non-small cell lung cancer. *J Exp Clin Cancer Res* 2019;38(1):478. doi: 10.1186/s13046-019-1479-2 [published Online First: 20191127]

8 Thesis

1. MiR-155-5p has been identified binding to tpn 3'UTR and upregulated the expression of tpn in different human melanoma cell lines resulting in an increased HLA-I surface expression thereby activating the antigen processing and presentation pathway as well as has clinical relevance.

2. The binding sequence of miR-155-5p for tpn has been identified including intrinsic suppressive activity as a silencer, which also suggest the new unconventional function of miR-155-5p that binding with a silencer.

3. HnRNP C has been identified to the 3'UTR of tpn. It can downregulate tpn expression thereby inhibiting the antigen processing and presentation pathway as well as has clinical relevance.

4. HnRNP C promote melanoma patients' metastasis and melanoma cell lines via epithelial-mesenchymal transition.

5. TAM interact with melanoma cell lines through CXCR3-hnRNP C-MIF axis and promote melanoma cells metastasis.

6. HnRNP C can affect tumor associated macrophages phenotypes as a M1-like macrophages.

Acknowledgement

Publication

1. Wang Y, Jasinski-Bergner S, Wickenhauser C, et al. Cancer Immunology: Immune Escape of Tumors—Expression and Regulation of HLA Class I Molecules and Its Role in Immunotherapies. *Advances in Anatomic Pathology* 2023;30(3):148-59.

2. Wang Y, Lazaridou M-F, Massa C, et al. 910 Overexpression of miR-155–5p can upregulate antigen processing and presentation pathway via targeting tapasin: BMJ Specialist Journals, 2021.

3. Massa C, Wang Y, Marr N, et al. Interferons and Resistance Mechanisms in Tumors and Pathogen-Driven Diseases—Focus on the Major Histocompatibility Complex (MHC) Antigen Processing Pathway. *International Journal of Molecular Sciences* 2023;24(7):6736.

4. Vaxevanis CK, Friedrich M, Tretbar SU, et al. Identification and characterization of novel CD274 (PD‐L1) regulating microRNAs and their functional relevance in melanoma. *Clinical and Translational Medicine* 2022;12(7):e934.

5. Liu X, Zhang M, Ying S, et al. Genetic alterations in esophageal tissues from squamous dysplasia to carcinoma. *Gastroenterology* 2017;153(1):166-77.

Declaration

Herein, I declare that this thesis is finished based on my own work in the past three years and it neither contains the materials published previously or written by other people, nor the substantial extent used to apply any other degree or diploma at any educational institutions, except the declaration made in the acknowledgment part in this thesis. Any contribution ma to this work by others is expressly acknowledged in this thesis.

Place and date

Signature: